UNIVERSITY OF CALIFORNIA SAN DIEGO

Allosteric mechanisms and consequences of Gi activation via the Guanine-nucleotide Exchange Modulator, GIV

A dissertation submitted in partial satisfaction of the
requirements for the degree
Doctor of Philosophy

in

Biomedical Sciences

by

Nicholas A. Kalogriopoulos

Committee in charge:

Professor Pradipta Ghosh, Chair
Professor Geoffrey Chang
Professor Steven Dowdy
Professor J. Silvio Gutkind
Professor Anthony Hunter

2019

The dissertation of Nicholas A. Kalogriopoulos is approved, and it is acceptable in quality and form for publication on microfilm and electronically:

_____

_____

_____

_____

_____

Chair

University of California San Diego

2019

DEDICATION

To:

Mama and Baba

EPIGRAPH

Failure is simply the opportunity to begin again,

this time more intelligently.

—Henry Ford

TABLE OF CONTENTS

LIST OF FIGURES

ACKNOWLEDGEMENTS

These few paragraphs do not begin to do justice to all the people I need to thank. So many people have helped shape me these past 6 years into the person and scientist I am today. They say all it takes is one mentor to guide, support, and believe in someone so they can succeed. During my time here, I have been incredibly fortunate to have had 5 amazing mentors in my thesis committee. Thank you to my thesis advisor, Pradipta, for pushing me and challenging me every single day to become a better scientist. I cannot put into words how much I have learned from you. It is obvious I would not be where I am today without you, so thank you. To the rest of my committee and mentors, Geoffrey, Steve, Silvio, and Tony, thank you for your never-ending support and guidance in all aspects of my professional career. The impact you all have had on my career will continue for many, many years to come.

Graduate school, and really science in general, can bring all sorts of different emotions: joy, sadness, excitement, surprise, anger, disgust. The Ph.D. is a roller coaster, and I want to thank all the people who were there with me through it all. To all my lab mates, especially Lee, Jason, Cristina, and Navin, every time I thought grad school knocked me down for the last time, you all were there to help me back up. I can confidently say that I would not have been able to do this without all of you. Thanks for all the late-night science talks, the mid-day coffee breaks, and the endless laughs. I can honestly say in the past 6 years there was not a single dull day, so thank you.

They say if a friendship lasts longer than seven years, then it will last a lifetime. Although I didn't make it to seven years (thankfully), grad school sometimes felt like waaaay more than seven years so I think that counts. To all my friends, Nate, Tim, James, Afsheen, Chelsea, Sarah, Nikos, Ian, David, and so many others, thank you for all the good times. Thanks for

occasionally reminding me that there is an outside world with real people and things in it. Thank you all for the endless scientific and personal support you have given me. I am so fortunate to have made life-long friends in all of you.

To the BMS Chair during my time here, Arshad, and to the BMS front office, Leanne, Gina, and Pat, thank you for making the BMS program an amazing place to get a Ph.D. Thank you for all the help, support, and guidance through my time here. I can't imagine a better place for grad school than the awesome scientific and social environment that you all created in the BMS program.

Finally, last but certainly not least, I want to thank my family. To Mama and Baba, I owe you everything. You have given me the world and I will never be able to thank you enough. Thank you for all your love and support and for giving me all the opportunities you have throughout my life, including the opportunity to pursue this Ph.D. To my siblings, Katie, John, and Stephanie, thanks for doing what you do and always being there for me... and it's Dr. Nick to you guys.

Chapter 1 in part is a reprint of material published in: Aznar N, **Kalogriopoulos NA**, Midde K, Ghosh P. 2016. "Heterotrimeric G protein signaling via GIV/Girdin: Breaking the rules of engagement, space, and time." *Bioessays.* 38:379-93. The dissertation author was a co-author.

Chapter 2 in part is a reprint of material submitted to be published in: **Kalogriopoulos NA***, Rees SD*, Ngo T, Kopcho N, Ilatovskiy A, Sun N, Komives E, Chang G, Ghosh P, Kufareva I. 2018. "Structural basis for GPCR-independent activation of heterotrimeric Gi proteins." *Under review*. The dissertation author was *co-first author.

Chapter 3 in part is material being prepared to be submitted for publication in: **Kalogriopoulos NA**, Lopez-Sanchez I, Lin C, Aznar N, Murray F, Garcia-Marcos M, Kufareva I, Ghassemian M, and Ghosh P. “Receptor tyrosine kinases activate Gi proteins by phosphorylating within the interdomain cleft of Gαi.” The dissertation author was the primary author.

Chapter 4 in part is a reprint of material published in: Aznar N, **Kalogriopoulos NA**, Midde K, Ghosh P. 2016. “Heterotrimeric G protein signaling via GIV/Girdin: Breaking the rules of engagement, space, and time.” *Bioessays.* 38:379-93. The dissertation author was a co-author.

VITA

2012	Bachelor of Science in Genetics and Molecular Biology, University of Wisconsin-Madison
2019	Doctor of Philosophy in Biomedical Sciences, University of California San Diego

PUBLICATIONS

Rakhmilevich A, Van de Voort T, Baldeshwiler M, Felder M, Yang RK, **Kalogriopoulos NA**, Koslov D, Sondel PM. Tumor-associated myeloid cells can be activated in vitro and in vivo to mediate antitumor effects. *Cancer Immunol Immunother*. 61:1683-97 (2012).

Yang RK*, **Kalogriopoulos NA***, Rakhmilevich AL, Ranheim EA, Seo S, Alderson KL, Gan J, Hank JA, Sondel PM. Intratumoral hu14.18-IL2 (IC) Induces Local and Systemic Antitumor Effects that Involve Both Activated T- and NK cells as well as Enhanced IC Retention. *J Immunol*. 189:2656-64 (2012).

Yang RK, **Kalogriopoulos NA**, Rakhmilevich AL, Ranheim EA, Seo S, Kim K, Alderson KL, Gan J, Reisfeld RA, Gillies SD, Hank JA, Sondel PM. Intratumoral treatment of smaller mouse neuroblastoma tumors with a recombinant protein consisting of IL-2 linked to the Hu14.18 antibody increases intratumoral CD8+ T and NK cells and improves survival. *Cancer Immunol Immunother*. 62:1303-13 (2013).

Ma G, Aznar N, **Kalogriopoulos NA**, Lopez-Sanchez I, Midde K, Dunkel Y, Muto J, Gallo R, Ghosh P. Therapeutic effects of cell-permeant peptides that activate G proteins downstream of growth factors. *Proc Natl Acad Sci*. 112:E2602-10 (2015).

Ma G, Lopez-Sanchez I, Aznar N, **Kalogriopoulos NA**, Pedram S, Midde K, Ciaraldi T, Henry RR, Ghosh P. Activation of G proteins by GIV-GEF is a pivot point for insulin resistance and sensitivity. *Mol Biol Cell*. 26:4209-23 (2015).

Lopez-Sanchez I, **Kalogriopoulos NA**, Lo I, Kabir F, Midde K, Wang H, Ghosh P. Focal adhesions are foci for tyrosine-based signal transduction via GIV/Girdin and G proteins. *Mol Biol Cell*. 26:4313-24 (2015).

Lopez-Sanchez I, Ma GS, Pedram S, **Kalogriopoulos NA**, Ghosh P. GIV/girdin binds exocyst subunit-Exo70 and regulates exocytosis of GLUT4 storage vesicles. *Biochem Biophys Res Commun*. 468:287-93 (2015).

Aznar N, **Kalogriopoulos NA**, Midde K, Ghosh P. Heterotrimeric G protein signaling via GIV/Girdin: Breaking the rules of engagement, space, and time. *Bioessays*. 38:379-93 (2016).

Ghosh P, Aznar N, Swanson L, Lo IC, Lopez-Sanchez I, Ear J, Rohena C, **Kalogriopoulos NA**, Joosen L, Dunkel Y, Sun N, Nguyen P, Bhandari D. Biochemical, Biophysical and Cellular Techniques to Study the Guanine Nucleotide Exchange Factor, GIV/Girdin. *Curr Protoc Chem Biol*. 8:265-298 (2016).

Aznar N, Ear J, Dunkel Y, Sun N, Satterfield K, He F, **Kalogriopoulos NA**, Lopez-Sanchez I, Ghassemian M, Sahoo D, Kufareva I, Ghosh P. Convergence of Wnt, growth factor, and heterotrimeric G protein signals on the guanine nucleotide exchange factor Daple. *Sci Signal*. 11(519) (2018).

* equal contribution

ABSTRACT OF THE DISSERTATION

Allosteric mechanisms and consequences of Gi activation via the Guanine-nucleotide Exchange Modulator, GIV

by

Nicholas A. Kalogriopoulos

Doctor of Philosophy in Biomedical Sciences

University of California San Diego, 2019

Professor Pradipta Ghosh, Chair

Heterotrimeric G proteins act as molecular switches that gate the flow of information from extracellular cues to intracellular effectors that control cell behavior. Canonically, G Protein-Coupled Receptors (GPCRs) activate G proteins by stimulating GDP to GTP exchange on the Gα subunit. It has also been extensively documented that G proteins can be non-canonically activated downstream of non-GPCRs, including Receptor Tyrosine Kinases (RTKs). RTKs are traditionally thought to transduce completely distinct signals via phosphorylation of downstream signaling adaptors, but increasing evidence suggests that these two signaling hubs cross-talk to

form an integrated signaling network. One recently discovered cross-talk mechanism is mediated via the novel guanine-nucleotide exchange modulator (GEM), GIV. GIV's C-terminus possesses a unique molecular make-up, containing an SH2-like domain and a GEM motif. The combination of these protein-binding modules allows the formation of RTK-GIV-Gαi complexes where GIV can activate Gαi in response to growth factor stimulation. Unlike canonical GPCR-mediated G protein signaling however, the structural basis for non-canonical GIV-mediated G protein activation, particularly downstream of growth factor stimulation, remained largely unknown. My dissertation work sought to fill this gap in knowledge by unravelling what binding of GIV may structurally do to Gαi to stimulate GDP release, as well as investigating alternative RTK-dependent and GIV-dependent mechanisms of G protein activation. Using structural, computational, and biochemical approaches, I revealed the structural and dynamical basis for GPCR-independent Gi activation by GEMs and found key similarities and differences between GPCR-dependent and -independent G protein activation, specifically identifying the hydrophobic core of Gαi as a common allosteric route toward GDP release utilized by both GPCRs and GEMs. Furthermore, I investigated an alternative but parallel GIV-dependent mechanism of RTK-mediated G protein activation via direct RTK phosphorylation of tyrosine residues within the interdomain cleft of Gαi. These RTK phosphorylated tyrosines are essential for Gαi activation and signaling in cells, and cancer mutation of these tyrosines results in hyperactive G protein. Taken together, my dissertation has formed a holistic understanding, at the atomic level, of the diverse allosteric mechanisms and consequences of non-canonical GIV-mediated G protein activation.

Chapter 1

Introduction: Cell Signaling Inside and Outside the Box

In its broadest sense, cell signaling, also referred to as signal transduction, is the transduction of one molecular event into another inside a cell. Transmembrane signaling refers to signals that are transmitted across the cell membrane. Cells use transmembrane signaling to communicate with their environment, sensing extracellular cues and transmitting those signals across the cell membrane to intracellular signaling pathways. This signal transduction allows cells to alter their behavior to respond to what is happening around them. Signal transduction involves a complex network of protein-protein interactions and feedback loops to coordinate the overall cellular response. This chapter will provide a general introduction to two of the major cell signaling hubs, G proteins and receptor tyrosine kinases, and discuss the cross-talk between them as well as their regulatory mechanisms.

1.1 Canonical Heterotrimeric G protein signaling

Heterotrimeric G proteins and G protein-coupled receptors

One of the major signaling pathways in eukaryotes is the heterotrimeric G protein signaling pathway. Heterotrimeric (or simply trimeric) G proteins work as molecular switches that control the flow of information from extracellular cues perceived at the cell surface to a wide array of intracellular effector proteins that control cell behavior (Gilman, 1987, Morris and Malbon, 1999). The molecular switch occurs when trimeric G proteins cycle between an inactive and active state in what is referred to as the G protein cycle (Figure 1.1). In the inactive state, G proteins are present as G$\alpha\beta\gamma$ trimers where the Gα subunit is bound to guanosine diphosphate (GDP); in the active state, the Gα subunit is bound to guanosine triphosphate (GTP) and is dissociated from the G$\beta\gamma$ heterodimer (Gilman, 1987, Morris and Malbon, 1999). Historically, the exchange of GDP for GTP is the key step in determining whether the G protein will be inactive or active, with GDP release being the rate limiting step of trimeric G protein activation (Ferguson et al., 1986).

Canonical heterotrimeric G protein signaling is mediated by the largest, most versatile, and most ubiquitous family of cell surface receptors, G protein-coupled receptors (GPCRs) (Gilman, 1987, Morris and Malbon, 1999, Lefkowitz, 2004, Wettschureck and Offermanns, 2005). There are about 1,000 GPCRs encoded by the human genome that sense and respond to sensory stimuli, hormones, neurotransmitters, and other paracrine factors (Bockaert et al., 2002, Fredriksson et al., 2003, Pierce et al., 2002, Rana and Insel, 2002, Vassilatis et al., 2003). Canonical G protein signaling is initiated at the plasma membrane when inactive trimers are activated by ligand-occupied G protein-coupled receptors (GPCRs). GPCRs are comprised

of seven transmembrane α-helical domains (7TM), an amino-terminal extracellular domain and an intracellular carboxyl terminus domain (Lefkowitz, 2004). GPCRs are receptor guanine nucleotide exchange factors (GEFs) for G proteins, meaning they promote the exchange of GDP for GTP on the Gα subunit and thereby activate the G protein (Ferguson et al., 1986). Upon activation, the monomeric GTP-bound Gα and the dissociated G$\beta\gamma$ dimer proceed to signal through various independent effectors. G protein signaling is terminated by the intrinsic GTPase activity of the Gα subunit, resulting in hydrolysis of the bound GTP into GDP and leading to reassociation of the Gα subunit with the G$\beta\gamma$ dimer.

Heterotrimeric G protein signaling is highly regulated. It is fine-tuned by a heterogeneous set of accessory proteins capable of modulating the activity of G proteins by various mechanisms (Figure 1.1). These accessory proteins include GTPase activating proteins (GAPs) that accelerate the intrinsic GTP hydrolysis rate of the G protein, guanine nucleotide dissociation inhibitors (GDIs) that inhibit the release of GDP from the Gα subunit, and non-receptor GEFs that again catalyze the exchange of GDP for GTP on the Gα subunit (Sato et al., 2006, Siderovski and Willard, 2005, Ross and Wilkie, 2000, Blumer et al., 2012, De Vries et al., 2000). In addition, canonical G protein signaling can also be regulated by desensitization and internalization of the GPCR (Kelly et al., 2008). In the classic model for this type of GPCR regulation, after agonist binding and GPCR activation, the third intracellular loop of the GPCR can be phosphorylated by G protein-couple receptor kinases (GRKs), which leads to desensitization through arrestin binding and receptor internalization (Stadel et al., 1983, Krupnick and Benovic, 1998, Pitcher et al., 1998, Ferguson, 2001, Willets et al., 2003, Benovic et al., 1986). Dephosphorylation and receptor recycling can resensitize GPCR signaling (Premont and Gainetdinov, 2007). The cumulative effect of these various regulatory mechanisms dictates the extent and duration of the

transduced G protein signal.

The evolution of numerous subtypes of G proteins and their modular architecture underlies the functional versatility of heterotrimeric G protein signaling (Wettschureck and Offermanns, 2005). The human genome contains 16 Gα, 5 Gβ, and 12 Gγ genes, with additional complexity provided by splice variants (McIntire, 2009). The Gα subunits define the basic properties of the heterotrimeric G proteins and are typically divided, largely based on sequence similarity, into four classes: Gαs, Gαi/Gαo, Gαq/Gα11, and Gα12/Gα13 (Wettschureck and Offermanns, 2005, Morris and Malbon, 1999, Wilkie et al., 1992). Gαs and Gαi regulate levels of the second messenger cAMP via stimulation or inhibition, respectively, of its producer adenylyl cyclase (McIntire, 2009). Gαq/Gα11 activates phosphoinositide-dependent phospholipase C (PLC), which produces the second messengers diacylglycerol and inositol trisphosphate, and Gα12/13 subunits signal to small monomeric G protein-dependent pathways (Milligan and Kostenis, 2006). $\beta\gamma$-dimers can regulate various ion channels (Wettschureck and Offermanns, 2005), as well as particular isoforms of adenylyl cyclase, PLC (Exton, 1996, Sunahara et al., 1996), and phosphoinositide-3-kinase (PI3K) (Vanhaesebroeck et al., 2001). With a few exceptions, the effector functions of the different $\beta\gamma$-combinations do not dramatically differ (Clapham and Neer, 1997). Of note, many individual GPCRs can couple to several G protein classes and respond to multiple ligands.

The incredibly large number of different ligand-GPCR-G protein combinations emphasizes the functional diversity and versatility that can arise from canonical G protein signaling. Thus, it is not surprising that GPCR/G protein signaling has been shown to play important roles in virtually every physiologic and pathologic process. Dysregulation of G protein signaling has been implicated in cancer, fibrosis, neurodegeneration, diabetes, and cardiovascular diseases,

among many other diseases (Schoneberg et al., 2004, Insel et al., 2007, Zhao et al., 2016, Hauser et al., 2018, Stoy and Gurevich, 2015, Wang et al., 2018). Accordingly, efforts to target GPCR/G protein pathways have been rewarded with tremendous success: GPCRs are targeted by about 40% of currently marketed drugs (Hopkins and Groom, 2002). Despite such success, continued development of new and/or improved therapeutics will depend on increased understanding of the structural mechanisms of GPCR and G protein function and activation.

Structural mechanism of GPCR-mediated G protein activation

Due to the long history and in-depth understanding of its importance in health and disease, the molecular mechanism and structural determinants of G protein activation and action have been a top priority in the field for decades, yielding over 70 publicly available structures in various conformations and complex compositions. X-ray crystallography has been the technique of choice to gain insights into the structural working of heterotrimeric G proteins. Early crystal structures of GDP-bound and GTP-bound (more accurately GTPγS-bound or GDP-AlF$_4^-$-bound) trimeric G proteins not only elucidated the overall structure of G proteins, but also quickly revealed surprisingly small differences between the inactive and active G protein states (Cabrera-Vera et al., 2003). The Gα subunit is comprised of two distinct domains, a GTPase or Ras-like domain (named based on its structural similarity to the Ras superfamily of small monomeric G proteins) and an all α-helical domain, with the nucleotide binding pocket residing within the interdomain cleft between the two domains. The GTPase domain is responsible for most of the nucleotide binding affinity, containing the GTPase G1-G5 binding motifs (Anand et al., 2006, Leipe et al., 2002). The inactive GDP-bound and active GTP-bound G protein conformations only differ in the position of three flexible regions, designated Switches I-III, which become more

rigid and well-ordered in the GTP-bound state (Cabrera-Vera et al., 2003, Sprang, 2016). In both the inactive and active conformations, Switch II forms a partial helix that is integral for its nucleotide-dependent interaction with G$\beta\gamma$, G protein modulators, and various effectors (Wall et al., 1995, Goricanec et al., 2016).

Because of the striking similarity between the inactive and active G protein structures, the mechanism of nucleotide exchange and the key determinants of G protein activation had challenged the field for decades. In the past 8 years however, the structural basis for GPCR-dependent G protein activation has been revealed by a series of landmark structural studies (Rasmussen et al., 2011, Koehl et al., 2018, Carpenter et al., 2016, Draper-Joyce et al., 2018, Dror et al., 2015). These studies demonstrated that GPCR-mediated nucleotide exchange proceeds through an intermediate, highly unstable nucleotide-free step; X-ray crystallography and cryo-EM structures of GPCRs bound to nucleotide-free G proteins have only been solved with the use of antibodies or nanobodies that trap and stabilize this transition state (Rasmussen et al., 2011, Zhang et al., 2017, Qi et al., 2019, Kang et al., 2018).

Other structural rearrangements observed in these ground-breaking structural studies confirm previous spectroscopic and biochemical data (Erlandson et al., 2018). Upon GPCR engagement, the carboxy-terminal α5 helix of the Gα subunit undergoes a rigid-body translation and rotation along its axis. This α5 motion is linked to G protein activation and domain opening; domain opening refers to the separation of the GTPase domain from the α-helical domain (Oldham et al., 2006). Domain opening exposes the nucleotide binding pocket (Van Eps et al., 2011), however molecular dynamics (MD) simulation studies suggest that domain opening is not sufficient to stimulate nucleotide release (Dror et al., 2015).

Insights into the precise mechanism of how GPCRs alter the GDP binding pocket and

stimulate GDP release came from the cumulative insights gained from structural, biochemical, and computational studies (Dror et al., 2013, Rasmussen et al., 2011, Van Eps et al., 2018, Gurevich and Gurevich, 2017, Dijkman et al., 2018, Latorraca et al., 2017). Collectively, these studies demonstrated that one of the key mechanisms of G protein activation by GPCRs involves perturbation of the so-called hydrophobic core of the Gα GTPase domain; the hydrophobic core is formed between the β2-β3 strands and the α1 and α5 helices (Kaya et al., 2014, Kaya et al., 2016). Displacement of the C-terminal α5 helix and insertion of the GPCRs intracellular loop 2 disturbs hydrophobic interactions with the β2-β3 strands and α1 helix; the resultant conformational changes are thought to be transmitted from α5 via β2-β3/α1 to Switch I and the phosphate binding loop, altering the GDP binding pocket, decreasing GDP affinity, and triggering GDP release (Kaya et al., 2014, Kaya et al., 2016).

1.2 Receptor tyrosine kinases and their cross-talk with GPCR/G proteins

Classical receptor tyrosine kinase signaling

Another major signaling pathway in eukaryotes is tyrosine-based signaling via receptor tyrosine kinases. Tyrosine phosphorylation is a highly regulated post-translational modification mediated by tyrosine kinases (Hubbard and Miller, 2007, Jin and Pawson, 2012, Hunter, 1995). Tyrosine kinases (TKs) are enzymes that catalyze the transfer of the γ-phosphate of adenosine triphosphate (ATP) to the hydroxyl group of tyrosine residues in protein substrates (Hunter, 2015). Receptor tyrosine kinases (RTKs) are transmembrane proteins on the surface of cells that bind to a subset of extracellular growth factors as ligands and transduce that signal to intra-

cellular signaling proteins (Hubbard and Miller, 2007). Humans have 58 known RTKs, which fall into 20 subfamilies (Robinson et al., 2000). All RTKs consist of an extracellular ligand-binding domain, a single transmembrane domain, and an intracellular region harboring a catalytic protein tyrosine kinase domain (Hubbard and Miller, 2007).

In general, signaling through RTKs is initiated by ligand-induced receptor dimerization (Ullrich and Schlessinger, 1990, Lemmon and Schlessinger, 2010). Dimerization activates the tyrosine kinase domain of the RTK and results in autophosphorylation of multiple tyrosines on its cytoplasmic tail. It should be noted that some RTKs, for example the insulin receptor, are expressed on the cell surface as dimers even in the absence of ligand, and in these cases ligand binding induces conformational changes in the dimeric receptor that activates its tyrosine kinase domains (Ward et al., 2007). The autophosphorylated tyrosines then serve as docking sites for the assembly and activation of various intracellular signaling proteins (Figure 1.2; Ullrich and Schlessinger, 1990, Lemmon and Schlessinger, 2010). Recruited signaling proteins include enzymes, such as the non-receptor TK c-src and PLCγ, as well as other adaptor/scaffolding proteins; these proteins typically bind to the activated RTK using Src homology-2 (SH-2) or phosphotyrosine-binding (PTB) domains that recognize phosphotyrosines (Pawson et al., 2001, Pawson, 2004, Jin and Pawson, 2012). Subsequent phosphorylation and activation of these proteins leads to the initiation of downstream signaling pathways, such as the MAP kinase and PI3K signaling pathways (Hubbard and Miller, 2007, McCain, 2013). Protein tyrosine phosphatases (PTPs), such as Src homology-2 domain-containing phosphatase-1 (SHP-1) and PTP1B, terminate RTK signaling by dephosphorylating the RTK autophosphorylation sites (Pawson et al., 2001, Pawson, 2004, Ledda and Paratcha, 2007, Kovalenko et al., 2000, Ostman et al., 2006, Persson et al., 2004).

RTK signaling has been shown to be critically important in a host of cellular programs, including cell proliferation, differentiation, migration, and survival (Ullrich and Schlessinger, 1990), and aberrant RTK signaling is known to contribute to or directly cause a wide variety of human diseases, including many developmental disorders and cancers (Takeuchi and Ito, 2011, Regad, 2015). In fact, deregulation of approximately fifty percent (30 of 58) of RTKs are associated with human tumors (Blume-Jensen and Hunter, 2001). Small molecule inhibitors and monoclonal antibodies targeting specific RTKs have had some clinical success treating cancers, however drug-resistant mutations continue to present challenging hurdles toward achieving sustained, long-term benefits (Gupta and El-Rayes, 2008, Esteva, 2004).

RTK-GPCR/G protein signaling cross-talk

Despite being distinct signaling pathways, it has been widely demonstrated that the RTK and GPCR/G protein pathways cross-talk to form an integrated signaling network; this signal cross-talk is referred to as transactivation (Lowes et al., 2002, Piiper and Zeuzem, 2004, Natarajan and Berk, 2006, Shah and Catt, 2004, Di Liberto et al., 2019). This transactivation has been shown to occur in both directions, i.e. a signal can be initiated in either pathway and then can access and be transduced through the other.

Transactivation of RTKs by GPCRs can be mediated via RTK ligand-dependent and ligand-independent mechanisms (Daub et al., 1996, Luttrell et al., 1999, Schafer et al., 2004). GPCRs can indirectly activate RTKs through a ligand-dependent triple-membrane-passing mechanism. In this mechanism, first an extracellular ligand binds and activates a GPCR, which transduces the signal across the plasma membrane (first membrane pass). Second, the transduced signal leads to the activation of membrane-bound matrix metalloproteases (MMPs) that

trigger the proteolytic cleavage of an extracellular RTK pro-ligand, generating a mature RTK ligand (second membrane pass). Finally, this mature RTK ligand binds and activates the RTK, which again transduces the signal across the plasma membrane to activate downstream signaling cascades (third membrane pass; Daub et al., 1996, Ohtsu et al., 2006, Prenzel et al., 1999). Ligand-independent transactivation, on the other hand, occurs through direct physical interaction between the GPCR and the RTK; physical association between the two receptors can result in allosteric effects that change the ligand recognition, effector recruitment, and/or trafficking of either receptor, all of which can alter signaling outputs (Guidolin et al., 2015).

In contrast, RTKs can activate G proteins as well, again by both GPCR ligand-dependent and ligand-independent mechanisms. Similar to transactivation of RTKs by GPCRs, transactivation of G proteins by RTKs can occur via production of GPCR-ligands (ligand-dependent) and physical interaction with GPCRs (ligand-independent) as previously discussed (Sun et al., 1995, Poppleton et al., 1996). Moreover, phosphorylation of GPCRs by RTKs is thought to be another regulatory mechanism for cross-talk from RTKs to G proteins (Marty and Ye, 2010). Such phosphorylation may alter the extent and duration of GPCR signaling by affecting G protein binding, arrestin binding, and/or receptor trafficking.

In addition, transactivation of G proteins by RTKs in a completely GPCR-independent manner has been suggested. There is some evidence for direct interaction between RTKs and G proteins (Patel, 2004). For example, EGFR may bind Gαi and Gαs through its juxtamembrane region to directly regulate G protein activity and function (Sun et al., 1995, Nair et al., 1990, Poppleton et al., 1996, Sun et al., 1997). Other studies have suggested similar interactions for the insulin receptor and IGF-I with various G proteins (Zick et al., 1986, O'Brien et al., 1987, Krupinski et al., 1988, Imamura et al., 1999, Okamoto et al., 1990, Okamoto et al., 1991),

although in many of these studies direct interaction between the RTK and G protein was not demonstrated.

G protein subunit phosphorylation as a regulatory mechanism

The field's growing understanding of the close interplay between kinases (both Ser/Thr and Tyr kinases) and G proteins within these complex signaling networks has spurred the identification of phosphorylation sites on G protein subunits that act to regulate G protein activity (Chakravorty and Assmann, 2018). Early subunit phosphorylation studies largely focused on kinases known to be downstream of classical G protein signaling, including the serine/threonine kinases protein kinase A (PKA) and protein kinase C (PKC). These studies identified phosphorylation sites on both the GTPase and helical domains of the G protein that regulate G protein function (Manganello et al., 2003, Wang et al., 1999, Glick et al., 1998, Gu et al., 2003, Chu et al., 2010, Navarro et al., 2007, Shi et al., 2007a, Shi et al., 2007b).

Although there are fewer examples, tyrosine phosphorylation has also been demonstrated to be a regulatory mechanism for mammalian Gα signaling (Chakravorty and Assmann, 2018). For example, upon GPCR stimulation, a C-terminal tyrosine (Y356) that is within the GPCR binding regions of Gαq and Gα11, has been shown to be phosphorylated and play a role in Gα coupling to both GPCRs and effectors, thereby regulating signal reception from the GPCR as well as downstream signaling (Umemori et al., 1997, Liu et al., 1996). Interestingly, this is not true for coupling of Gαq and Gα11 to all GPCRs as this tyrosine phosphorylation appears to be necessary for Gαq and Gα11 coupling to metabotropic glutamate, but not for Gαq and Gα11 coupling to thrombin receptors (Umemori et al., 1997).

The non-receptor tyrosine kinase c-src has been shown to phosphorylate and regulate

the activity of several G proteins, including Gαi1, Gαi2, Gαi3, Gαo, Gαt, and Gαs (Hausdorff et al., 1992). c-src phosphorylation of Gαs was the most rigorously investigated. c-src phosphorylates two tyrosines in Gαs, Y37 and Y391 (Moyers et al., 1995); Y37 is on the N-terminal helix near the site of G$\beta\gamma$ binding, while Y391 aligns with Y356 in Gαq. The individual effects of these two tyrosines was not investigated, but the combined tyrosine phosphorylation on Gαs was shown to stimulate GTPγS binding and receptor-stimulated GTP hydrolysis (Hausdorff et al., 1992). It has been speculated that c-src phosphorylation on the other Gα subunits may similarly regulate G protein activity.

In addition, studies have also suggested that some receptor tyrosine kinases can directly phosphorylate G protein subunits as well. Direct phosphorylation of G proteins by RTKs has been suggested in contexts where there was already evidence for direct interaction between the RTK and the G protein, as in the cases discussed earlier (Poppleton et al., 2000, Patel, 2004). These studies propose that, following direct interaction, EGFR may phosphorylate Gαs on two tyrosine residues and, though these tyrosines have not been identified, their phosphorylation may affect G protein activity (Poppleton et al., 1996). Such phosphorylation apparently does not occur in the case of EGFR and Gαi even though EGFR can also directly interact with Gαi (Liang and Garrison, 1991, Nair et al., 1990, Poppleton et al., 1996, Sun et al., 1997). Similar reports have suggested that the insulin receptor may phosphorylate Gαi and Gαo, as well (O'Brien et al., 1987, Krupinski et al., 1988). However, in-depth mechanisms into how these phosphorylations occur and function in cells are lacking, and thus the phenomenon as a whole has remained controversial.

1.3 GIV is a new link between RTKs and G proteins

Non-canonical G protein signaling via GIV

Adding to the intricate interplay between RTKs and G proteins is a recently discovered, non-canonical set of cytosolic G protein modulators called guanine-nucleotide exchange modulators (GEMs) (Gupta et al., 2016, Ghosh et al., 2017). GEMs are cytosolic proteins that uniquely act as non-receptor GEFs to activate Gαi and as guanine-nucleotide dissociation inhibitors (GDIs) to inhibit Gαs, all using the same 31 aa evolutionarily conserved GEM motif (Gupta et al., 2016). The first and most well-studied member of the GEM family is Gα-Interacting Vesicle associated protein (GIV or Girdin).

GIV is a large (about 250 kDa) multi-modular signal transducer that contains various domains that facilitate protein-protein interactions including a microtubule-binding hook domain, an oligomerization coiled-coil domain, a nucleotide-independent Gα-binding domain, a phosphatidylinositol-4-phosphate (PI4P)-binding domain, a nucleotide-dependent GEM motif, a phosphotyrosine-binding SH-2-like domain, and protein kinase B (AKT)- and actin- binding domains (Figure 1.3; Aznar et al., 2016, Lin et al., 2011, Ghosh et al., 2008, Garcia-Marcos et al., 2011, Garcia-Marcos et al., 2010, Garcia-Marcos et al., 2009, Ghosh, 2015). GIV's unique combination of domains enables transactivation of G proteins in response to a wide variety of stimuli by engaging a diverse array of receptors, including GPCRs, integrins, and RTKs (Garcia-Marcos et al., 2009, Ghosh et al., 2010).

Its ability to modulate G protein activation downstream of many different receptors places GIV as a key signal integrator within large signaling networks (Figure 1.4). Multiple studies have interrogated the impact of GIV-dependent G protein activation on downstream signaling

pathways in cell lines expressing a GIV mutant (F1685A) that is selectively GEM deficient and cannot bind G protein (Ghosh, 2015). These studies found that the signaling network triggered in cells expressing wild-type GIV is a mirror image of the network in cells expressing the GEM-deficient GIV mutant, i.e. signals enhanced in cells that are GEM-proficient are suppressed in cells that are GEM-deficient, and vice versa. Furthermore, cells can alter (increase or decrease) the levels of GIV mRNA/protein or selectively modulate GIV's GEM activity to modulate growth factor signaling pathways across a range of intensities (Lopez-Sanchez et al., 2013), and thus our group described GIV as a cellular rheostat for signal transduction (Ghosh et al., 2011).

Consistent with its ability to integrate signals downstream of multiple receptors, GIV modulates diverse cellular processes, including cell motility, golgi structure and secretory function, autophagy, endosome maturation, cell survival, cell polarity, cell division, endo- and exocytosis, and cell-cell junctions (Garcia-Marcos et al., 2011, Garcia-Marcos et al., 2010, Garcia-Marcos et al., 2009, Lo et al., 2015, Beas et al., 2012, Lopez-Sanchez et al., 2014, Sasaki et al., 2015, Lopez-Sanchez et al., 2015, Ichimiya et al., 2015). Furthermore, GIV-dependent signaling has been implicated in a number of pathophysiologic conditions, including organ fibrosis, wound healing, nephrotic syndrome, insulin resistance, and cancers, among others (Leyme et al., 2015, Bhandari et al., 2015, Lopez-Sanchez et al., 2014, Ma et al., 2015, Wang et al., 2015, Hartung et al., 2013). In every case where it has been tested, GIV's ability to regulate these diverse processes and diseases is dependent its ability to bind and modulate G proteins downstream of specific cell surface receptors (Garcia-Marcos et al., 2011, Garcia-Marcos et al., 2010, Garcia-Marcos et al., 2009, Lo et al., 2015, Beas et al., 2012, Lopez-Sanchez et al., 2014, Sasaki et al., 2015, Lopez-Sanchez et al., 2015).

GIV-mediated G protein activation downstream of RTKs

Although GIV can activate G proteins downstream of multiple different receptors, the molecular mechanisms that govern how GIV couples G proteins to receptors are best understood in the context of RTKs. GIV has been shown to directly bind the tyrosine-phosphorylated intracellular tails of EGFR, insulin receptor β, and VEGFR2, suggesting a conserved and general mechanism of binding for other RTKs (Lin et al., 2014, Ghosh et al., 2010). Structural insights into RTK-GIV interactions have only recently been elucidated (Lin et al., 2014). A stretch of approximately 110 aa in the C-terminal domain of GIV appears to display structural plasticity, i.e. it is capable of transitioning from a disordered state to an SH2-like folded domain capable of binding phosphotyrosine ligands. When a critical residue in this domain is mutated, binding to phosphotyrosines is lost and GIV no longer transduces signals downstream of RTKs, even in the presence of an intact GEM motif (Lin et al., 2014). Taken together, these findings delineate a signal transduction mechanism in which trimeric G proteins become activated by RTKs via GIV; an RTK-GIV-G protein complex forms when autophosphorylated RTK tails recruit the SH2-like domain of GIV, and GIV in turn recruits and activates G proteins via its GEM motif (Figure 1.5).

Furthermore, upon RTK ligand stimulation, two tyrosines within the C-terminus of GIV, Y1764 and Y1798, are phosphorylated by the RTK (Lin et al., 2011). These phosphorylated tyrosines enable the direct binding of GIV to p85α, a regulatory subunit of PI3K, by creating docking sites for the SH2 domains of p85α (Lin et al., 2011). This interaction stabilized receptor association with PI3K and enhanced PI3K activity at the plasma membrane (Lin et al., 2011). Downstream, this results in enhanced activation of AKT and actin remodeling that ultimately triggers cell migration (Lin et al., 2011). Importantly, tyrosine phosphorylation of GIV did not affect the GIV-Gαi interaction, and tyrosine phosphorylation of GIV and its downstream signaling

effects did not depend on GIV's GEM function (Lin et al., 2011).

Interestingly, FRET studies in living cells revealed that although the extent of G protein activation downstream of RTKs and GPCRs appear similar, the spatiotemporal dynamics of non-canonical G protein activation by GIV represents a clear deviation from the dynamics of canonical G protein signaling that is triggered by GPCRs. Canonical signal transduction via trimeric G proteins is spatially and temporally restricted, i.e. triggered exclusively at the PM by agonist activation of GPCRs via a process that completes within a few hundred milliseconds (Lohse et al., 2008); this temporal regulation of GPCR signaling is largely mediated by G protein-coupled receptor kinases (GRKs) (Ribas et al., 2007) and by β-arrestins (DeWire et al., 2007). Non-canonical transactivation of trimeric G proteins by RTKs via the GIV-CT platform has distinctive features– 1) can occur at the PM and on internal membranes discontinuous with the PM (Garcia-Marcos et al., 2011, Lo et al., 2015), and 2) can continue for prolonged periods of time (several minutes) (Midde et al., 2015). How these distinct GIV-mediated signaling dynamics are achieved in cells has remained incompletely understood.

To better understand how GIV-mediated G protein activation is achieved in cells, multiple studies set out to elucidate the structural basis for GIV binding to G protein (Garcia-Marcos et al., 2011, Garcia-Marcos et al., 2010, Garcia-Marcos et al., 2009). In these studies, a combination of homology modeling and site-directed mutagenesis provided some structural insights into the assembly of the GIV-Gαi complex (Garcia-Marcos et al., 2009, Garcia-Marcos et al., 2012). These revealed that conserved hydrophobic residues that align on one side of a short aliphatic helix in GIV engage with a hydrophobic cleft between the switch II and the α3 helix of Gαi, a mechanism distinct from how Gα subunits engage with GPCRs (Rasmussen et al., 2011). This proposed mode of binding seems to explain GIVs inability to bind active Gαi because the con-

formation of the switch II helix in Gαi-GTP occludes the predicted binding site (Coleman et al., 1994). Furthermore, the proposed GIV-binding interface on Gαi shares significant overlap with the binding interface for G$\beta\gamma$, potentially explaining GIV's ability to compete with and displace G$\beta\gamma$ from Gαi (Garcia-Marcos et al., 2009). How much of GIV's action is mediated by G$\beta\gamma$ subunits that are physically displaced from Gαi versus those that are mediated by activation of Gαi remains unexplored.

1.4 Outline of the dissertation

The insights gained within the past decade has shaped a paradigm of GIV-dependent non-canonical G protein signaling by receptors that are typically not believed to signal via G proteins. Despite these insights, it is clear that a lot remains unknown. GIV-mediated G protein activation downstream of RTKs remains incompletely understood. Although homology modeling has proven insightful thus far, obtaining further structural insights into how GIV engages with Gα-subunits is an urgent and unmet need. It is still unclear how exactly GIV binding to Gαi stimulates nucleotide exchange and activates the G protein. Such insights are expected to greatly facilitate the development of small molecules that can selectively target the GIV-Gαi interface. In addition, parallel mechanisms of RTK-dependent, GIV-dependent G protein activation in the context of the RTK-GIV-G protein complex demand further investigation.

In the rest of the dissertation, I will describe my Ph.D. work and how it has focused on answering some of these remaining mysteries regarding RTK-dependent, GIV-mediated G protein activation. I will describe my main work investigating the structural basis of GPCR-independent GIV-mediated activation of Gαi (Chapter 2) and touch on my work investigating the deregulation of GIV-dependent direct phosphorylation of Gαi by RTKs within the RTK-GIV-Gαi

ternary complex (Chapter 3). I will conclude by discussing where the field has come and where it is going, my thoughts on what I have accomplished throughout my dissertation work, and what I think are the remaining unmet needs in understanding non-canonical GIV-dependent G protein signaling (Chapter 4).

Acknowledgements

This research was funded by NIH (R01CA160911 and DK099226), as well as an NIH predoctoral fellowship (F31 CA206426) and T32 training grants T32CA067754 and T32DK007202.

Chapter 1 in part is a reprint of material published in: Aznar N, **Kalogriopoulos NA**, Midde K, Ghosh P. 2016. “Heterotrimeric G protein signaling via GIV/Girdin: Breaking the rules of engagement, space, and time.” *Bioessays.* 38:379-93.

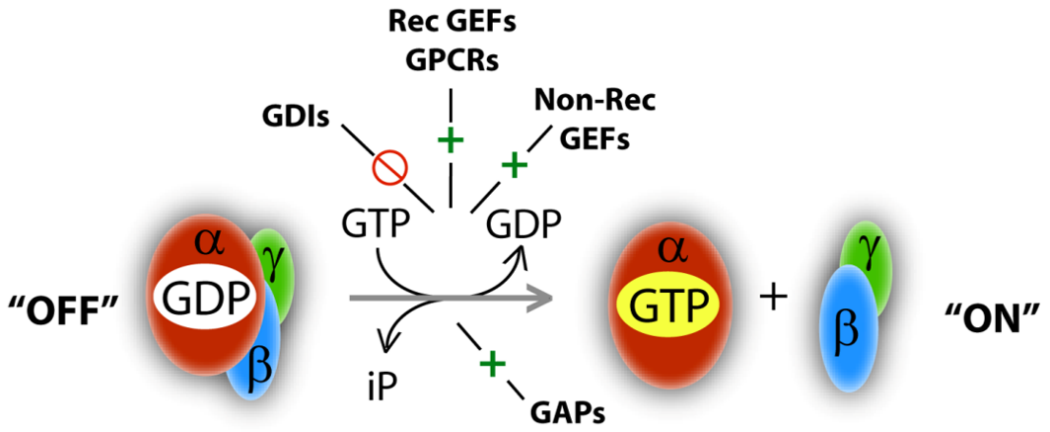

Figure 1.1: The heterotrimer G protein cycle. Schematic displaying the cycling between the inactive GDP-bound trimeric and active GTP-bound dissociated G protein states. Regulators of G protein activity and their effects are also shown.

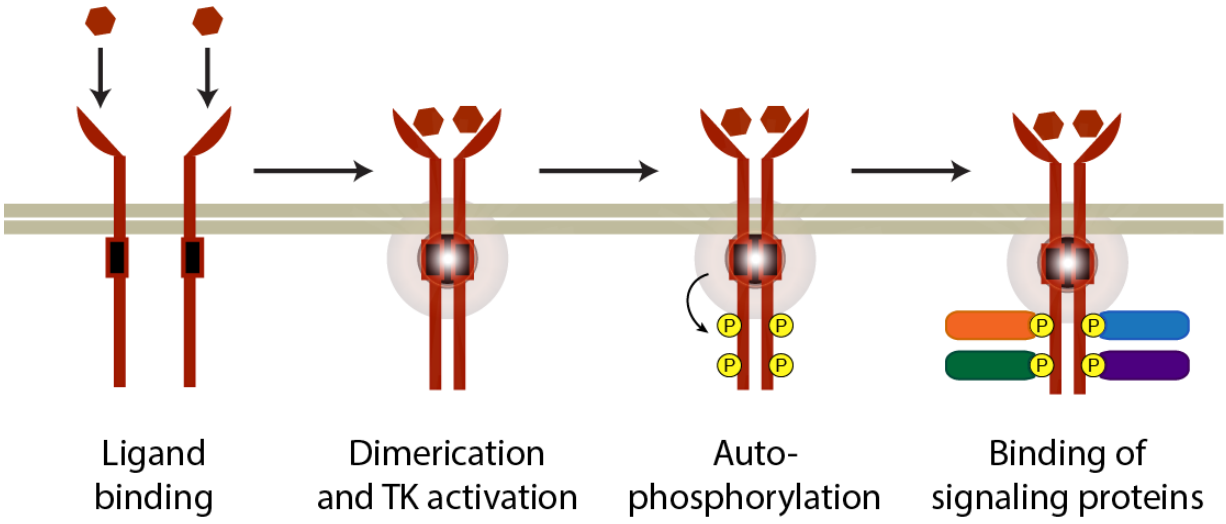

Figure 1.2: Receptor tyrosine kinase activation. Schematic displaying the key events during receptor tyrosine kinase activation.

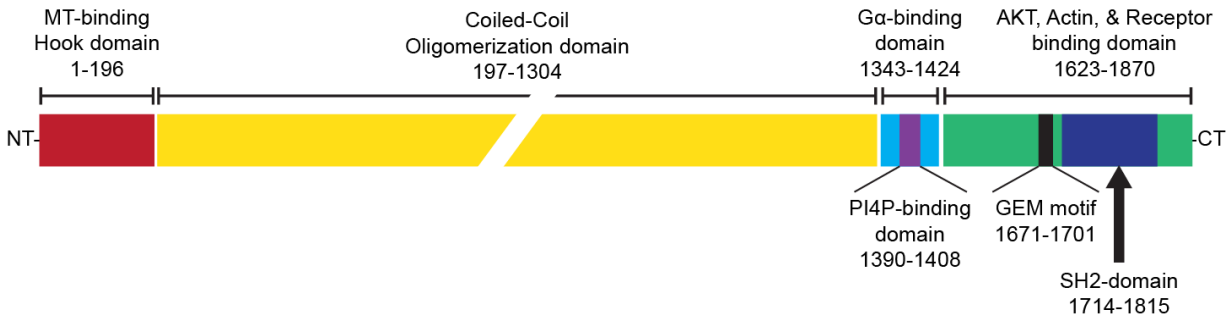

Figure 1.3: GIV is a large multi-domain protein. Schematic displaying the various distint domains within GIV that promote protein-protein interactions.

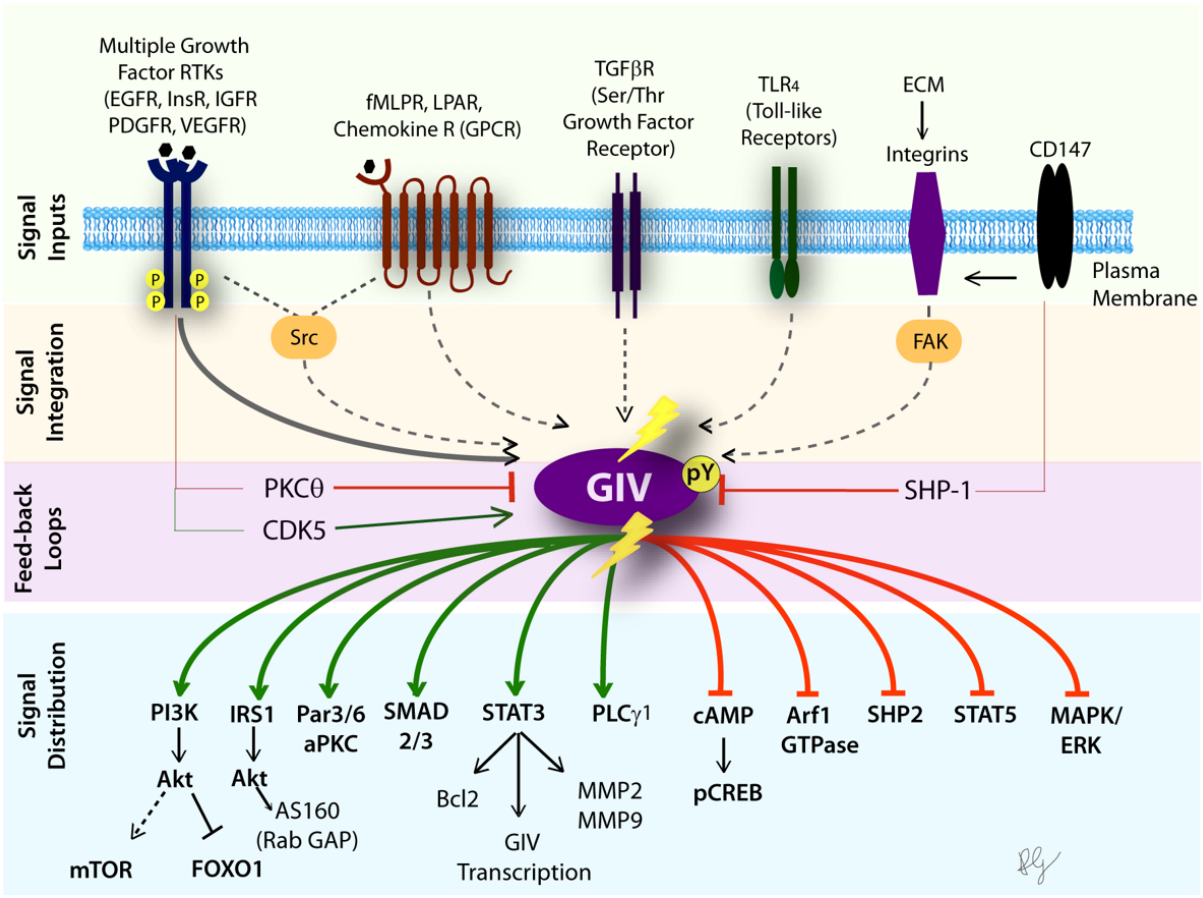

Figure 1.4: GIV regulates a broad signaling network. Schematic presenting GIV's role in many signal transduction pathways downstream of diverse cell surface receptors.

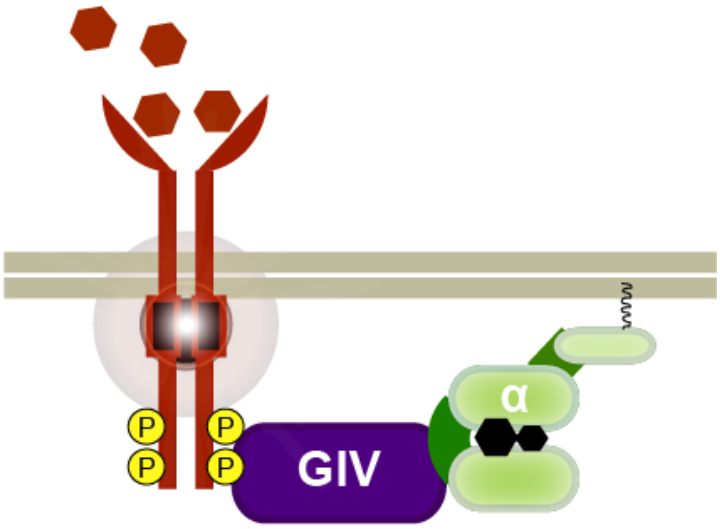

Figure 1.5: The RTK-GIV-Gαi complex. Schematic showing how GIV is able to simultaneously bind activated RTKs and Gα subunits to form RTK-GIV-Gαi complexes.

Chapter 2

Structural basis for GPCR-independent activation of heterotrimeric Gi proteins

Heterotrimeric G proteins are key molecular switches that control cell behavior. The canonical activation of G proteins by agonist-occupied G protein-coupled receptors (GPCRs) has recently been elucidated from the structural perspective. In contrast, the structural basis for GPCR-independent G protein activation by a novel family of Guanine-nucleotide Exchange Modulators (GEMs) remains unknown. Here, we present a 2.0 Å crystal structure of Gαi in complex with the GEM motif of GIV/Girdin. Nucleotide exchange assays, molecular dynamics simulations, and hydrogen-deuterium exchange experiments demonstrate that GEM binding to the conformational switch II causes structural changes that allosterically propagate to the hydrophobic core of the Gαi GTPase domain. Rearrangement of the hydrophobic core appears to

be a common mechanism by which GPCRs and GEMs activate G proteins, although with different efficiency. Atomic-level insights presented here will aid structure-based efforts to selectively target non-canonical G protein activation.

2.1 Introduction

Heterotrimeric G proteins act as molecular switches that gate the flow of information from extracellular cues to intracellular effectors that control cell behavior (Gilman, 1987, Morris and Malbon, 1999). Canonically, heterotrimeric G protein signaling is initiated at the plasma membrane where agonist-bound G protein-coupled receptors (GPCRs) trigger the dissociation of GDP from G$\alpha\beta\gamma$ trimers and release of G$\beta\gamma$ subunits; in other words, GPCRs serve as guanine nucleotide exchange factors (GEFs) (Gilman, 1987). This signal is fine-tuned by GTPase activating proteins (GAPs), guanine-nucleotide dissociation inhibitors (GDIs), and other accessory proteins (Siderovski and Willard, 2005).

Among these accessory proteins, the recently delineated family of guanine-nucleotide exchange modulators, or GEMs (Aznar et al., 2016, Ghosh et al., 2017), stands out due to their ability to modulate heterotrimeric G proteins independently of GPCRs. GEMs are cytosolic proteins that uniquely act as GEFs for Gαi and as GDIs for Gαs, all using the same evolutionarily conserved GEM motif (Garcia-Marcos et al., 2009, Gupta et al., 2016). The motif was initially identified based on homology to the synthetic peptide KB752 that can bind and activate Gαi (Johnston et al., 2005); however, the motif has since been found in several naturally occurring proteins (Ghosh et al., 2017). The ability of GEMs to activate Gαi in live cells downstream of diverse classes of receptors has been demonstrated by various approaches: dissociation of G$\beta\gamma$ subunits from Gαi was shown using FRET- and BRET-based reporters (Ma et al., 2015,

Midde et al., 2015, Parag-Sharma et al., 2016), Gαi activation by conformation-specific antibodies (Lopez-Sanchez et al., 2014), and reduction in cellular cAMP by radioimmunoassay (Lopez-Sanchez et al., 2014). These cited studies also demonstrated that the spatiotemporal patterns of GEM-mediated Gαi signaling are remarkably distinct from those triggered by GPCRs (Aznar et al., 2016). Furthermore, published work has provided insight into GEM biology and demonstrated translational relevance of dysregulated GEM signaling in disease (Ghosh, 2015), including cancer, organ fibrosis, and diabetes.

Because heterotrimeric G proteins are expressed in virtually all cell and tissue types, and are involved in most physiologic and pathologic processes, the molecular mechanism and structural determinants of G protein activation and action have been a top priority in the field, yielding over 70 publicly available structures in various conformations and complex compositions. The structural basis for GPCR-dependent G protein activation had challenged the field for decades but was revealed in the past 8 years by a series of landmark structural studies (Rasmussen et al., 2011, Koehl et al., 2018, Carpenter et al., 2016, Draper-Joyce et al., 2018, Dror et al., 2015). These studies have demonstrated that one of the key mechanisms of G protein activation by GPCRs involves perturbation of the so-called hydrophobic core (Kaya et al., 2014, Kaya et al., 2016) of the Gα GTPase domain, which is mediated by displacement of the C-terminal α5 helix and insertion of the GPCRs intracellular loop 2 (Rasmussen et al., 2011, Koehl et al., 2018, Carpenter et al., 2016, Draper-Joyce et al., 2018, Dror et al., 2015).

In contrast to these insights, the structural basis of GPCR-independent G protein activation has remained elusive. The present study reveals, at an atomic resolution, the structural and dynamical basis for Gαi activation by GEMs. These insights would be invaluable for efforts of selective pharmacological targeting of GEMs to treat GEM-driven diseases.

2.2 Results

Unique from GPCRs, GIV-GEM binds and stabilizes Switch II of Gαi

The first and most well-studied member of the GEM family is Gα-Interacting Vesicle-associated protein or GIV/Girdin. GIV is a large, multi-domain (Figure 2.1a) signal transducer that mediates G protein activation downstream a variety of cell-surface receptors to modulate diverse cellular processes (Garcia-Marcos et al., 2015, Aznar et al., 2016). GIV-dependent signaling has been implicated in a number of pathophysiologic conditions, including diabetes, fibrosis, and cancer (Aznar et al., 2016).

Here, the 31 aa GEM motif of GIV/Girdin (aa 1671-KTGSPGSEVVTLQQFLEESNKLTSVQIKSSS-1701) was co-crystallized with GDP-bound rat Gαi3 (henceforth Gαi:GDP). In the crystallization construct, the flexible 25-aa long N-terminal helix of Gαi was deleted as done previously (Johnston et al., 2005), and replaced by a His-tag followed by a short linker (SSGLVPRGSHM; Figure 2.1b, henceforth referred to as His-tag linker). The structure was determined to 2.0 Å resolution (Figure 2.1, Figure 2.2a-b).

The structure demonstrated that GIV-GEM binds at the typical effector binding interface: the hydrophobic pocket between Sw-II and the α3-helix of Gαi (Figure 2.2a-b). By forming a short anti-parallel β-sheet with Sw-II residues Q204-R208 (Flock et al., 2015), the peptide stabilizes Sw-II in a unique elevated conformation (Figure 2.2b-d). Key polar contacts at the interface include hydrogen-bonding of GIV E1678 and E1688 to Gαi R208, around which the peptide folds in a loop-helix conformation, and a hydrogen bond from GIV Q1683 with Gαi Q204, a residue known for its role in GTP-hydrolysis (Sprang, 2016). The interface also features hydrophobic packing of GIV's F1685 against W211, I212, F215, and W258 of Gαi, consistent

with the established role of F1685 as the key interaction determinant (Garcia-Marcos et al., 2009). Residues L1682-N1690 of GIV form an α-helix that packs favorably across the α3-helix of Gαi (Figure 2.2b-d).

A number of Gαi residues engaged by GIV-GEM are shared by G$\beta\gamma$ and GoLoco GDIs (Figure 2.2d-g, Figure 2.3): e.g. R208 is important for RGS14, and K209 is critical for G$\beta\gamma$. These findings provide insight into the mutual exclusivity of GIV and G$\beta\gamma$, or GIV and Goloco GDI, binding to Gαi (Garcia-Marcos et al., 2009, Garcia-Marcos et al., 2011a). Although paralleling the phenomenon of G$\beta\gamma$ displacement by GPCRs, this mutual exclusivity has a different basis, as in the case of GIV, it is not mediated by nucleotide exchange. Instead, the plausible mechanism of GIV-G$\beta\gamma$ competition is similar to that employed by Goloco GDIs and involves GIV capturing the post-GTP-hydrolysis Gαi molecules thus preventing their re-associating with G$\beta\gamma$.

The basis for the previously described phosphoregulation of GEM activity of GIV (Bhandari et al., 2015, Lopez-Sanchez et al., 2013) is evident from the structure and molecular modeling. A phosphate on the N-terminal S1674 of GIV-GEM is predicted to improve binding by creating an additional polar contact with Gαi R208 (Figure 2.4a-b). By contrast, a phosphate on the C-terminal S1689 of GIV-GEM would disrupt a key hydrogen bond that this residue forms with W258 of Gαi (Figure 2.4c). These findings explain the opposing roles of the two phosphoevents: the former is known to enhance and the latter to abrogate the ability of GIV to bind and activate Gαi (Bhandari et al., 2015, Lopez-Sanchez et al., 2013).

Homology modeling of other GEM family members, Daple and NUCB1, suggested a conserved mode of binding with a few subtle differences that corroborate prior mutagenesis findings (Garcia-Marcos et al., 2010, Aznar et al., 2015, Garcia-Marcos et al., 2011b) (Figure

2.5a-e). Both Daple and NUCB1 appear to form a salt bridge with Gαi K248 (Figure 2.5d-e), which is not available to GIV due to a non-acidic residue in the position of Q1683 (Figure 2.5c). Yet GIV and Daple, but not NUCB1, form a hydrogen bond with Gαi W258, due to a Ser-to-Thr substitution in NUCB1 (Figure 2.5c-d). The presence of both hydrogen bonds in Daple explains its tolerance towards individual mutations of K248 or W258, whereas binding of GIV and NUCB1 to Gαi is lost exclusively upon mutations of W258 or K248, respectively (Garcia-Marcos et al., 2010, Aznar et al., 2015, Garcia-Marcos et al., 2011b). Interestingly, the GEM motif of NUCB1 maps onto one of the EF-hand motifs of this protein (de Alba and Tjandra, 2004); modeling suggests not only full compatibility of the EF-hand topology with Gαi Sw-II binding, but also structural mimicry between such binding and the canonical EF-hand-mediated molecular fold (Figure 2.5f).

In our structure, the His-tag linker of each molecule binds to its symmetry neighbor, positioning the linker Arg and surrounding residues across the nucleotide cleft in a manner similar to GoLoco GDIs (Kimple et al., 2002) (Figure 2.6a-c). Removal of the His-tag linker or changing its position produced no crystals, suggesting that the linker trapped an otherwise transient and likely non-crystallizable GEF-induced conformation of Gαi:GDP. Although often overlooked, crystal packing against Sw-I is in fact quite prevalent in published Gαi crystal structures (Raw et al., 1997, Morris and Malbon, 1999). Here we sought to directly assess if the observed packing confounded any of the structural findings related to the GIV-GEM interface with Gαi. To this effect, we determined the structure of the His-tag linker-containing Gαi:GDP with KB752 (Figure 2.6a and 2.6e-f) and compared it to a previously published complex without the His-tag linker (Johnston et al., 2005) (PDB: 1Y3A). No discernible differences were noted in the Gαi-KB752 interface (Figure 2.6f, Figure 2.7), suggesting that the observed features at the Gαi-GIV-GEM

interface are also representative of the native interactions. By contrast, pronounced differences were observed in the position of Gαi Sw-I, which is found in an inward, collapsed conformation in the linker-free structure of Gαi-KB752 complex (Johnston et al., 2005) but is propped by the crystal neighbor's His-tag linker in an outward conformation in our linker-containing structure of the same complex (Figure 2.7). Consequently, we use caution in our interpretation of Sw-I position in the Gαi-GIV-GEM structure, and henceforth validate all structural observations with orthogonal biochemical, biophysical, and computational methods.

GIV-GEM binding disfavors the high-GDP-affinity conformations of Gαi SwII and Q204

Upon binding, GIV-GEM accelerates the basal nucleotide exchange of monomeric Gαi (Garcia-Marcos et al., 2009). To understand the structural basis for this phenomenon, we compared the newly determined structure with all previously crystallized GDP-bound complexes of Gαi. The complexes were organized in order of decreasing GDP affinity, from GoLoco GDI-bound and G$\beta\gamma$-bound (high GDP affinity), through GDP-only (basal affinity) to KB752- and GIV-bound (low GDP affinity). A clear trend emerged in the position of Sw-I and the molecular contacts of Q204 in Sw-II. In high-GDP-affinity states, Q204 appears to stabilize Sw-I in an outward position, away from the nucleotide-binding pocket (Figure 2.8a-b). By contrast, in the KB752-bound Gαi structures [(Johnston et al., 2005) and this work], Q204 is displaced away from Sw-I; in the His-tag linker-free structure (Johnston et al., 2005), this allows Sw-I to collapse towards the bound nucleotide (Figure 2.8d). GIV-GEM produces a similar but more exacerbated effect: it stabilizes an elevated conformation of Sw-II, hydrogen-bonds to Gαi Q204 via Q1683 and pulls it approximately 11 Å away from Sw-I, leading to an even greater contraction of the

GDP phosphate binding site that also involves a displacement of the β2-strand (Figure 2.8e-f). Despite this collapse, the N-terminal part of Sw-I is found in the outward position, due to the His-tag linker-mediated crystal packing (Figure 2.8e).

These observations prompted us to probe the role of Gαi Q204 in GIV-GEM-mediated GDP-release. A Q204A mutant was generated and tested in a kinetic assay where GDP released from Gαi is replaced by MANT-GTPγS, a non-hydrolyzable fluorescent GTP analogue (Remmers, 1998, Goricanec et al., 2016). Because GDP release is the rate-limiting step of nucleotide exchange, increases in MANT-GTPγS incorporation rate by Gαi reflect the acceleration of GDP release (Ferguson et al., 1986). Gαi(Q204A) fully retained its ability to bind GTP (Figure 2.9a). Compared to WT, Gαi(Q204A) displayed a small but consistent increase in the basal GDP exchange rate (1.28-fold; Figure 2.8g-h). However, the mutant was significantly more sensitive to activation by GIV-GEM (3.25-fold compared to 1.84-fold for WT Gαi; Figure 2.8g-h). These findings suggest that Q204 indeed negatively regulates GDP release, likely by stabilizing Sw-I in the high-GDP-affinity state. Interestingly, the direct contact between GIV Q1683 and Gαi Q204 appears unnecessary for accelerated nucleotide exchange because a GIV(Q1683A) mutant fully retained its GEF function (Figure 2.9b-c).

Binding of GIV-GEM to Gαi overcomes the allosteric GDP-stabilizing role of hydrophobic residues in SwII

Besides Q204, GIV-GEM directly engages the aromatic residues W211 and F215 in Sw-II of Gαi; these residues were previously proven critical for GIV-GEM binding (Garcia-Marcos et al., 2009). Structural comparisons suggest that each of these residues is stabilized by GIV-GEM in a different position as compared to the high GDP-affinity G$\beta\gamma$- (PDB 1GP2 (Wall et al., 1995))

or GoLoco-bound (PDB 1KJY (Kimple et al., 2002)) states (Figure 2.10). The root-mean-square deviation (RMSD) of the W211 side chain between the GIV-GEM bound and GoLoco-bound structures is 2.7 Å, and its rotamer states are completely different. The side-chain of F215 is also displaced 6.4 Å in GIV-GEM-bound structure as compared to the heterotrimer structure. These findings suggest that the conformations of W211 and F215 in Gαi Sw-II may be important for regulating GDP-affinity, and that the packing of these bulky hydrophobic residues against the β-barrel of the GTPase domain may stabilize GDP in the basal state (Figure 2.11a). If so, binding of GIV-GEM to Sw-II may neutralize such GDP-stabilizing effects to stimulate GDP release. Corroborating this hypothesis, alanine mutants W211A or F215A retained the ability to bind GTP (Figure 2.12a) but resulted in substantial increases in the basal nucleotide exchange rate of Gαi in MANT-GTPγS incorporation assays (2.48- and 1.84-fold increases, respectively; Figure 2.11b-c). By contrast, mutation of V218A, a hydrophobic residue on Sw-II that is not necessary for GIV-GEM binding, showed a small decrease in nucleotide exchange rate (Figure 2.11b-c). Consistent results were obtained in thermal stability assays where the two fast-exchanging Gαi mutants, W211A and F215A, displayed lower melting temperatures in both the native and GDP-bound states compared to WT Gαi and Gαi(V218A) (Figure 2.12b-c). These results support the idea that W211 and F215 on Sw-II contribute to stabilization of the bound GDP, an effect that is neutralized by GIV-GEM binding.

To understand the global allosteric changes in Gαi caused by the loss of bulky hydrophobic residues in Sw-II, we subjected WT and mutant Gαi to hydrogen-deuterium exchange mass spectrometry (HDX-MS): a sensitive technique that uses deuterium labeling of protein backbone amides (Wales and Engen, 2006) to probe conformational dynamics and mutation-induced allostery (Peacock et al., 2018, Kant et al., 2016). The V218A mutant showed only slight de-

creases in deuterium uptake compared to WT Gαi, notably in the C-terminal end of the α3-helix through the α3-β5 loop (residues F250-S263, 3.0% decrease) and the C-terminal end of the α5-helix (residues A338-N347, 2.3% decrease) (Figure 2.11d, Figure 2.13). By contrast, the fast-exchanging W211A mutant exhibited regions of higher deuterium uptake indicative of increased dynamics. The segment spanning Sw-I and the β2-strand (residues R176-F191) showed the highest increase in deuterium uptake in the W211A mutant compared to the WT protein (7.2% increase; Figure 2.11e, Figure 2.13). Other regions with more modest increased deuterium uptake in the mutant include the αA-αB loop and part of the αB helix (residues K92-L107, 2.5% increase), the αD-αE loop including the so-called NDS motif (residues F140-Y154, 4.2% increase), part of the αG-α4 loop and α4-helix (residues I285-A301, 3.3% increase), the C-terminal end of the α4-helix through the β6-strand (residues N311-F323 and E308-F323, 5.6% increase), and the C-terminal end of the α5-helix (residues A338-N347, 3.0% increase) (Figure 2.11e, Figure 2.13). Although it is impossible to state whether these changes are a trigger or a consequence of GDP release, the findings are consistent with the role of W211 on Sw-II as an allosteric stabilizer of Sw-I and the β2-strand of Gαi, and thus, of the overall high-GDP-affinity state of the protein. Of note, the relatively small magnitude of the observed changes in deuteration was not unexpected, as these changes were determined in comparison to monomeric WT GDP-bound Gαi, whose basal state is very dynamic when it is not stabilized by G$\beta\gamma$.

Interestingly, at an earlier 1 min time point, four regions within the W211A mutant (residues T120-C139, C224-D231, F267-F274 and V335-D341) showed reduced deuterium uptake as compared to WT (Figure 2.13). In other words, for these regions, the localized motions which gradually exposed amide protons to deuterium exchange appeared partially slowed by the W211A mutation, with uptake into the W211A mutant reaching that of WT Gαi only by 5

minutes of incubation with deuterium. These segments stand out in contrast to the enhanced dynamics observed for SwI, β2-strand, α4-β6 loop, and NDS loop, where greater deuterium uptake was observed throughout all measured time points. The reason for these differences may be entropic compensation, a known phenomenon (Anand et al., 2002) whereby reduced dynamics of some regions in the protein structure compensates for an enhancement in others.

Molecular dynamics simulations reveal GIV-induced rearrangements in the hydrophobic core of Gαi

To gain further insights into the allosteric regulation of Gαi and the mechanism by which GIV-GEM accelerates GDP release, we carried out molecular dynamic (MD) simulations. Using the crystallized conformation of Gαi:GDP as a starting point, 350 ns of protein dynamics were simulated in triplicates for the GDP only and GIV-GEM-bound states (1050 ns total for each state), and 3200 ns were simulated in the GIV-GEM+His-tag linker bound state. A root mean square fluctuation (RMSF) analysis of the centers of mass of Gαi residues demonstrates that Sw-II is highly dynamic in the GDP-only simulation (Figure 2.14a-b), in agreement with its invariably disordered state in WT Gαi:GDP crystal structures (Raw et al., 1997, Coleman and Sprang, 1998, Kapoor et al., 2009) (Figure 2.14c). Binding of GIV-GEM to Gαi Sw-II increased its rigidity as expected, but it also unexpectedly stabilized Sw-III that has no direct contact with the peptide (Figure 2.14a-c). The most striking increase in dynamics was observed in the C-terminal region of Sw-I and the β2-β3 strands (Figure 2.14b-c), which normally pack against the α1 and α5 helices of Gαi to form the hydrophobic core (Kaya et al., 2016) of the GTPase domain. When simulations were run in the presence of the His-tag linker, the dynamics of Sw-II was unchanged with respect to the GIV-bound state, the high mobility of Sw-III was restored to the GDP-only

level, and the GIV-induced increase in Sw-I and β2-β3 strand dynamics was partially negated, in agreement with a potential role of the His-tag linker in stabilizing GIV-GEM-bound Gαi and facilitating its crystallization (Figure 2.15a). These data support the idea that binding of GIV-GEM to Sw-II allosterically perturbs Sw-I and the β2-strand; it also suggests that the perturbation is further propagated to the hydrophobic core of the GTPase domain of Gαi.

To pinpoint the dominant allosteric changes in Gαi induced by GIV-GEM, we projected the pairwise Gαi residue (center of mass) distances onto a lower-dimension space via principal component analysis (PCA; Figure 2.15b). Sw-II was excluded from the PCA to selectively detect allosteric changes rather than direct consequences of GIV-GEM binding. In the first principal component, the largest contributions were from the residue distances within the hydrophobic core of the GTPase domain that changed consistently and substantially upon GIV-GEM-binding: those from the β2-β3 strands to helix α1 systematically increased, and those from α1 to α5 systematically decreased (Figure 2.14d-f, Figure 2.15c). Analysis of representative Gαi conformations from different areas in the PC space demonstrates that GIV-GEM binding allosterically induces an outward motion of the β2-β3 loop with a concomitant tilting of the C-terminal part of the α5 helix towards the β2-β3 strands, drastically perturbing the intramolecular packing in the hydrophobic core (Figure 2.14e). Moreover, the tilted α5 conformation was recently proposed to correlate with GDP-release (Sun et al., 2018). In addition, GIV-GEM binding resulted in a distance increase between GDP and R178 (a residue known to stabilize GDP) and a concomitant decrease in distance between the GDP and the αF-helix (preceding Sw-I) (SI Appendix, Figure 2.15d-f), indicative of inward collapse of Sw-I as predicted (Figure 2.8). Many of the Gαi residues highlighted by this analysis were retrospectively found to play important roles in GDP binding (Sun et al., 2015).

GDP dissociation did not occur over the course of our 3350 ns simulations with GIV-GEM, consistent with the reported high affinity of GDP to Gαi and its ability to stay bound through much longer simulations (total 42 μs simulation for Gαi-GDP only) unless the protein conformation is substantially perturbed (Dror et al., 2015).

2.3 Discussion

The present work provides the first atomic-level structure of a naturally occurring GEM bound to Gαi. The structure provides mechanistic insights into key aspects of GEM biology, including the mutual exclusivity of GEM binding with G$\beta\gamma$ (which promotes G$\beta\gamma$ signaling) and GoLoco-containing proteins (which antagonizes the GDI action of such proteins) (Garcia-Marcos et al., 2009, Garcia-Marcos et al., 2011a). Furthermore, the structure explains the basis for phosphoregulation of GIV-GEM.

This study also elucidates the mechanism by which GEMs accelerate GDP release from Gαi. MD simulations, HDX-MS, and nucleotide exchange experiments reveal a previously unknown role of Gαi Sw-II in nucleotide affinity. Stabilization of the elevated Sw-II conformation by GIV-GEM releases conformational constraints on Sw-I and β2-β3 strands of Gαi, allowing for inward collapse of the former and higher mobility of the latter. This perturbation propagates to the hydrophobic core in the center of the GTPase domain that was previously shown to contribute to both basal and GPCR-accelerated nucleotide exchange in Gαi (Kaya et al., 2014, Kaya et al., 2016). Structures of GPCR-bound G proteins demonstrate that GPCRs perturb the hydrophobic core directly by displacing the C-terminal α5 helix of Gαi and also inserting a hydrophobic residue from the intracellular loop 2 into the core (Rasmussen et al., 2011, Koehl et al., 2018, Carpenter et al., 2016, Draper-Joyce et al., 2018). Thus, our findings suggest that despite bind-

ing at non-overlapping interfaces on Gαi, GEMs and GPCRs converge on a similar mechanism for acceleration of GDP release by either directly or allosterically perturbing the intramolecular packing in the hydrophobic core of the GTPase domain of Gαi (Figure 2.16). These similarities escaped detection in earlier studies employing molecular modeling (Garcia-Marcos et al., 2009) and NMR (de Opakua et al., 2017).

The presented data and model of GIV-GEM-triggered Gαi activation are in agreement with the findings of a prior study (de Opakua et al., 2017) where the authors investigated the same complex by NMR. The two studies converge on an almost identical set of GIV-GEM-induced increases in the dynamics of Gαi regions, including Sw-I, the β2-β3, α3-β5 and α4-β6 loops, and the NDS motif of the helical domain. In fact, the only difference between the two studies is found in the phosphate-coordinating P-loop of Gαi, where de Opaqua et al. (de Opakua et al., 2017) report an increase in dynamics while we observe no significant difference by either HDX or MD. However, it is important to note that our experiments are conducted in the absence of excess GDP, by inherently different techniques, and, in the case of HDX, on a mutant rather than the Gαi complex with GIV; therefore, subtle variations in findings are expected. Despite this difference, the proposed dynamic model of GIV-GEM-mediated GDP release is fully consistent between the two studies, with the advance of our work being in providing, for the first time, an atomic resolution insight into the details of GIV-GEM binding and action.

Our MD simulations of GIV-GEM-bound Gαi:GDP closely recapitulates the findings from the HDX studies of the GEM-mimicking mutant W211A. In the HDX studies of the mutant, several regions showed increased deuterium incorporation, with the largest increases observed in the β2 strand, α4-β6 loop, NDS loop, and α5 helix; these findings were corroborated by the MD simulations. The main difference between the HDX and MD studies was in the αD-αE loop

where increased dynamics was observed in HDX but not in MD. The αD-αE loop is important for stabilizing the contacts between the Gαi GTPase and α-helical domain, thus regulating domain separation. The observed difference could be explained by insufficient sampling due to moderate length of our MD simulations (total of about 1 μs) where much longer simulations may be required to observe spontaneous domain opening (e.g. the total 42 μs Gαi-GDP as in Dror et al., 2015).

Recent studies have suggested the existence of a transition state intermediate in G protein activation (Sun et al., 2018, Du et al., 2019, Liu et al., 2019). These studies utilize HDX-MS, hydroxyl radical mediated protein footprinting (HRF)-MS, and computational methods to gain insight into structural changes early in the G protein activation process. These studies identified increased dynamics in the C-terminal region of the α5-helix and β1-β3 strands to be some of the earliest motions that occur during GPCR-mediated G protein activation, and suggest that disruption of interactions between the α5 helix and the αN/β1 hinge and β sheets (i.e. disruption of the hydrophobic core) may be sufficient to destabilize the nucleotide-binding pocket. In the present study, we also observe similar motions in the β2-β3 and α5 regions in both our HDX and MD studies, supporting the idea that these motions may also be part of an early event in G protein activation and GDP release triggered by GEMs. Therefore, the recent computational studies (Sun et al., 2018, Du et al., 2019, Liu et al., 2019) are fully consistent with the results presented here and in the prior NMR study of GIV-GEM (de Opakua et al., 2017).

Because nucleotide exchange is an inherently dynamic process, our serendipitously identified His-tag linker has likely facilitated the crystallization of an otherwise unstable and transient complex, much like crystal packing for a previously crystallized accelerated exchange mutant (Kapoor et al., 2009) or the intentionally introduced conformation-specific nanobodies in

other GEF-bound structures of G proteins (Che et al., 2018, Huang et al., 2015, Rasmussen et al., 2011, Kruse et al., 2013). Several lines of evidence support this claim. First, no crystals were obtained when the His-tag linker was removed or placed in a different position, suggesting that the linker assisted in crystallization. Second, MD simulations with and without the His-tag linker showed pronounced differences, where the presence of the linker reversed the de-stabilizing effects of the GIV-GEM peptide and stabilized the hydrophobic core (the region of the protein that is associated with nucleotide exchange). Finally, the similarities in Sw-I interactions between the His-tag linker and GoLoco GDIs suggested a possible mechanistic basis by which the linker counteracts the GEF action of the GIV-GEM peptide. Importantly, despite its role in crystallization, the His-tag linker did not affect the Gαi-GEM interaction interface, as demonstrated by the comparison of our His-tag linker-containing Gαi-KB752 structure with the previously solved linker-free structure of the same complex. However, it clearly influenced the position of Sw-I, which was expected to be found in an inward-collapsed low-GDP-affinity conformation but was instead propped in a partial outward high-GDP-affinity-like conformation. This illustrates that the insights from the structure alone may be limited by its static nature, and that only the orthogonal computational, biophysical, and biochemical experiments can provide a holistic understanding of the diverse mechanisms for allosteric regulation of Gαi.

Finally, our study reveals similarities between the mechanism of action of GIV-GEM and the activation of small GTPases. It has been postulated that a common ancestor of the GTPase fold provided a structural framework that can be perturbed by the interruption of α5-α1 contacts (Flock et al., 2015). GPCRs trigger the perturbation by directly binding to α5 of their effector trimeric G protein, whereas GEFs of small GTPases typically act via binding to Sw-I and Sw-II. Our study not only supports the conserved nature of the ancestral α5-α1 activation mechanism,

but also suggests that similarities between monomeric GTPases and trimeric G proteins extend beyond it, because just like for small GTPases, Sw-I and Sw-II in Gαi may serve as allosteric "handles" by which the conserved exchange mechanism is accessed by modulators.

2.4 Materials and Methods

Plasmid constructs and mutagenesis

All restriction endonucleases and Escherichia coli strain DH5 were purchased from New England Biolabs (Ipswich, MA). For crystallization, biochemical experiments, and HDX-MS, rat Gαi3 (Uniprot P08753-1) was cloned into a pET28b vector using NdeI and XhoI restriction sites, resulting in an N-terminal 6xHis tag separated from the Gαi3 protein by the sequence SSGLVPRGSHM. The nucleotide sequences encoding for the tag and the linker was: ATGGGCAGCAGCCATCATCATCATCATCACAGCAGCGGCCTGGTGCCGCGCGGCAGC CAT- followed by the start ATG codon of WT Gαi3; this construct is referred to 6xHis-Gαi3. In the construct used for crystallization, the N-terminal 25 amino acids of Gαi3 were removed to facilitate crystallization as previously done (Johnston et al., 2005); this construct will be referred to as 6xHis-ΔN25-Gαi3. For GST pull down assays, full length Gαi3 was cloned into a pGEX vector with an N-terminal GST-tag, resulting in a GST-Gαi3. All site-directed mutagenesis (Gαi3 Q204A, R208Q, K209M, K210M, W211A, H213F, F215A, and V218A, were carried out using QuikChange II site-directed mutagenesis kit (Agilent Technologies; Santa Clara, CA; Ca200524) as per the manufacturers protocol. In the main text, all three constructs (6xHis-Gαi3, 6xHis-ΔN25-Gαi3, and GST-Gαi3) are referred to as Gαi; in the methods below, specific constructs used in each experiment are detailed.

Sequences

Cloned full length Rattus norvegicus Gαi3 sequence:

MGSSHHHHHHSSGLVPRGSHMGCTLSAEDKAAVERSKMIDRNLREDGEKAAKEVKLLLLGA
GESGKSTIVKQMKIIHEDGYSEDECKQYKVVVYSNTIQSIIAIIRAMGRLKIDFGEAARADDARQ
LFVLAGSAEEGVMTSELAGVIKRLWRDGGVQACFSRSREYQLNDSASYYLNDLDRISQTNY
IPTQQDVLRTRVKTTGIVETHFTFKELYFKMFDVGGQRSERKKWIHCFEGVTAIIFCVALSDYDL
VLAEDEEMNRMHESMKLFDSICNNKWFTDTSIILFLNKKDLFEEKIKRSPLTICYPEYTGSNTY
EEAAAYIQCQFEDLNRRKDTKEVYTHFTCATDTKNVQFVFDAVTDVIIKNNLKECGLY

Cloned 25aa N-terminally truncated Rattus norvegicus Gαi3 sequence:

MGSSHHHHHHSSGLVPRGSHMDGEKAAKEVKLLLLGAGESGKSTIVKQMKIIHEDGYSEDEC
KQYKVVVYSNTIQSIIAIIRAMGRLKIDFGEAARADDARQLFVLAGSAEEGVMTSELAGVIKRLW
RDGGVQACFSRSREYQLNDSASYYLNDLDRISQTNYIPTQQDVLRTRVKTTGIVETHFTFK
ELYFKMFDVGGQRSERKKWIHCFEGVTAIIFCVALSDYDLVLAEDEEMNRMHESMKLFDSI
CNNKWFTDTSIILFLNKKDLFEEKIKRSPLTICYPEYTGSNTYEEAAAYIQCQFEDLNRRKDTKE
VYTHFTCATDTKNVQFVFDAVTDVIIKNNLKECGLY

Peptides

Peptides were synthesized by three companies independently [LifeTein (Somerset, NJ), Chempeptide (Shanghai, China), and AbClonal (Woburn, MA)] and all displayed comparable effects in assays. Peptides were synthesized with L-amino acids at $\geq$95% purity and kept frozen at -80°C as 10 mM stocks in DMSO.

KB-752 peptide sequence:

1-NH2-SRVTWYDFLMEDTKSR-COOH-16

GIV-WT GEM-motif peptide sequence:

1671-NH2-KTGSPGSEVVTLQQFLEESNKLTSVQIKSSS-COOH-1701

GIV-Q1683A GEM-motif peptide sequence:

1671-NH2-KTGSPGSEVVTLAQFLEESNKLTSVQIKSSS-COOH-1701

Expression and purification of Gαi3

6xHis-tagged Gαi3 constructs (6xHis-Gαi3, 6xHis-ΔN25-Gαi3, or single-point mutants of thereof) were transformed into E. coli BL21 (DE3; Invitrogen) cells. Cells were grown in 1 L flasks at 37C until OD reached 0.8-1.0, then induced overnight at 25°C with 1 mM isopropyl β-d-1-thiogalactopyranoside (IPTG). Cells were harvested via centrifugation and lysed at 15,000 PSI by a single pass through a cell disruptor (TS-Series; Constant Systems, Inc) in Running Buffer (RB; 50 mM NaH_2PO_4 pH 7.4, 300 mM NaCl, and 0.5 mM EDTA) supplemented with 2x Protease Inhibitors (Roche Life Science) and 10 mM imidazole. Cell debris was removed by ultracentrifugation at 45,000 x g for 40 min, and the supernatant was loaded on a NiNTA His60 Superflow resin (Qiagen) affinity column via fast protein liquid chromatography (AKTA, GE Life Sciences). The resin was washed with RB+60 mM imidazole, and eluted with RB+300 mM imidazole. The eluted protein was concentrated at 1500 x g (Amicon Ultra-15 30 MWCO centrifugal filter; Millipore) and subjected to size exclusion chromatography via Superdex 200 resin (GE Healthcare) equilibrated with storage buffer (20 mM Tris-HCl pH 7.4, 20 mM NaCl, 1 mM $MgCl_2$, and 5% glycerol). Fractions from major peak were pooled, usually resulting in 1-5 mg/mL Gαi protein. Protein was then aliquoted, flash frozen, and stored at -80°C. Protein

concentration and purity were checked throughout purification via SDS-PAGE and comparison to known amounts of Bovine Serum Albumin (BSA).

GST-alone and GST-tagged Gαi3 constructs (wild type and mutant proteins) were expressed and purified from Escherichia coli strain BL21 (DE3; Invitrogen) as described previously. Briefly, cells were grown in 1 L flasks at 37°C until OD reached 0.8-1.0, then induced overnight at 25°C with 1 mM IPTG. A bacterial pellet from 1 L of culture was resuspended in 10 ml of GST-lysis buffer (25 mM Tris-HCl, pH 7.5, 20 mM NaCl, 1 mM EDTA, 20% [vol/vol] glycerol, 1% [vol/vol] Triton X-100, 2 protease inhibitor cocktail [Complete EDTA-free; Roche Diagnostics]). Cell lysates were sonicated (4 x 20 s, 1 min between cycles) and then centrifuged at 12,000 x g at 4°C for 20 min. Solubilized proteins were affinity purified on glutathione-Sepharose 4B beads (GE Healthcare) by incubation for 4 hours at 4°C. Beads were washed 3 x with 50 mM Tris pH 8 and then eluted with GST elution buffer (50 mM Tris pH 8, 10 mM reduced glutathione). Eluted proteins were dialyzed overnight at 4°C against phosphate-buffered saline (PBS), and stored at -80°C in aliquots.

Co-crystallization of Gαi3 with KB-752 and GIV-GEM

Purified 3 mg/mL 6xHis-ΔN25-Gαi3 (either freshly prepped or freeze-thawed once) was incubated overnight in storage buffer (20 mM Tris-HCl pH 7.4, 20 mM NaCl, 1 mM $MgCl_2$, and 5% glycerol) at a 3:1 (peptide:Gαi3) molar ratio at 4°C, then concentrated to 15 mg/mL and set on 288-well Intelli-Plate trays (Art Robbins Instruments) in 1:1, 1.5:1, and 2:1 volume ratios with mother liquor (12-16% PEG 3350, 0.2 M NH_4Cl) at room temperature. Crystals appeared after 1-2 days and grew to full size in 5-7 days. Crystals were cryoprotected by soaking in mother liquor supplemented with 10% glycerol and flash-frozen with liquid nitrogen.

X-ray data collection and structure determination of Gαi3-peptide co-crystal structures

X-ray diffraction data were collected at 100 K at the Lawrence Berkeley National Laboratory Advanced Light Source (8.2.2) and Stanford Synchrotron Radiation Lightsource (9-2) at a single wavelength. All diffraction data were indexed and integrated with MOSFLM, processed with AIMLESS, and truncated with CTRUNCATE within the CCP4 suite of programs (51-53) (v.7.0.056). Phases were estimated via molecular replacement in Phaser (McCoy et al., 2007) (v.2.8.1), using a previously published model of human Gαi1 (PDB 1y3a, for Gαi3:GDP with KB-752) or human Gαi3 (PDB 4g5r, for Gαi3:GDP with GIV-GEM) as a search model. Models underwent rigid-body and restrained positional refinement using PHENIX.REFINE in the PHENIX software suite (Adams et al., 2010) (v.1.13-2998) against a maximum likelihood target function, alternated with manual inspection against electron density maps in Coot (Emsley et al., 2010) (v.0.8.2 for Windows). Peptides were manually modeled in Coot and refined in the final rounds of refinement, which also included the application of hydrogens to their riding positions and simulated annealing. The resulting refinement statistics for each model are included in Table S1. Figures displaying crystal packing were prepared using PyMOL (v.1.8.3.2, http://www.pymol.org), and atomic coordinates and structure factors were deposited in the Protein Data Bank (accession codes 6MHE and 6MHF for KB752 and GIV-GEM co-crystal structures, respectively).

Cell culture

Cells were cultured according to American Type Culture Collection (ATCC) guidelines. Briefly, HeLa cells were grown in high glucose DMEM (Sigma; CaD5796) supplemented with

10% (vol/vol) FBS (HyClone; CaSH30071.03) and penicillin-streptomycin-glutamine (Gibco; Ca10378-016). For cell lysates, HeLa cells were grown on 10-cm plates and harvested by scraping into 0.5 mL of lysis buffer [20 mM HEPES pH 7.4, 5 mM Mg-acetate, 125 mM K-acetate, 0.4% Triton X-100, 1 mM DTT, 1 Complete Protease Inhibitor Mixture (Roche; Ca11873580001), and 1 Phosphatase Inhibitor Mixtures 2 and 3 (Sigma; CaP5726 and P0044, respectively)] on ice. Cell lysates were incubated for 10 min at 4°C and were centrifuged at 12,000 x g for 10 min. Clarified cell lysates were subsequently used in GST pulldown assays.

In vitro GST pulldown assays

Purified GST-Gαi3 or GST-alone (5 μg) were immobilized on glutathione-Sepharose beads and incubated with binding buffer [50 mM Tris-HCl (pH 7.4), 100 mM NaCl, 0.4% (vol/vol) Nonidet P-40, 10 mM $MgCl_2$, 5 mM EDTA, 30 μM GDP, 2 mM DTT, 1 Complete Protease Inhibitor Mixture (Roche; Ca11873580001)] for 90 min at room temperature as described before (24, 57-59). Lysates (250 μg protein) of HeLa cells were added to each tube, and binding reactions were carried out for 4 hr at 4°C with constant tumbling in binding buffer [50 mM Tris-HCl (pH 7.4), 100 mM NaCl, 0.4% (vol/vol) Nonidet P-40, 10 mM $MgCl_2$, 5 mM EDTA, 30 M GDP, 2 mM DTT]. Beads were washed (4X) with 1 mL of wash buffer [4.3 mM Na_2HPO_4, 1.4 mM KH_2PO_4 (pH 7.4), 137 mM NaCl, 2.7 mM KCl, 0.1% (vol/vol) Tween-20, 10 mM $MgCl_2$, 5 mM EDTA, 30 μM GDP, 2 mM DTT] and boiled in Laemmli's sample buffer for 10min. For immunoblotting, rabbit anti-Gβ primary antibody (M-14; Casc-261) and anti-GIV-CT primary antibody (T-13; Casc-133371) were obtained from Santa Cruz Biotechnology (Dallas, TX). IRDye 680RD goat anti-rabbit secondary antibody (Ca926-68071) and IRDye 800 goat anti-mouse secondary antibody (Ca926-32210) were from Li-Cor Biosciences (Lincoln, NE). Protein samples were sepa-

rated by SDS-PAGE and transferred to PVDF membranes (Millipore). Membranes were blocked with PBS supplemented with 5% nonfat milk before incubation with primary antibodies (1:500 dilutions overnight at 4°C). Blots were washed 3 times in PBS-T [4.3 mM Na_2HPO_4, 1.4 mM KH_2PO_4 (pH 7.4), 137 mM NaCl, 2.7 mM KCl, 0.1% (vol/vol) Tween-20] and incubated with secondary antibodies (1:20,000 dilutions at room temperature for 1 hour). Blots were then washed 3 times in PBS-T and once with PBS before infrared imaging following the manufacturer's protocols using an Odyssey imaging system (Li-Cor Biosciences).

Molecular modeling

Models of Gαi:GDP with (pS1674)GIV-GEM, Gαi:GDP with Daple-GEM, and Gαi:GDP with NUCB1-GEM were constructed by homology with the structure of Gαi:GDP with GIV-GEM using ICM versions 3.8-6 to 3.8-7a (Molsoft LLC, San Diego, CA).

The GEM motif peptides from (pS1674)GIV (1671-KTG-pS1674-PGSEVVTLQQFLEESNK-1691) and Daple (1663-ASPSSEMVTLEEFLEESNR-1681) were built ab initio; the GEM motif peptide from NUCB1 (305-DTNQDRLVTLEEFLASTQRKEF-326) was extracted from the NMR structure of NUCB1 (PDB 1snl (de Alba et al., 2004)). The backbone atoms of the peptides were confined to the crystallographic coordinates of the corresponding atoms of GIV-GEM (residues 1676-GSEVVTLQQFLEES-1689 only) via a set of harmonic distance restraints (tethers); the peptide flanks and side-chains were kept unrestrained. Full-atom conformational sampling of the peptides (backbone, side-chains, and positional variables) and the surrounding side-chains of Gαi was performed using 5106 steps of biased probability Monte Carlo optimization (Abagyan and Totrov, 1994) as implemented in ICM, with the repulsive part of the Van der Waals potential capped at 20 kJ/mol. The top

scoring pose of each peptide was selected for analysis.

Gαi3-limited proteolysis assay

6xHis-Gαi3 or 6xHis-ΔN25-Gαi3 (0.25 mg/ml) was incubated for 150 min at 30°C in buffer (20 mM HEPES pH 8, 100 mM NaCl, 1 mM EDTA, 10 mM $MgCl_2$, and 1 mM DTT) supplemented with GDP (30 μM) or GTPγS (30 μM). After incubation trypsin was added to the tubes (final concentration 6.25 μg/ml) and samples were incubated for 10 min at 30°C. Samples were rapidly transferred to ice, reactions were stopped by the addition of Laemmli sample buffer, after which the samples were boiled for 10min. Proteins were separated by SDSPAGE and stained with Coomassie blue.

MANT-GTPγS incorporation assays

MANT-GTPγS incorporation assays in Figure 2 were done using full length 6xHis-ΔN25-Gαi3, whereas incorporation assays in Figure 3 were done using the 6xHis-Gαi3 construct. For Gαi3 incorporation assays in the presence of peptide, peptide was pre-bound to Gαi3 prior to running the assay. To equilibrate and pre-bind peptide to Gαi3, 111 nM His-Gαi3 WT or mutants were first incubated in reaction buffer (20 mM HEPES pH 8, 100 mM NaCl, 1 mM EDTA, 10 mM $MgCl_2$, and 1 mM DTT) in 30°C water bath for 30 min with or without varying concentrations of peptide in a final incubation volume of 250 μL. After equilibration, 72 μL protein-peptide complexes were transferred to a pre-warmed 384-well black flat-bottom plate (in triplicates). The reaction was initiated by injecting 8 μL of 250 nM MANT-GTPγS (Abcam, Cambridge, MA) in each well for a final reaction volume of 80 μL and final concentrations of 100 nM Gαi3, 25 nM MANT-GTPγS and the indicated concentrations of the peptide. MANT-GTPγS incorporation into

Gαi3 was quantified, either by FRET (ex = 280; em = 440) or by direct MANT excitation (ex = 350; em = 440), using a microplate fluorescence reader (TECAN Spark 20M). Fluorescence was measured every 30 sec starting immediately after injection of MANT-GTPγS. Raw fluorescence was plotted over time and observed rates (kobs) were determined by fitting a one-phase association curve to the data (GraphPad Prism v.7).

Differential scanning fluorimetry (thermal shift assays)

6xHis-Gαi3 WT and mutants (5 μM) were taken in their native state (as purified) or loaded with GDP by incubating it for 150 min at 30°C in buffer (20 mM HEPES, pH 8, 100 mM NaCl, 1 mM EDTA, 10 mM $MgCl_2$, and 1 mM DTT) supplemented with GDP (1 mM). After loading, 45 μL of 5 μM His-Gαi3 was pipetted into PCR tubes (in triplicates) and 5 μL 200X SYPRO Orange solution freshly made in the same buffer from 5000X stock (Life Technologies S-6650) was added to the protein. A buffer + dye only (no protein) control was also included. Thermal shift assays were run on an Applied Biosystems StepOnePlus Real-Time PCR machine. Mixed protein and dye samples were subjected to increasing temperatures from 25 to 95°C in half degree increments, holding each temperature for 30 sec and measuring SYPRO fluorescence (using filter 3 for TAMRA^{TM} and NED^{TM} dyes) at each temperature. Melting temperatures were defined as the temperature at which the maximum value for the derivative of signal fluorescence (dF/dt) is achieved (GraphPad Prism v.7).

Hydrogen-deuterium exchange mass spectrometry (HDX-MS)

HDX-MS measurements were made using a Synapt G2Si system (Waters Corporation). Deuterium exchange reactions were carried out by a Leap HDX PAL autosampler (Leap Tech-

nologies, Carrboro, NC). Deuterated buffer was prepared by lyophilizing 10 mL of 20 mM Tris-HCl pH 7.4, 20 mM NaCl, 5 μM GDP and 5% glycerol and resuspending it in 10 mL 99.96% D2O immediately before use. Each deuterium exchange time point (0 min, 1 min, 2.5 min, 5 min) was measured in triplicate. For each measurement, 5 μL of 100 M 6xHis-Gαi3 protein [in storage buffer (20 mM Tris-HCl pH 7.4, 20 mM NaCl, 1 mM $MgCl_2$, and 5% glycerol) was mixed with 55 μL of D2O buffer at 25°C. Deuterium exchange was quenched by combining 50 μL of the deuterated sample with 50 μL of 0.1% formic acid and 3 M guanidinum-HCl for 1 min at 1°C. The quenched sample was then injected in a 50 μL sample loop and digested by an inline pepsin column (Pierce, Inc.) at 15°C. The resulting peptides were captured on a BEH C18 Vanguard precolumn, separated by analytical chromatography (Acquity UPLC BEH C18, 1.7 m, 1.0 50 mm, Waters Corporation) using 785% acetonitrile in 0.1% formic acid over 7.5 min, and analyzed in a Waters Synapt G2Si quadrupole time-of-flight mass spectrometer following electrospray injection.

Data were collected in Mobility, ESI+ mode, mass acquisition range of 200-2000 (m/z), scan time 0.4 sec. Continuous lock mass correction was performed using infusion of leu-enkephalin (m/z = 556.277) every 30 sec (mass accuracy of 1 ppm for calibration standard). For peptide identification, data were instead collected in MS E (mobility ESI+) mode. Peptides masses were identified following triplicate analysis of 10 μM Gαi3, and were analyzed using PLGS 2.5 (Waters Corporation). Peptides masses were identified using a minimum number of 250 ion counts for low energy peptides and 50 ion counts for their fragment ions; with the additional constraint that peptide size was greater than 1500 Da. The following parameters were used to filter peptide sequence matches: minimum products per amino acid of 0.2, minimum score of 7, maximum MH+ error of 5 ppm, and a retention time RSD of 5%, and the peptides

had to be present in two of the three ID runs collected. After identification in PLGS, peptides were analyzed in DynamX 3.0 (Waters Corporation). Deuterium uptake for each peptide was calculated by comparing the centroids of the mass envelopes of the deuterated samples with the undeuterated controls. To account for back-exchange and systematic autosampler sample handling differences between the shorter 1 min and longer 2.5 min and 5 min deuteration times, the uptake and standard deviation values were divided by 0.79 and 0.75, respectively. Data were plotted as number of deuterons incorporated vs time. The Y-axis limit for each plot reflects the total number of amides within the peptide that can possible exchange. Each plot includes the peptide MH+ value, sequence, and sequential residue numbering.

Molecular dynamic (MD) simulations

MD simulations were performed with AMBER package (v. 16) in periodic boundary conditions. Three different complexes were created and refined in ICM v. 3.8-7a (Molsoft LLC, San Diego, CA), and then used to create Amber topology files: Gαi:GDP, Gαi:GDP with GIV-GEM, and Gαi:GDP with GIV-GEM and His-tag linker (amino acid residues GLVPRGS from the linker of the crystallographic neighbor molecule). In all cases, the Gαi molecule contained residues 30-347 only. Residue protonation states were assigned by the convertObject utility in ICM, followed by pdb4amber conversion. The proteins were represented using the ff14SB force-field. The parameters for GDP were taken from the AMBER parameter database (www.pharmacy.manchester.ac.uk/bryce/amber) (Meagher et al., 2003).

Each system was solvated with explicitly represented water (TIP3P model, 12 Å margin). K^+ and Cl^- ions were added to maintain neutrality of the system and represent approximately 150 mM K^+. The system compositions were as follows. The Gαi:GDP system consisted of

47,571 atoms in the 97 x 83 x 73 Å box, including 14,121 water molecules, 39 K^+ ions and 30 Cl^- ions. The Gαi:GDP + GIV-GEM system consisted of 50,454 atoms in the 97 x 83 x 77 Å box, including 15,000 water molecules, 42 K^+ ions and 30 Cl^- ions. The Gαi:GDP + GIV-GEM + His-tag linker system consisted of 50,463 atoms in the 97 x 83 x 77 Å box, including 14,969 water molecules, 42 K^+ ions and 31 Cl^- ions. The systems were minimized with restrained heavy atoms of the solute, followed by an unrestrained minimization.

The systems were slowly heated (1 K/ps) up to 310 K with Langevin thermostat (γ = 1 ps-1). The density of the systems was equilibrated in a series of short (20 ps) simulations at isotropic pressure of 1 bar with MC barostat. All bond lengths to hydrogen atoms were constrained with SHAKE algorithm (ntc = 2, ntf = 2). The non-bonded interactions cutoff was 12 Å. The time step was 0.5 fs. Additionally, the systems were equilibrated in the NPT ensemble for 10 ns with time step of 2 fs.

The production runs were started in triplicates from the last frame of the equilibration stage. The simulations were carried out in the same NPT ensemble (310 K, 1 bar), non-bonded cutoff (12 Å) and time step (2 fs) for 100 ns. Each run started with a unique random seed that affects the thermostat.

The MD simulations were performed with GPU-accelerated PMEMD using SPFP precision model on Nvidia GeForce GTX 680 and GTX TITAN cards.

MD trajectory analysis

MD simulation analyses were performed in ICM v.3.8-7a (Molsoft LLC, San Diego, CA), unless otherwise stated. Replicate simulations of a single condition were concatenated together for analysis.

For Root Mean Square Fluctuation (RMSF) analysis, MD frames from each condition were superimposed by the backbone (C, N, O and C atoms), using cpptraj, within the AMBER package (Roe and Cheatham, 2013) (v.16). To trace intramolecular motions in Gαi induced by GIV-GEM, Euclidean distances between centers of mass of amino-acid residue pairs, or between residues and GDP (50,721 pairs total), were calculated for each frame of the simulation. Residue pairs were filtered to retain only 1658 pairs that satisfied the following criteria: (1) they were at least two residues apart in the sequence; (2) they were separated by less than 12 Å in at least one MD frame; (3) their distances displayed less than 75% overlap in frequency distribution between the Gαi:GDP and Gαi:GDP+GIV-GEM simulations; (4) they did not involve Sw-II residues (residues 202 to 218). To calculate the overlap between the distance frequency distributions, the distance range was broken into *b* 0.2 Å intervals.

The 1658 non-trivial residue pairs were subjected to principal component (PC) analysis to identify those pairs whose changing distances contribute the most to the dominant modes of motion upon GIV-GEM binding, in an unbiased manner. Only the first PC was analyzed because it correctly discriminated the simulation conditions (SI Appendix, Fig. S7b). Residue pairs assigned with the largest weights and associated with the first PC were mapped onto the crystal structure for visualization.

Statistical analysis

Each experiment presented in the figures is representative of at least three independent repeats (with at least two technical repeats for each condition within each repeat). Statistical significance between the differences of means was calculated using multiple comparisons in one-way nonparametric ANOVA. All statistics and graphical data presented were prepared using

GraphPad Prism v.7. Histograms of MD simulation data were generated in R v.3.4.4. All error bars are standard deviation.

Data availability

Atomic coordinates and structure factors were deposited in the Protein Data Bank (accession codes 6MHE and 6MHF for KB752 and GIV-GEM co-crystal structures, respectively). Raw data for Fig. 5 and SI Appendix, Fig. S6 is provided in the form of SI Appendix, Table S3. Raw data for Fig. 6 and SI Appendix, Fig. S7 is provided in the form of SI Appendix, Table S4.

Acknowledgements

Authors thank Drs. Barry Grant and Xinqiu Yao for fruitful discussions about MD trajectory analyses, Dr. Mikel Garci-Marcos for insightful discussions regarding crystallization conditions, and Dr. Suchismita Roy for help with HDX-MS interpretation. This work was partially supported by NIH R01 grants AI118985 and GM117424 to I.K, CA100768, CA160911 and DK099226 to P.G, and NSF grant IOS-1444435 to G.C. and S.D.R. N.A.K was supported by a NIH predoctoral fellowship (F31 CA206426), and T32 training grants T32CA067754 and T32DK007202. S.D.R. was supported by the Frontiers of Innovation Scholarship Program, the UCSD Stem Cell Innovative Projects Award, and T32 training grants T32GM007752 and T32 GM008326. T.N. is supported by a NHMRC C. J. Martin Early Career Fellowship 1145746. N.K. was supported by the Frontiers of Innovations Scholarship Program, the UCSD Stem Cell Innovative Projects Award, and T32 training grant T32GM008326. A.I was supported by NIH R01 GM071872. The Synapt G2Si was obtained from NIH grant S10 OD016234. This research was

supported in part by the W. M. Keck Foundation through computing resources at the W. M. Keck Laboratory for Integrated Biology at UCSD. We thank Advanced Light Source (ALS), Advanced Photon Source (APS), Stanford Synchrotron Radiation Laboratory (SSRL), and Canadian Light Source (CLS) for screening crystals and subsequent data collection.

Chapter 2 in part is a reprint of material submitted to be published in: **Kalogriopoulos NA***, Rees SD*, Ngo T, Kopcho N, Ilatovskiy A, Sun N, Komives E, Chang G, Ghosh P, Kufareva I. 2018. “Structural basis for GPCR-independent activation of heterotrimeric Gi proteins.” *Under review*. The dissertation author was *co-first author.

Figure 2.1: Gαi construct design and crystallization. a, Schematic representation of the domain organization of GIV, adapted from (Ma et al., 2015). b, Design of the rat Gαi3 construct that was used to produce protein for crystallography in this study. The 25 aa N-terminal helix of Gαi3 was removed and replaced by an N-terminal His-tag separated from the β1-strand by an 11-residue linker (construct referred to as ΔN25-HisGαi3; linker referred to as His-tag linker). c, SDS-PAGE analysis and Coomassie-Blue staining of the purified ΔN25-HisGαi3 side-by-side with bovine serum albumin (BSA) standards confirms the expected molecular weight, purity, and high yield for ΔN25-HisGαi3. d, Sequence alignment of GIV-GEM with the previously described synthetic peptide, KB752 (Johnston et al., 2005). e, Unit cell and crystal image for our solved KB752-bound Gαi:GDP structure. Yellow, Gαi; purple, His-tag linker; cyan, KB752. f, Unit cell and crystal image for our solved GIV-GEM-bound Gαi:GDP structure. Structure is colored as in d except GIV-GEM is in red.

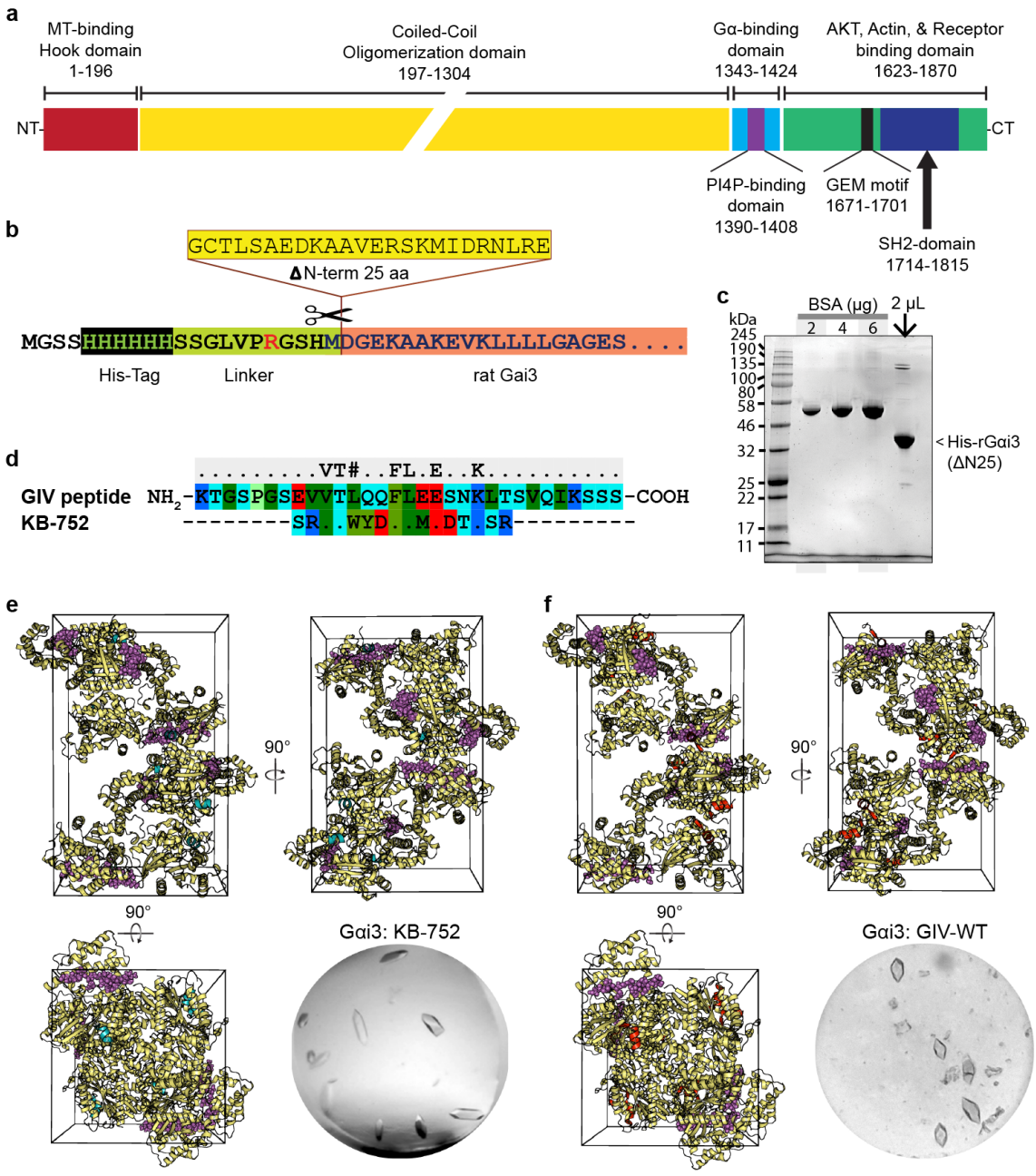
a
MT-binding
Hook domain
1-196
Coiled-Coil
Oligomerization domain
197-1304
Gα-binding
domain
1343-1424
AKT, Actin, & Receptor
binding domain
1623-1870
NT-
-CT
PI4P-binding
domain
1390-1408
GEM motif
1671-1701
SH2-domain
1714-1815
b
GCTLSAEDKAAVERSKMIDRNLRE
ΔN-term 25 aa
MGSSHHHHHHSSGLVPRGSHMDGEKAAKEVKLLLLGAGES....
His-Tag
Linker
rat Gαi3
c
kDa
245
190
135
100
80
58
46
32
25
22
17
11
BSA (μg)
2
4
6
2 μL
< His-rGαi3
(ΔN25)
d
GIV peptide
KB-752
NH2-KTGSPGSEVVTLQQFLEESNKLTSVQIKSSS-COOH
.....VT#..FL.E..K.....
--------SR..WYD..M.DT.SR---------
e
90°
90°
90°
Gαi3: KB-752
f
90°
90°
Gαi3: GIV-WT

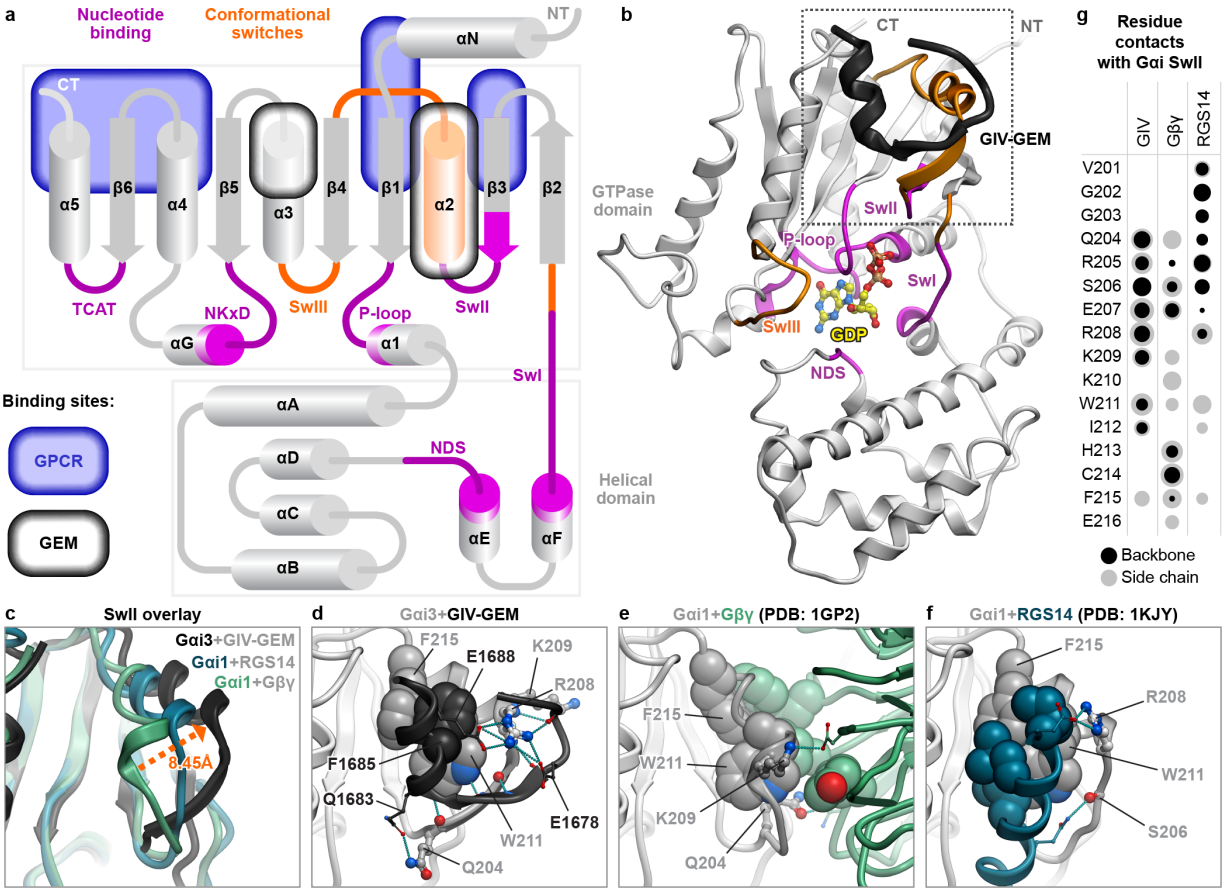

Figure 2.2: GIV-GEM binds Sw-II of Gαi. a, Topology of the Gαi protein with conformational switches and binding sites of key interactors marked. b, Crystal structure of Gαi with GIV-GEM peptide bound at Switch (Sw)-II. c, Overlay of Gαi Sw-II from G$\beta\gamma$-bound, GDI-bound, and GIV-GEM-bound crystal structures. d, A close-up view of the interaction interface between Gαi and GIV-GEM. e-f, Close-up views of Gαi Sw-II bound to G$\beta\gamma$ (e, PDB 1GP2 (Wall et al., 1995)) or GoLoco-motif GDI RGS14 (f, PDB 1KJY (Kimple et al., 2002)). Key Sw-II residues shared by GIV and at least one of G$\beta\gamma$ or RGS14 are shown as spheres (aromatic/aliphatic) or sticks (polar). g, Bubble plot displaying the strength and the nature of contacts that Gαi Sw-II residues make with GIV-GEM, G$\beta\gamma$ or RGS14. The size of the dot is proportional to the strength of the contact (Kufareva et al., 2011); backbone and side-chains contacts are shown in black and grey, respectively.

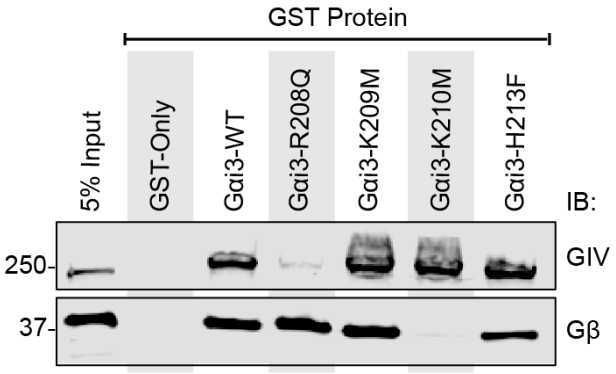

Figure 2.3: Biochemical confirmation of crystal structure findings. Western blot of GST pull-down assay of WT and mutant GST-tagged Gαi with GIV and G$\beta\gamma$ from HeLa lysate.

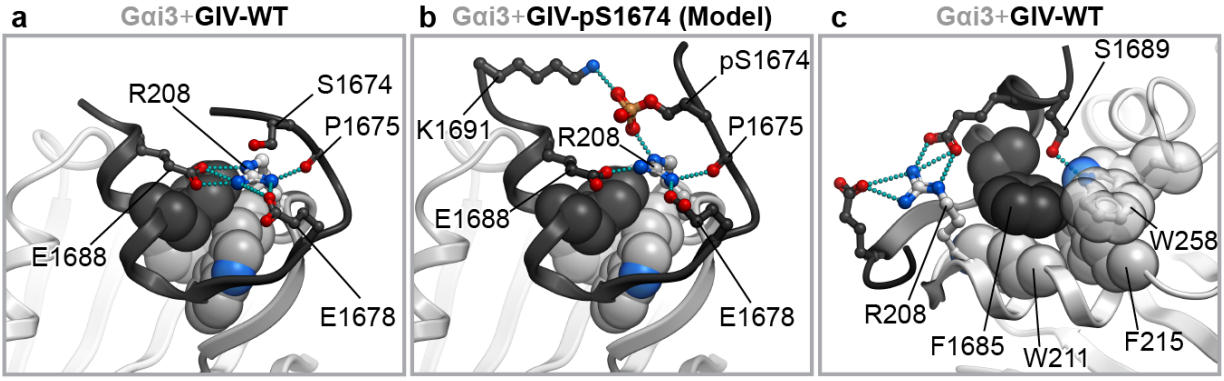

Figure 2.4: Structural basis for phosphoregulation of GIV binding and activity towards Gαi. a, Structure of WT GIV-GEM, highlighting unphosphorylated S1674 and the various contacts of R208 of Gαi. b, Model of (pS1674)GIV-GEM highlighting the formation of an additional direct contact with R208. c, Structure of WT GIV-GEM, highlighting a polar contact that unphosphorylated S1689 makes with W258 of Gαi.

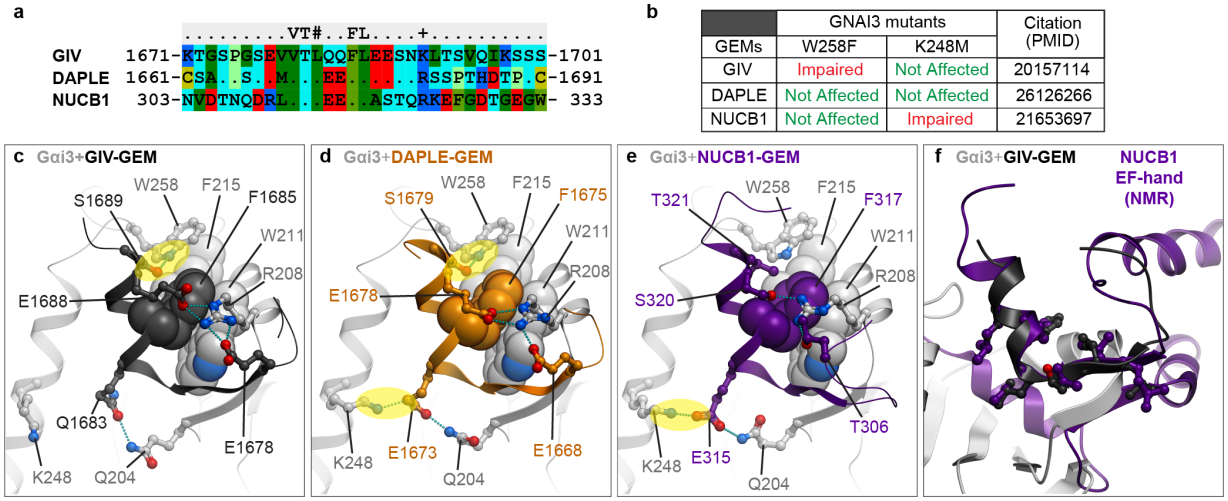

Figure 2.5: Homology models of Gαi:GDP bound to the various members of the GEM family suggest a conserved mechanism of binding and action. a, Sequence alignment of the GEM motifs within human GIV, Daple, and NUCB1 (Calnuc) sequences. b, Table summarizing previous mutagenesis studies. c, Crystal structure of GIV-GEM bound to Gαi. d-e, Homology models of (d) Daple and (e) NUCB1 bound to Gαi created using the GIV-GEM-bound structure as template. Hydrogen bonds explaining the mutagenesis in b are highlighted. f, Overlay of our GIV-GEM-bound Gαi structure with the EF-hand motif of NUCB1, previously determined by NMR (PDB 1SNL).

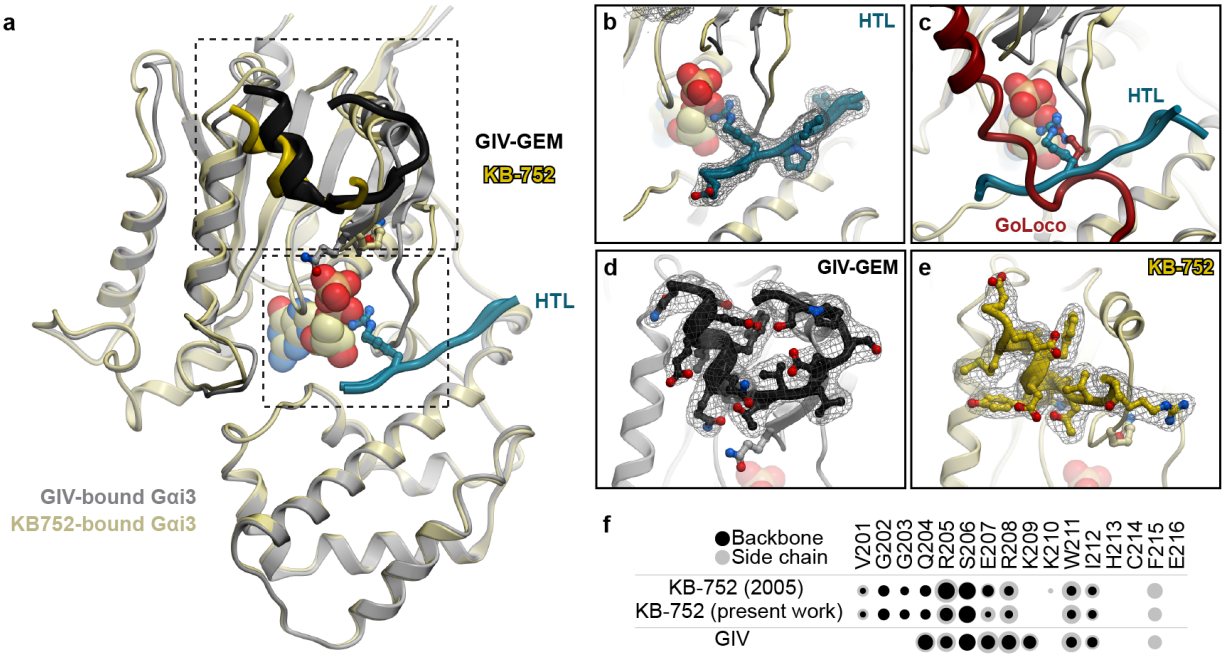

Figure 2.6: Structures of KB752-bound and GIV-GEM-bound Gαi:GDP. a, Overlay of our solved KB752-bound and GIV-GEM-bound Gαi:GDP structures. Boxed regions are highlighted in b-e. b, Fo-Fc electron density map around the His-tag linker in the Gαi:GDP structure with GIV-GEM is contoured at 3σ. c, Overlay of the His-tag linker with the GoLoco motif of GDI RGS14 (PDB 1KJY (Kimple et al., 2002)). d-e, Fo-Fc electron density maps around the GIV-GEM peptide (d) or KB752 (e) are contoured at 3σ. f, Bubble plot of the contacts between Sw-II residues of Gαi and the GIV peptide or the KB752 peptide, as seen in the previously published (2005) KB752-bound structure without the His-tag linker and our solved structures with the His-tag linker. The size of the dot is directly proportional to the strength of the contact (Kufareva et al., 2011).

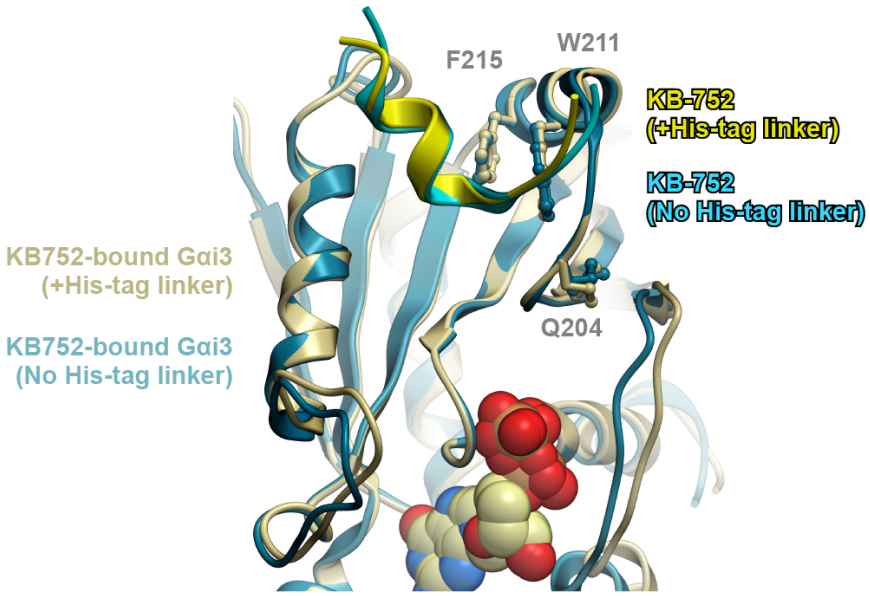

Figure 2.7: Comparison of structures of KB752-bound Gαi:GDP with (this work) and without (PDB 1Y3A) the His-tag linker. For clarity, only the GTPase domains of the G proteins are shown. The overlay demonstrates that the peptide interface is indistinguishable between the two structures.

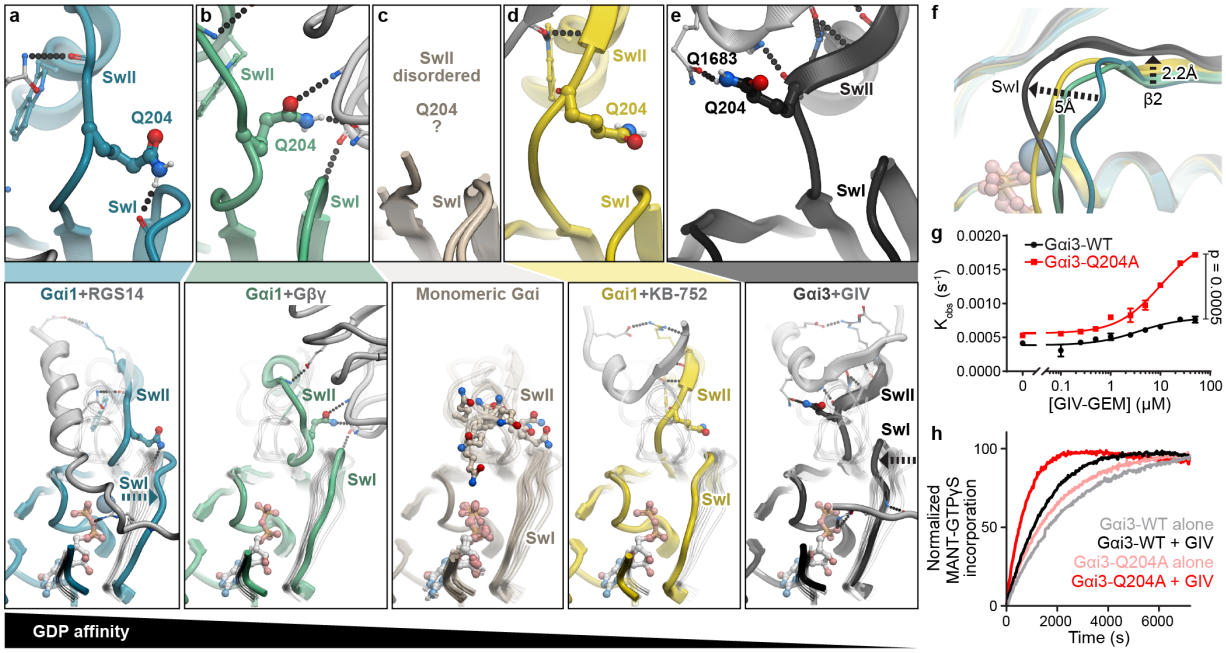

Figure 2.8: GIV binding to Sw-II of Gαi disrupts GDP-stabilizing interactions between Sw-II and Sw-I and induces a low-GDP-affinity conformation of Gαi. a-e, Comparison of Sw-I, Sw-II, and Q204 in various GDP-bound structures of Gαi, arranged from high (left) to low (right) GDP-affinity states. In the top part of (c), the only two existing structures of GDP-bound monomeric WT Gαi are shown, PDB: 1BOF and 1GDD, both with disordered Sw-II. f, Overlay of structures shown in a-b and d-e, highlighting differences in Sw-I and the β2-strand. g, MANT-GTPγS incorporation into WT and Q204A Gαi proteins was assessed in the presence of varying concentrations of WT GIV-GEM peptide. Findings are displayed as a line graph showing observed rates (kobs, s^{-1}) for nucleotide incorporation. Data shown is triplicates from a representative experiment; n = 3. h, Same data as in g presented as a line graph showing average nucleotide incorporation over time in the presence or absence of 50 μM WT GIV-GEM peptide. Statistical significance between means was calculated using multiple comparisons in one-way nonparametric ANOVA.

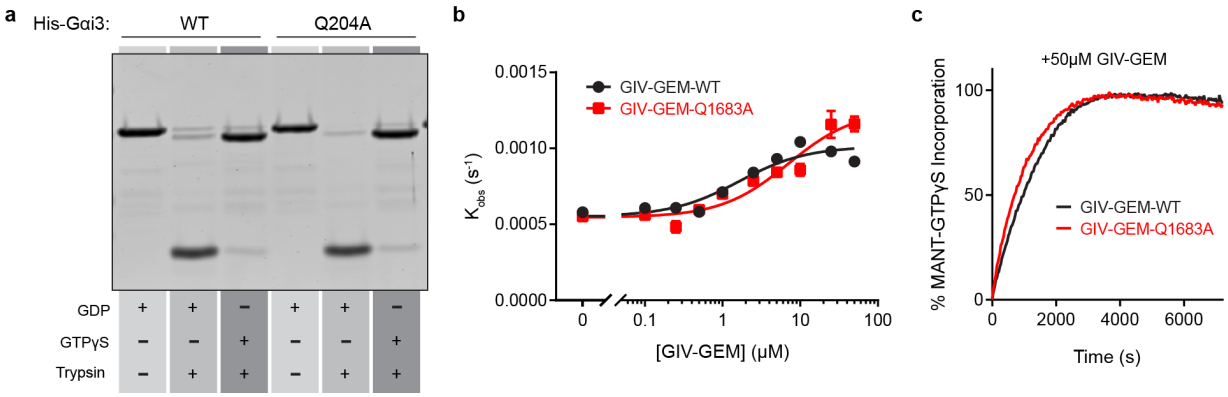

Figure 2.9: The polar contact observed in the crystal structure between GIV Q1683 and Gαi Q204 is dispensable for activation of Gαi by GIV-GEM. a, Coomassie stain of a trypsin proteolysis assay performed on WT and Q204A mutant Gαi proteins loaded with GDP or GTPγS. b-c, MANT-GTPγS incorporation into Gαi was assessed in the presence of increasing concentrations of WT and Q1683A mutant GIV-GEM proteins. Findings are displayed as a line graph (b) showing observed rates (kobs, s^{-1}) for nucleotide incorporation and as line graphs (c) showing average nucleotide incorporation over time. Data shown is triplicates from a representative experiment; n = 3.

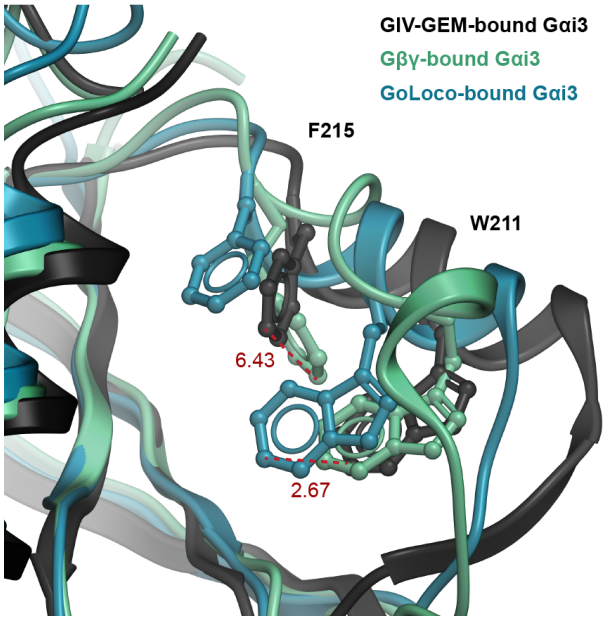

Figure 2.10: Positions of W211 and F215 in various Gαi3 structures. Overlay of the Sw-II regions of our solved GIV-GEM-bound Gαi:GDP structure, the G$\beta\gamma$-bound Gαi:GDP structure (PDB 1GP2 (Wall et al., 1995)), and the GoLoco-bound Gαi:GDP structure (PDB 1KJY (Kimple et al., 2002)). Side chains of W211 and F215, as well as distances of these residues between structures, are displayed.

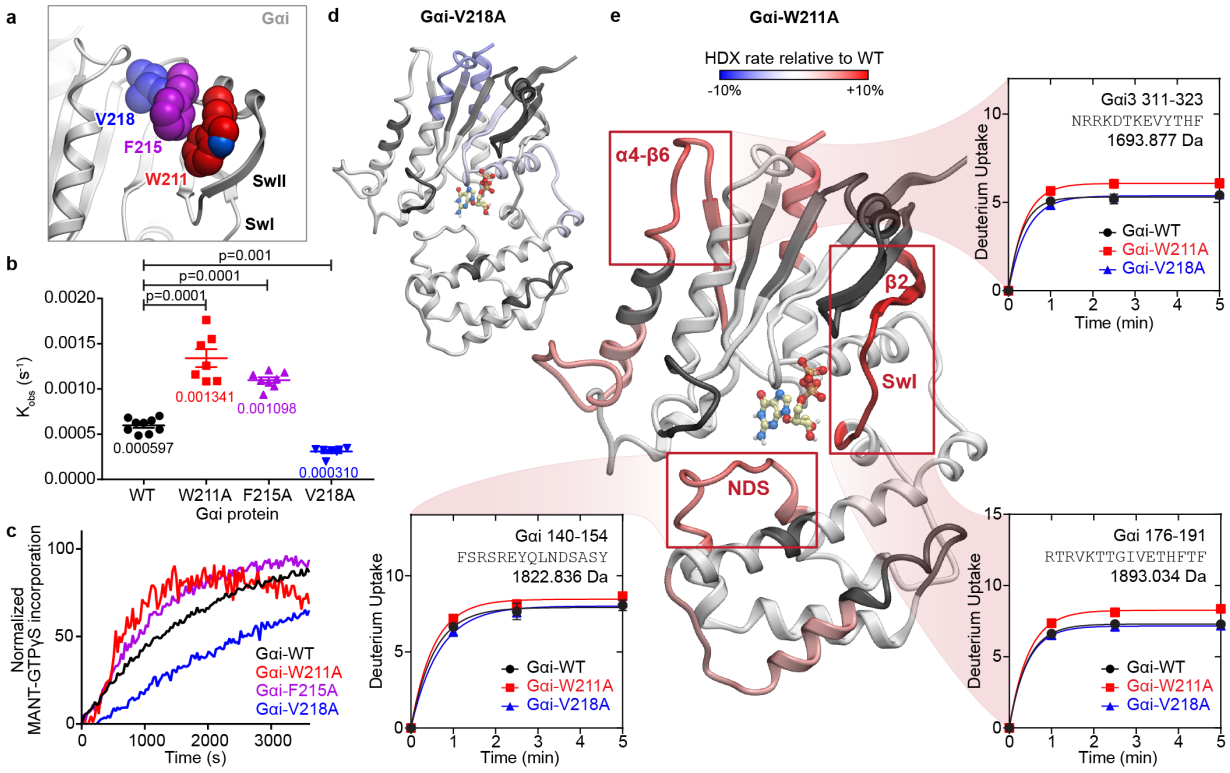

Figure 2.11: Bulky hydrophobic residues in Sw-II of Gαi that are engaged by GIV stabilize GDP and influence the dynamics of Sw-I and the β2-strand. a, Structure showing hydrophobic residues in Sw-II of Gi that were subjected to mutagenesis. b-c, MANT-GTPγS incorporation into WT, W211A, F215A, and V218A Gαi. Findings are displayed as a dot plot (b) showing the observed nucleotide incorporation rates (kobs, s^{-1}) and as line graphs (c) showing average nucleotide incorporation over time. Data shown is from three independent experiments; n = 9, 7, 8 and 7 for WT, W211A, F215A, and V218A, respectively. d-e, Differences in relative deuterium uptake between V218A and WT Gαi (d) and between W211A and WT Gαi (e) at 5 min, as determined by triplicate HDX-MS assays. Blue and red coloring corresponds to -10% and +10% change, respectively, black indicates regions that were not mapped. Regions exhibiting increased uptake in the W211A mutant are highlighted and the corresponding deuterium uptake plots shown (standard deviation error bars are within the symbols). Statistical significance between means was calculated using multiple comparisons in one-way nonparametric ANOVA.

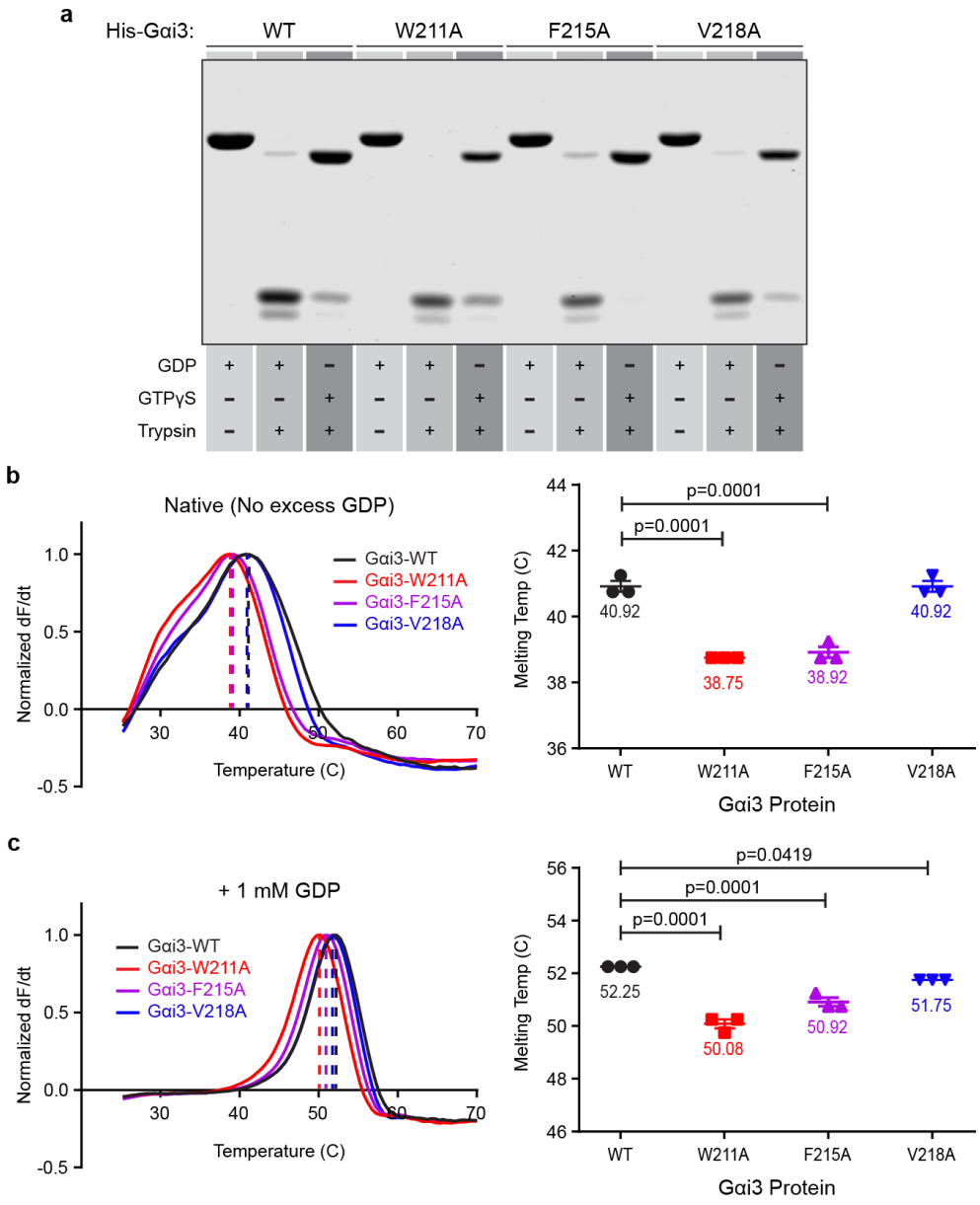

Figure 2.12: Trypsin proteolysis and thermal shift assays support the GDP-stabilizing role of Sw-II residues W211 and F215. a, Coomassie stain of a trypsin proteolysis assay performed on WT and Sw-II mutant Gαi proteins loaded with GDP or GTPγS. b, WT and Sw-II mutant Gαi proteins were subjected to increasing temperatures in differential scanning fluorimetry (thermal shift) assay. Findings are displayed as a line graph (left) showing average normalized dF/dt curves of native (no excess GDP added) WT and Sw-II-mutant Gαi proteins or as dot plot (right) showing the melting temperatures of native WT and Sw-II-mutant Gαi proteins. Peaks of the curves (left) represent protein melting temperatures. Data shown are triplicates from a representative experiment; n = 3. c, Same as in b except 1 mM GDP was added.

Figure 2.13: Coverage map and deuterium uptake plots for HDX assays. a, Sequence coverage of Gαi following pepsin digestion, LC separation, and MS/MS detection. Blue bars represent distinct peptides. b, Plots showing deuterium uptake for distinct peptides at various time points. Experiments were performed in triplicate and standard deviation error bars are shown (although most are within the symbols).

a **Total: 21 Peptides, 72.0% Coverage, 1.11 Redundancy**

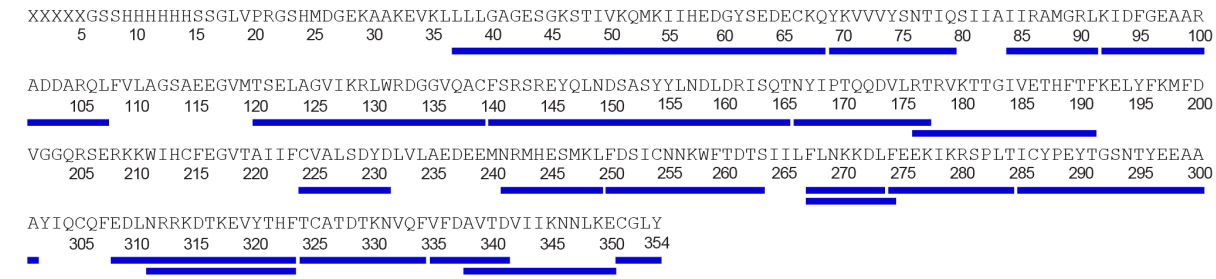

b

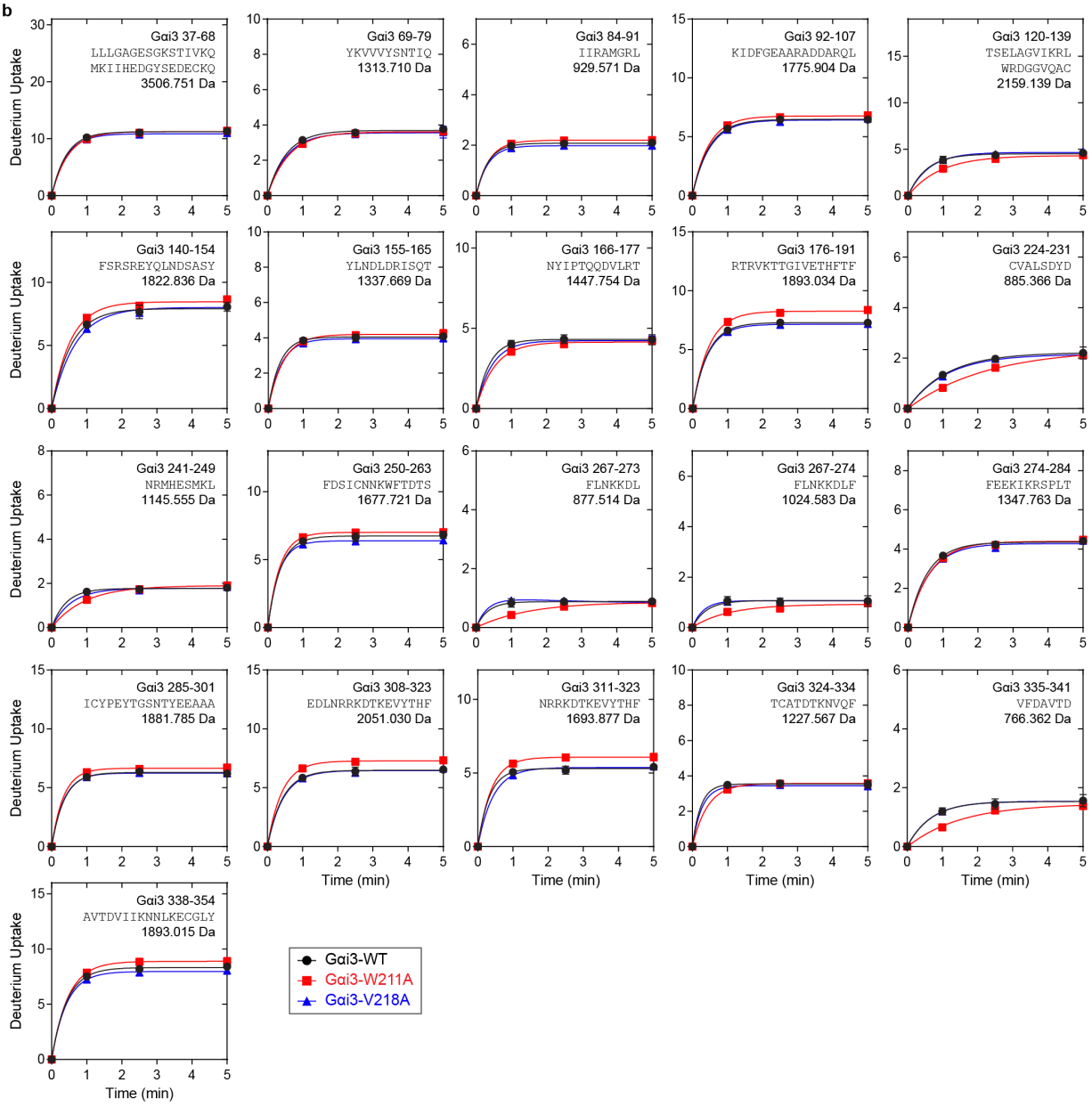

Figure 2.14: Binding of GIV-GEM overcomes the GDP-stabilizing role of Sw-II and releases conformational constraints on Sw-I, β2-β3 strands, and the hydrophobic core of the GTPase domain. a, Root Mean Square Fluctuations (RMSF, Å) of Gαi residues as determined by molecular dynamics simulations under the three specified conditions. b, Representative histograms showing the distribution, across all simulation frames, of residue Root Mean Square Deviation (RMSD) in relation to the mean position of the same residue (F191 in the left panel and Q204 in the right panel). c, Residue RMSF differences between the GIV-GEM-bound Gαi:GDP and Gαi:GDP alone mapped onto the structure of Gαi. d, Intramolecular distances where the most significant changes between the two simulation conditions (as in c), as determined by PCA, are shown as dotted lines; significant distances beyond the hydrophobic core are colored silver. e, Representative frames from the MD simulations highlighting the conformational changes allosterically induced by GIV-GEM, and perturbation of key interactions in the hydrophobic core of Gαi. f, Distribution of inter-residue distances for the indicated residue pairs throughout the molecular dynamics simulations.

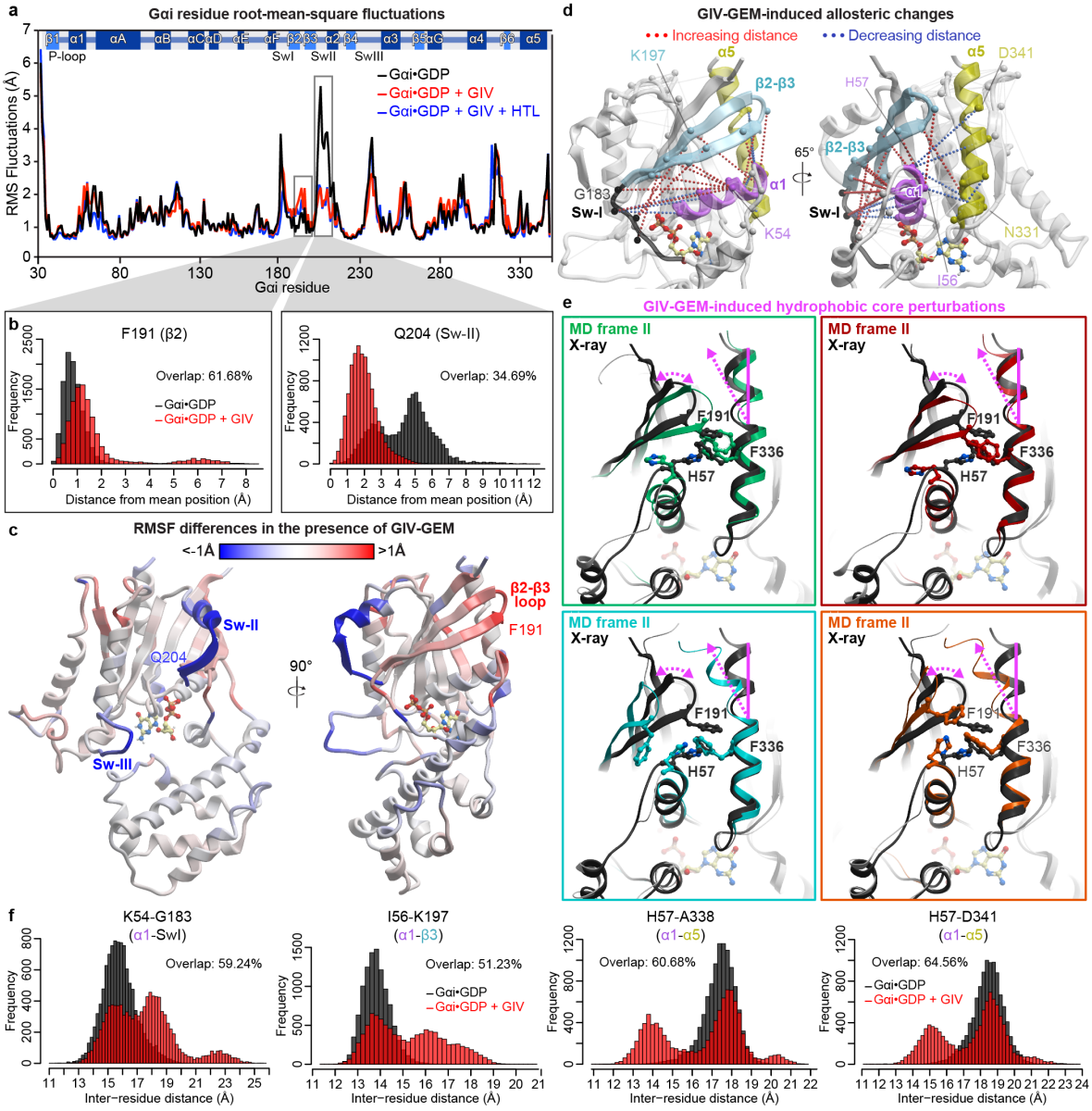
a
Gαi residue root-mean-square fluctuations
RMS Fluctuations (Å)
Gαi residue
P-loop
SwI
SwII
SwIII
–Gαi•GDP
–Gαi•GDP + GIV
–Gαi•GDP + GIV + HTL
b
F191 (β2)
Overlap: 61.68%
Q204 (Sw-II)
Overlap: 34.69%
Frequency
Distance from mean position (Å)
c
RMSF differences in the presence of GIV-GEM
<-1Å
>1Å
Sw-II
Sw-III
Q204
β2-β3 loop
F191
90°
d
GIV-GEM-induced allosteric changes
Increasing distance
Decreasing distance
K197
α5
β2-β3
α1
G183
Sw-I
K54
H57
D341
65°
N331
I56
e
GIV-GEM-induced hydrophobic core perturbations
MD frame II
X-ray
F191
F336
H57
f
K54-G183
(α1-SwI)
Overlap: 59.24%
I56-K197
(α1-β3)
Overlap: 51.23%
H57-A338
(α1-α5)
Overlap: 60.68%
H57-D341
(α1-α5)
Overlap: 64.56%
Inter-residue distance (Å)

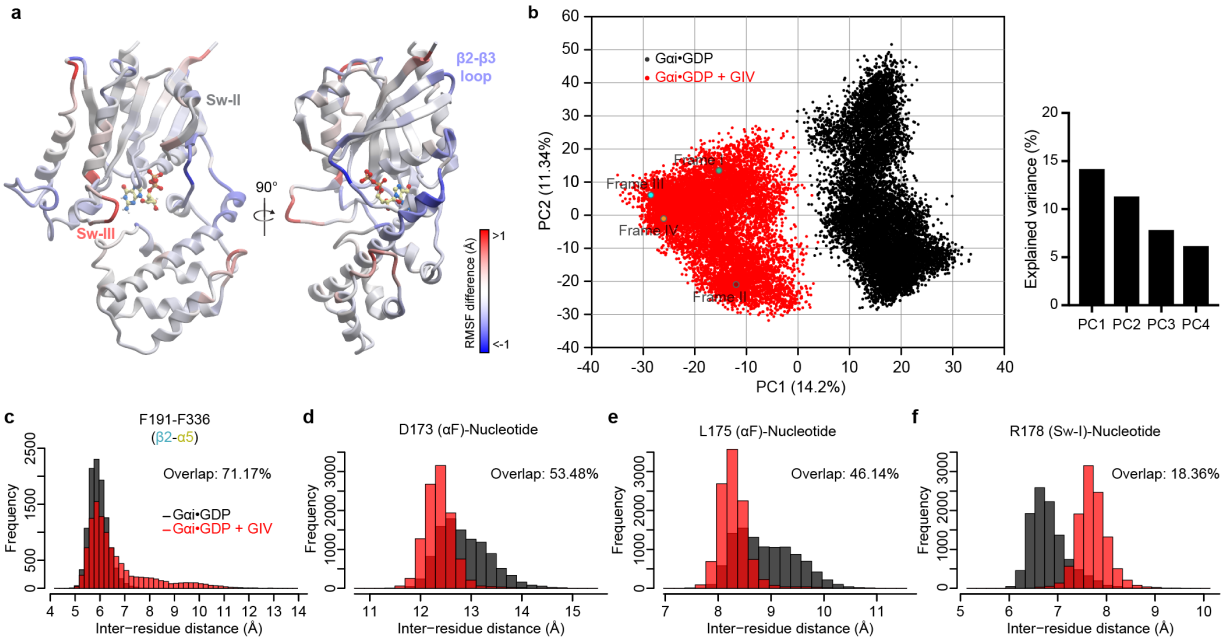

Figure 2.15: MD simulations support the stabilizing role of the His-tag linker and identify GIV-GEM-induced structural changes. a, Residue RMSF differences between the GIV-GEM-bound Gαi:GDP with the His-tag linker and GIV-GEM-bound Gαi:GDP without the His-tag linker are mapped onto the structure of Gαi. b, (Left) Plot displaying first two principal components as identified by the Principal Component Analysis (PCA) of inter-residue distances in the Gαi:GDP and GIV-GEM-bound Gαi:GDP simulations. Each dot represents an MD frame taken with an interval of 100 ps. (Right) Bar graph showing % variance explained by each of the first four principal components. The position of the representative frames depicted in Figure 6e are highlighted and color matched to each respective protein backbone color. c-f, Histograms showing inter-residue distances (c) or the distances between the indicated residues and GDP (d-f) throughout the duration of molecular dynamics simulations.

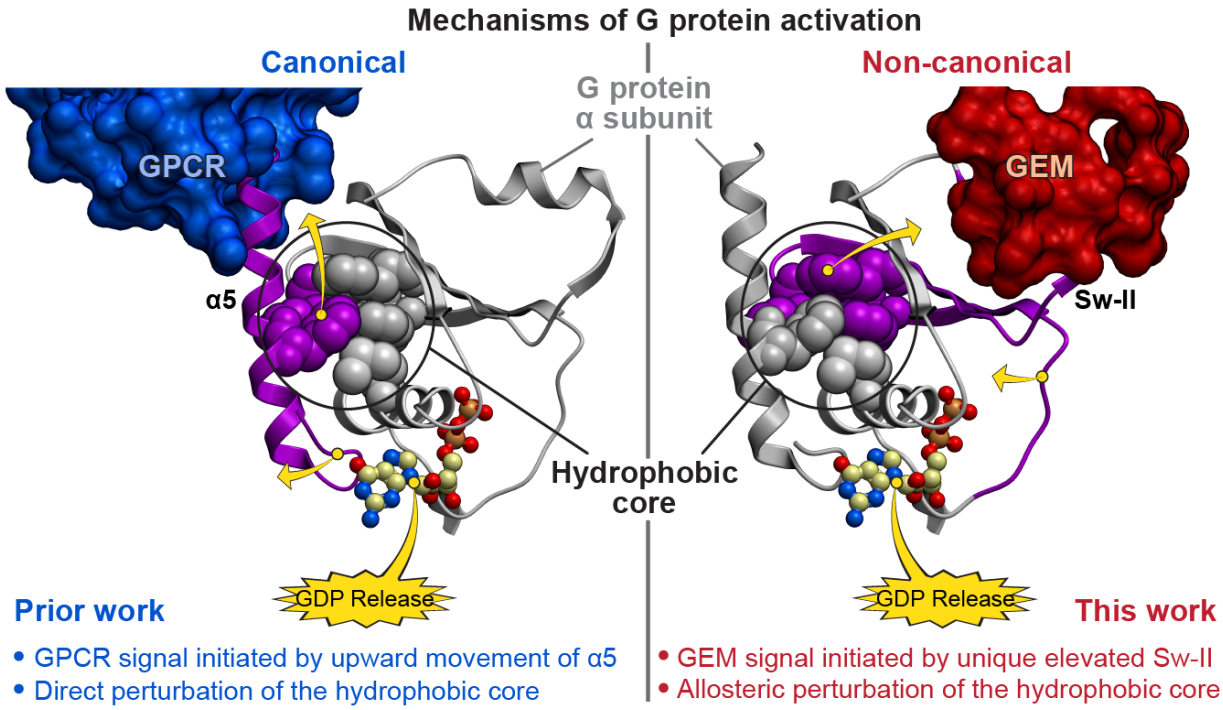

Figure 2.16: GEMs and GPCRs bind at non-overlapping interfaces on Gαi but both perturb the hydrophobic core of the GTPase domain to stimulate GDP release. Left, Structure displaying GPCR interface and subsequent Gαi dynamics that ultimately result in GDP release. Right, Structure displaying GEM interface and subsequent Gαi dynamics that ultimately result in GDP release. Purple color highlights regions of Gαi that move during activation, while yellow arrows describe the direction those regions move. For clarity, only part of the GTPase domain of Gαi is shown.

Chapter 3

Other contributions: Investigating a novel RTK-G protein cross-talk pathway and its potential role in cancer progression

The molecular mechanisms by which receptor tyrosine kinases (RTKs) and heterotrimeric G proteins, two major signaling hubs in eukaryotes, independently relay signals across the plasma membrane have been extensively characterized. How they may work together has been a long-standing question in the field of signal transduction but remains understudied. Previously, our lab used linear-ion-trap mass spectrometry in combination with biochemical, cellular, and computational approaches to unravel a unique mechanism of activation of heterotrimeric G proteins via direct phosphorylation by RTKs. Upon growth factor

stimulation, the guanine-nucleotide exchange modulator, GIV, dissociates resting Gαi$\beta\gamma$ trimers to bring monomeric Gαi subunits to the proximity of RTKs and facilitates their direct phosphorylation on two tyrosines located within the inter-domain cleft. Such tyrosine phosphorylation triggers activation of Gαi to modulate second messenger (cAMP) levels. Since the discovery of this unpublished novel cross-talk mechanism between RTKs and Gαi, I have worked to further characterize these phosphorylation events and investigate how this pathway may be aberrantly regulated in cancer and contribute to cancer progression. Both phospho-mimics and cancer mutations on these tyrosine residues disrupt an intricate network of hydrogen bonds within Gαi, resulting in decreased G protein thermal stability, increased G protein activation, and altered cell behavior.

3.1 Introduction

The phenotypic response of a cell is determined by the transduction and integration of a wide variety of extracellular signals to the interior of the cell. The transmission of these molecular signals is mediated by a complex array of proteins at the plasma membrane that partake in defined signaling pathways. In eukaryotes, two of the most widely studied signaling pathways are receptor tyrosine kinase (RTK) signaling and heterotrimeric G protein signaling.

Upon ligand binding, growth factor receptor tyrosine kinases (RTKs) become autophosphorylated on their cytoplasmic tails, creating docking sites for the recruitment and phosphorylation of a variety of adaptor proteins that propagate the signal to the cells interior (Gschwind et al., 2004). In contrast, heterotrimeric G proteins serve as molecular switches, canonically acting downstream of 7 transmembrane domain G protein-coupled receptors (GPCRs) (Gilman, 1987, Morris and Malbon, 1999). Agonist-bound GPCRs act as receptor guanine-nucleotide

exchange factors (GEFs) for heterotrimeric G proteins, triggering Gα GDP to GTP exchange and the release of G$\beta\gamma$ subunits; GTP-bound Gα subunits and G$\beta\gamma$ dimers go on to bind and transduce signals via a variety of effectors.

Despite being distinct signaling pathways, it has been widely demonstrated that RTK and GPCR/G protein pathways cross-talk to form an integrated signaling network (Lowes et al., 2002, Piiper and Zeuzem, 2004, Natarajan and Berk, 2006, Shah and Catt, 2004, Di Liberto et al., 2019). G protein-dependent activation of RTKs and RTK-dependent activation of GPCR/G protein intermediates can both occur indirectly by upregulation of ligand synthesis as well as directly by physical interaction (Daub et al., 1996, Luttrell et al., 1999, Schafer et al., 2004, Ohtsu et al., 2006, Prenzel et al., 1999, Guidolin et al., 2015, Sun et al., 1995, Poppleton et al., 1996, Marty and Ye, 2010, Nair et al., 1990, Sun et al., 1997). The close interplay between kinases (RTKs and non-RTKs) and G proteins within these networks has spurred the identification of phosphorylation sites on G protein subunits that act to regulate G protein activity, however in-depth mechanisms into how these phosphorylations occur and function are lacking (Poppleton et al., 1996, Liang and Garrison, 1991, Nair et al., 1990, Sun et al., 1997, O'Brien et al., 1987, Krupinski et al., 1988).

Adding to the intricate interplay between RTKs and G proteins is a recently discovered, non-canonical set of G protein modulators, guanine-nucleotide exchange modulators (GEMs) (Gupta et al., 2016, Ghosh et al., 2017). GEMs are cytosolic proteins that uniquely act as non-receptor GEFs to activate Gαi and as guanine-nucleotide dissociation inhibitors (GDIs) to inhibit Gαs, all using the same evolutionarily conserved GEM motif (Gupta et al., 2016). The first and most well-studied member of the GEM family is Gα-Interacting Vesicle associated protein (GIV or Girdin). GIV is a large, multi-domain signal transducer that modulates G protein signaling

downstream a myriad of cell surface receptors, including growth factor RTKs, integrins, and GPCRs (Aznar et al., 2016, Lin et al., 2011, Ghosh et al., 2008, Garcia-Marcos et al., 2011, Garcia-Marcos et al., 2010, Garcia-Marcos et al., 2009, Ghosh, 2015). The unique combination of the GEM motif and an SH2-like domain within GIV's C-terminus stimulates the formation of an RTK-GIV-Gαi ternary complex, resulting in Gαi activation downstream of activated, autophosphorylated RTKs (Lin et al., 2014, Ghosh et al., 2010). GIV-dependent signaling has been implicated in a number of pathophysiologic conditions, including diabetes, fibrosis, and cancer (Leyme et al., 2015, Bhandari et al., 2015, Lopez-Sanchez et al., 2014, Ma et al., 2015, Wang et al., 2015, Hartung et al., 2013).

3.2 Summary of key discoveries prior to my arrival

RTKs phosphorylate Gαi within the inter-domain cleft in a GIV-dependent manner

Prior works have suggested that RTKs and downstream activated non-receptor tyrosine kinases (non-RTKs) phosphorylate G proteins (Chakravorty and Assmann, 2018). Previous studies (largely high throughput mass spectrometry studies) also documented phosphorylation of Gαi on a handful of tyrosines (Figure 3.1); among these, phosphorylation or Gαi by the non-RTK c-src has been the most studied (Hausdorff et al., 1992, Moyers et al., 1995).

When I entered the lab, it had recently been discovered that Gαi (but not Gαs or Gαo) is directly and abundantly (70%) phosphorylated by multiple growth factor RTKs in vitro (Figure 3.2a). The lab previously demonstrated that, upon ligand stimulation, the GEM protein GIV directly and simultaneously binds both Gαi3 and the autophosphorylated cytoplasmic tails of activated RTKs to form ternary RTK-GIV-Gαi3 signaling complexes (Figure 3.2b; (Lin et al.,

2014, Ghosh et al., 2010)). Thus, the obvious question was whether the close proximity of Gαi3 to the RTK in the RTK-GIV-Gαi3 complex may allow direct phosphorylation of Gαi3 by RTKs in cells. Using WT and a GEM-deficient mutant (F1685A) GIV that cannot bind Gαi, it was shown that Gαi is phosphorylated in cells, the GIV-Gαi interaction is necessary for the assembly of ternary RTK-GIV-Gαi complexes, and the GIV-Gαi interaction is essential for RTKs to phosphorylate Gαi in cells (Figure 3.2c).

Phosphorylation on Y154, Y155, and Y320 of Gαi by RTKs is essential for G protein activation

To determine the RTK phosphorylated tyrosines in Gαi3, the lab used linear-Ion-Trap mass spectrometry (Douglas et al., 2005) to analyze both in vitro EGFR phosphorylated Gαi3 and Gαi3 phosphorylated in cells in response to EGF stimulation. Using this method, three novel sites of EGFR tyrosine phosphorylation were identified in both the in vitro and in cell phosphorylated samples, namely Y154, Y155, and Y320 (Figure 3.3a). The same approach with insulin-stimulated cells showed phosphorylation at the same three sites, indicating that this signaling mechanism is not limited to EGFR and is conserved across multiple RTKs. Individual and combinatorial non-phosphorylatable Tyr to Phe mutations in Gαi3 at these RTK-targeted sites (Y154F, Y155F, Y320F) confirmed that these are the only substrate sites for RTKs in vitro (Figure 3.3b), and they account for the observed tyrosine phosphorylation in vivo after EGF and insulin stimulation.

In vitro kinase assays and in cell phosphorylation assays with either overexpression of constitutively active Src kinase or inhibition of Src family kinases with PP2 also demonstrated that the RTK phosphorylation sites on Gαi are non-overlapping with those that are targeted by

Src. Moreover, using the phosphorylation-deficient Tyr to Phe mutants, tyrosine phosphorylation of Gαi was shown to be essential for enhanced and sustained activation of the G protein (by active conformation Gαi:GTP-specific antibodies (Lane et al., 2008) and by Gαi FRET activity reporter (Bunemann et al., 2003)) and inhibition of cellular cAMP (by radioimmunoassay (Lin et al., 2014)) in cells responding to growth factors (EGF and insulin).

Gαi-Y154H cancer mutation results in a hyperactive G protein

In addition, genetic alteration of this pathway was found to occur in tumors. Using the cBioPortal database, it was found that both of the key RTK-phosphorylated tyrosines (Y154 and Y155) on Gαi are mutated in cancers of the liver (Y154H, 3 tumors), lung (Y155S, 2 tumors), and blood (Y154D, 1 tumor). Since Y154 was the most phosphorylated tyrosine by mass spectrometry and since Y154H was the most common mutation found at these sites, the Y154H mutation was chosen to move forward with for further investigation. A Gαi3-Y154H mutant exhibited increased basal nucleotide exchange in vitro and a higher basal activation state in cells (by Gαi FRET activity reporter).

3.3 My contributions

My contributions to this project focused on further validating and characterizing phosphorylation at these RTK targeted tyrosines within Gαi, as well as further investigating the role of phosphorylation and mutation of these tyrosines on G protein structure and activity and how they may affect overall cell behavior.

Further validation of the RTK-targeted phosphorylation sites

To further validate these RTK phosphorylation sites, we developed a custom antibody against the dually phosphorylated pY154/pY155 Gαi3 protein; this antibody will henceforth be referred to as the pYpY-Gαi antibody. In vitro EGFR kinase assays were conducted on various Tyr to Phe Gαi3 mutants, ran on Phos-tag SDS-PAGE gels to separate proteins by size and phosphorylation status (Kinoshita et al., 2006, Kinoshita-Kikuta et al., 2007), and then immunoblotted with the pYpY-Gαi antibody (Figure 3.4a). We found that multiple phospho forms of Gαi3 are detected by the pYpY-Gαi antibody after in vitro EGFR phosphorylation of Gαi3-WT (Figure 3.4a); this is consistent with several phosphorylated forms being detected by mass spectrometry as well. Mutating either Y154 or Y155 to a non-phosphorylatable phenylalanine completely abolished the phosphorylation detected by the pYpY-Gαi antibody, while the Gαi3-Y320F mutant showed comparable levels of phosphorylation to Gαi3-WT (Figure 3.4a).

Impact of RTK phosphorylation and Y154H cancer mutation on Gαi3 structure and activity

The location of the RTK-targeted tyrosines within the folded G protein structure provides clues about what the structural consequences of such tyrosine phosphorylation may be (Figure 3.4b). Y154 and Y155 are positioned within the inter-domain cleft on the αE helix facing towards the αF helix and Sw-I (Figure 3.4b). All currently available structures of inactive (GDP-bound) Gαi and active (GDP-AlF4- or GTPγS-bound) Gαi show that Y154 and Y155 are not accessible and thus cannot be phosphorylated when Gαi is bound to nucleotide. The fact that Y154 and Y155 are in the inter-domain cleft and inaccessible in the closed, nucleotide-bound state led us to hypothesize that perhaps domain opening and nucleotide release are required to expose the

tyrosines prior to phosphorylation. However, the several available structures of nucleotide-free Gαi bound to GPCRs (Rasmussen et al., 2011, Zhang et al., 2017, Qi et al., 2019, Kang et al., 2018) reveal that Y154 and Y155 are still not accessible for phosphorylation in the open, nucleotide-free state. Moreover, phosphorylation of Y154 and Y155 is predicted to disrupt an intricate network of hydrogen bonds between the αE helix, αF helix, and Sw-I (Figure 3.4c) and destabilize the overall G protein structure. This suggests that a novel structural alteration of the G protein is necessary to accommodate phosphorylation of these tyrosines.

In order to assess the structural and functional consequences that disruption of this hydrogen bond network may cause, we used WT and mutant G protein constructs in differential scanning fluorimetry (thermal shift) and nucleotide exchange assays. The phospho-deficient Y154F/Y155F/Y320F (referred to as 3YF) Gαi3 mutant was used to assess what effect the absence of these hydrogen bonds would have, and a phospho-mimicking Y154E mutant was also made to assess what the consequences of phosphorylation at that site would be. After numerous purification attempts, we were unable to purify a Y155E Gαi protein. It should be acknowledged that although Tyr to Glu mutations are rather poor phospho-tyrosine mimics in terms of shape and size, they can be informative in regard to the possible consequences of a negative charge at that site. Furthermore, we also tested the Y154H cancer mutation to see its affects on G protein stability.

Using limited proteolysis assay, we first confirmed that all WT and mutant Gαi proteins being tested were capable of binding nucleotides and adopting an active conformation. We then conducted thermal shift assays to determine if the overall thermal stability of the protein had been affected by the mutations. We found that the Y154E mutation most greatly affected Gαi protein stability. In fact, the melting temperature (Tm) of Gαi3-Y154E in the native state

could not be determined in these experiments because the protein was so unstable (Figure 3.5a). Furthermore, the Tm of nucleotide-bound Gαi3-Y154E was significantly lower compared to nucleotide-bound WT protein (-10.75°C Tm change for the GDP-bound state and -7.5°C Tm change for the GTPγS-bound state; Figure 3.5b-c). In addition, Gαi3-Y154H was also less thermally stable compared to Gαi3-WT in the native (-2°C Tm change), GDP-bound (-5.75°C Tm change), and GTP-bound (-4.5°C Tm change) states (Figure 3.5a-c). Notably, the Gαi3-3YF mutant exhibited comparable thermal stability to the WT protein in all states (Figure 3.5a-c). Collectively, these results suggest that loss of the hydrogen bond network in the αE-αF region alone is not sufficient to significantly alter G protein stability. The Y154E and Y154H mutations must further alter intramolecular interactions to produce the observed decrease in thermal stability.

To determine if the structural changes in the Gαi3-Y154E and Gαi3-Y154H mutants that were causing decreased thermal stability affected G protein activation, we conducted nucleotide exchange assays to measure the rate of GDP to GTP exchange in the WT and mutant Gαi3 proteins (Figure 3.6a-b). Indeed, we found that both the Y154E and Y154H G protein mutants had increased rates of basal nucleotide exchange compared to Gαi3-WT (15.6-fold and 5-fold increases, respectively; Figure 3.6a-b). No significant difference in basal nucleotide exchange rate was detected between Gαi3-WT and Gαi3-3YF (Figure 3.6a-b). These results suggest that cancer mutations at Y154 or Y155, and perhaps tyrosine phosphorylation at these sites as well, regulate G protein activation.

Gαi3-Y154H mutation alters tumor cell behavior

The lab previously described that GIV-dependent activation of Gαi3 promotes behavioral features of metastatic tumor cells such as enhanced cell migration and PI3K-Akt signaling (Ghosh et al., 2011). We reasoned that tyrosine phosphorylation of Gαi may play a role in these processes as well because it also enhances G protein activation and depends on GIV. Thus, we investigated what effect the Gαi3-Y154H cancer mutant may have on cell migration. Using 2D scratch wound migration assays, we found that cells expressing the Gαi3-Y154H cancer mutant exhibited increased cell migration compared to Gαi3-WT expressing cells under 2% FBS conditions (23.9% more wound closure; Figure 3.7a-b). Cells expressing Gαi3-3YF did not show any significant change in wound closure compared to cells expressing Gαi3-WT (Figure 3.7a-b). These data suggest that enhanced signaling through this novel RTK-G protein signaling pathway, via mutation or phosphorylation of the RTK-targeted tyrosines, can drive a pro-metastatic tumor cell phenotype.

3.4 Discussion

The main goal of my contributions to this project was to investigate the consequences of tyrosine phosphorylation and tyrosine mutation on Gαi protein stability and activity. Here we used a Y154E mutation to assess the effect that phosphorylation of Y154 may have on G protein structure and function. As mentioned previously, Tyr to Glu mutations are poor phospho-tyrosine mimics in terms of shape and size. An alternative approach for mimicking a phospho-tyrosine would be to utilize the non-natural amino p-carboxylmethylphenylalanine (pCMF). Incorporation of pCMF at sites 154 and 155 of Gαi would likely provide a more biologically accurate tool to

study the consequences of phosphorylation at these tyrosine sites.

It is interesting to consider how Y154 and Y155 become exposed in order to be phosphorylated. Gαi domain opening is clearly required but apparently not sufficient to make the tyrosines accessible to RTKs. Moreover, it is well-established that kinases in general prefer linear substrates (Kettenbach et al., 2012, Ubersax and Ferrell, 2007). Since Y154 and Y155 are on the small αE helix, partial unfolding of the G protein helical domain (or at least of the αE helix) is likely also necessary to fully expose these tyrosines in a linear form that can be subsequently targeted and phosphorylated by RTKs. Thus, just as the field was unaware of G protein domain opening and closing a mere decade ago, there are likely still important dynamic motions taking place throughout the G protein activation process that are yet to be discovered.

It is not entirely clear what structural changes occur upon phosphorylation of Y154 and Y155, or in cancer mutations at these sites, that result in decreased stability and increased G protein activation. We speculate that there are several structural changes occurring simultaneously to alter G protein stability and function. The position of Y154 and Y155 within the inter-domain cleft near the packing contacts between the Ras-like and Helical domains of the G protein leads us to believe that phosphorylation may affect domain opening. Recently, MD simulation studies have suggested that domain opening is not sufficient for GDP release (Dror et al., 2015), but nonetheless, altered domain opening may affect overall stability of the G protein. In addition, the proximity of Y154 and Y155 to the nucleotide binding pocket raises the possibility that tyrosine phosphorylation may affect residues that have direct contact with the nucleotide, with the most likely candidate being the αD-αE loop that includes the so-called NDS motif. Alternatively, a parallel mechanism may involve Sw-I. A recent study by our group investigating the structural mechanism of GIV-mediated Gαi activation identified Sw-I as a key determinant of

an allosteric activation mechanism that proceeds through the hydrophobic core of the G protein (Chapter 2). Because Y154 and Y155 both face towards αF and Sw-I, particularly Y155, we believe that phosphorylation of these tyrosines would likely affect the position and stability of Sw-I and may affect G protein function through this allosteric activation mechanism. This possible shared mechanism may also explain potential synergy between G protein activation mediated directly by GIV-binding and by tyrosine phosphorylation.

The novel signaling cross-talk described here between RTKs and G proteins has vast implications for disease. Data presented here demonstrate that this RTK-dependent G protein phosphorylation pathway can be hijacked by cancers to promote a pro-metastatic phenotype. In this study, we investigated a cancer mutation at Y154, however it is likely that cancers can also hijack this pathway through upregulation of the pathway, resulting in hyper G protein phosphorylation and again pro-tumor behaviors. For example, studies have shown that upregulation of GIV in tumors is correlated with poorer prognosis (Dunkel et al., 2016), possibly in part due to a concomitant increase in G protein tyrosine phosphorylation. Furthermore, many primary and therapy-resistant tumors are driven by overexpression of RTKs or mutations in RTKs that make them constitutively active (Regad, 2015); in these contexts, hyper G protein phosphorylation is again likely to be observed. These cases may represent opportunities for novel therapeutic intervention by targeting this RTK-dependent G protein phosphorylation pathway.

3.5 Materials and Methods

Reagents and antibodies

Unless otherwise indicated, all reagents were of analytical grade and obtained from Sigma-Aldrich. Cell culture media were purchased from Invitrogen. EGF and insulin were obtained from Invitrogen and Novagen, respectively. Recombinant EGFR, PDGFR, VEGFR, InsR and Src were purchased from Cell Signaling Technology. PP2 was obtained from Calbiochem. Silencer Negative Control scrambled (Scr) siRNA and Gαi3 siRNA were purchased from Ambion and Santa Cruz Biotechnology, respectively. Antibodies against GIV that were used in this work include affinity-purified anti-GIV coiled-coil IgG and anti-GIV-CT (Santa Cruz Biotechnology). Anti-Gαi3:GTP (6-F12) was a gift from Dr. Graeme Milligan. Rabbit polyclonal antibodies used in this work were Gαi3 (C-10) and pan-Gβ (M-14) (Santa Cruz Biotechnology) and phospho-AKT Ser 473 (Cell Signaling). The rabbit anti-Gαi-pY154/pY155 (pYpY-Gαi) antibody was custom made (21st Century) for use in these studies. Mouse mAbs against pTyr (BD Biosciences), hexahistidine, FLAG and α-tubulin (Sigma) were obtained commercially. Control mouse and rabbit IgGs for immunoprecipitations were purchased from Bio-Rad and Sigma, respectively.

Plasmid constructs, mutagenesis and protein expression

Cloning of Gαi1/2/3, Gαs, Gαo and GIV-CT into pGEX-4T-1 or pET28b and rat Gαi3 and GIV into p3XFLAG-CMVTM-14 were described previously (Garcia-Marcos et al., 2009). GST-TrkA-CT (aa 448-552) was a gift from Dr M.G. Farquhar and was used previously (Garcia-Marcos et al., 2009). Mutants of rat Gαi3 (Y154F, Y155F, Y320F, Y154/155F, Y155/320F, and Y155/155/320F) were generated using QuickChange II (Stratagene) and specific primers

(sequence available upon request) following the manufacturers instructions and Gαi3-W258F-FLAG was described before (Garcia-Marcos et al., 2010). All constructs were checked by DNA sequencing.

Expression and purification of His-tagged proteins

His-tagged constructs were expressed and purified from Escherichia coli strain BL21 (DE3; Invitrogen) as described previously. Briefly, cells were grown in 1 L flasks at 37°C until OD reached 0.8-1.0, then induced overnight at 25°C with 1 mM IPTG. A bacterial pellet from 1 L of culture was resuspended in 10 ml of His lysis buffer (50 mM NaH_2PO_4 pH 7.4, 300 mM NaCl) supplemented with 2x Protease Inhibitors (Roche Life Science). Cell lysates were sonicated (4 x 20 s, 1 min between cycles) and then centrifuged at 12,000 g at 4°C for 20 min. Solubilized proteins were affinity purified on His (cobalt or nickel) beads (GE Healthcare) by incubation for 4 hours at 4°C. Beads were washed 3 x with 50mM Tris pH 8 and then eluted with His elution buffer (50 mM NaH_2PO_4 pH 7.4, 300 mM NaCl, 300 mM imidazole). Eluted proteins were dialyzed overnight at 4°C against phosphate-buffered saline (PBS), and stored at -80°C in aliquots. His-tagged Gαi3 proteins were stored in storage buffer containing 20 mM Tris-HCl pH 7.4, 20 mM NaCl, 1 mM $MgCl_2$, and 5% glycerol).

Cell culture, transfection, lysis, and quantitative immunoblotting

HeLa cells were cultured according to American Type Collection guidelines. Cells were transfected using Genejuice (Novagen) or polyethylenimine for DNA plasmids and Oligofectamine (Invitrogen) for siRNA oligos following the manufacturers protocols. HeLa cell lines stably expressing Gαi3 wild-type (HeLa-Gαi3-WT), Gαi3-Y155/155/320F (HeLa-Gαi3-3YF), or Gαi3-

Y154H were generated as described previously (Garcia-Marcos et al., 2009). These cell lines were maintained in the presence of G418 (500 g/ml). Lysates for immunoprecipitation assays were prepared by resuspending cells in lysis buffer [20 mM HEPES, pH 7.2, 5 mM Mg-acetate, 125 mM K-acetate, 0.4% Triton X-100, 1 mM DTT, supplemented with sodium orthovanadate (500 μM), phosphatase (Sigma) and protease (Roche) inhibitor cocktails], after which they were passed through a 28G needle at 4°C, and cleared (10,000 x g for 10 min) before use in subsequent experiments. For immunoblotting, protein samples were separated by SDS-PAGE and transferred to PVDF membranes (Millipore). Membranes were blocked with PBS supplemented with 5% nonfat milk (or with 5% BSA when probing for phosphorylated proteins) before incubation with primary antibodies. Infrared imaging with two-color detection and quantification were performed using a Li-Cor Odyssey imaging system. All Odyssey images were processed using Image J software (NIH) and assembled for presentation using Photoshop and Illustrator softwares (Adobe).

2D scratch wound migration assay

Scratch-wound assays were done as described previously (Ghosh et al., 2008). Briefly, monolayer cultures (100% confluent) of HeLa cells stably expressing WT, Y154/155/320F, or Y154H Gαi were scratch-wounded using a 10-l pipette tip and incubated in 2% FBS media. The cells were subsequently monitored by phase-contrast microscopy over the next 30 hr. To quantify cell migration (expressed as percent of wound closure), images were analyzed using ImageJ software to calculate the difference between the wound area at 0 hrs and that at 20 hrs divided by the area at 0 hrs x 100.

In vitro kinase and in cell phosphorylation assays

In vitro phosphorylation assays were carried out using purified His-Gαi3 wild-type or mutants (3-5 μg/reaction) and commercially obtained recombinant kinases (50-100 ng/reaction). The reactions were started by addition of 1 mM of ATP and carried out at 25C in 50 μl of kinase buffer [60 mM Hepes (pH 7.5), 5 mM $MgCl_2$, 5 mM $MnCl_2$, 3 μM Na_3OV_4] for 60 min. Phosphorylated His-tagged proteins were detected by immunoblotting with mouse pTyr antibody and the total amount of proteins used in the assay were visualized by Ponceau S staining. For in vivo phosphorylation assays on Gαi3, Cos-7 cells were transfected with Gαi3-FLAG wild-type or mutants and serum-starved for 16 h (0% FBS) prior to stimulation with EGF (50 nM, 5 min) or insulin (100 nM, 5 min). Reactions were stopped using PBS that was chilled to 4°C and supplemented with 200 μM sodium orthovanadate, and immediately scraped and lysed for immunoprecipitation followed by immublotting.

Immunoprecipitation

HeLa cell lysates (12 mg of protein) were incubated 3 h at 4°C with 2 μg of antibody (FLAG, Gαi3 or Gαi3:GTP, depending on the experiment) followed by incubation with protein G or A-agarose beads at 4°C for an additional 60 min. Beads were washed (x4) with 1 ml of wash buffer (4.3 mM Na_2HPO_4, 4 mM KH_2PO_4, pH 7.4, 137 mM NaCl, 2.7 mM KCl, 0.1% (v/v) Tween 20, 10 mM $MgCl_2$, 5 mM EDTA, 2 mM DTT), and the bound immune complexes were eluted by boiling in SDS sample buffer.

Limited trypsin proteolysis assays

His-Gαi3 wild-type or His-Gαi3 mutants (0.5 mg/ml) were incubated for 120 min at 30°C in the presence of GDP (30 μM) or GDP-AlF_4^- (30 μM GDP, 30 μM $AlCl_3$, 10 mM NaF). After incubation, samples were first in vitro phosphorylated by EGFR or directly treated with trypsin (final concentration, 12.5 μg/ml) and incubated for an additional 10 min at 30°C. Reactions were stopped by adding SDS-PAGE sample buffer and boiling. Proteins were resolved by SDS-PAGE and stained with Coomassie Blue and/or immunoblotted with specific antibodies.

GTPγS incorporation assays

A volume of 72 μL of His-Gαi3 at 1 μM in reaction buffer (20 mM HEPES pH 8, 100 mM NaCl, 1 mM EDTA, 10 mM $MgCl_2$, and 1 mM DTT) was transferred to a pre-warmed 384-well black flat-bottom plate (in triplicates). The reaction was initiated by injecting 8 μL of 1 mM GTPγS (Abcam, Cambridge, MA) in each well for a final reaction volume of 80 μL and final concentrations of 100 nM Gαi3, 100 μM GTPγS. Reactions were carried out at 30°C. GTPγS incorporation into Gαi3 was quantified by direct tryptophan fluorescence (ex = 280; em = 350), using a microplate fluorescence reader (TECAN Spark 20M). Fluorescence was measured every 30 sec starting immediately after injection of GTPγS. Raw fluorescence was plotted over time and observed rates (kobs) were determined by fitting a one-phase association curve to the data (GraphPad Prism v.7).

Differential scanning fluorimetry (thermal shift assays)

His-Gαi3 (5 μM) was taken in their native state (as purified) or nucleotide loaded by incubating it for 150 min at 30°C in buffer (20 mM HEPES, pH 8, 100 mM NaCl, 1 mM EDTA,

10 mM $MgCl_2$, and 1 mM DTT) supplemented with 1 mM GDP or 40 μM GTPγS. After loading, 45 μL of 5 μM His-Gαi3 was pipetted into PCR tubes (in triplicates) and 5 μL 200X SYPRO Orange solution freshly made in the same buffer from 5000X stock (Life Technologies S-6650) was added to the protein. A buffer + dye only (no protein) control was also included. Thermal shift assays were run on an Applied Biosystems StepOnePlus Real-Time PCR machine. Mixed protein and dye samples were subjected to increasing temperatures from 25 to 95°C in half degree increments, holding each temperature for 30 sec and measuring SYPRO fluorescence (using filter 3 for TAMRATM and NED^{TM} dyes) at each temperature. Melting temperatures were defined as the temperature at which the maximum value for the derivative of signal fluorescence (dF/dt) is achieved (GraphPad Prism v.7).

Linear-ion-trap Mass Spectrometry

To determine in vivo phosphorylation states of the FLAG-Gnai3 we used the QTRAP 5500 in the MRM mode to scan for all possible phospho-forms of this protein. For this purpose, MRM methods were developed for all possible tryptic peptides in phosphorylated and non-phosphorylated states. The ABSCIEX MRM PilotTM software was used for MRM method development. Ultimately a method with 210 MRM transitions states was developed for phosphorylated and non-phosphorylated tryptic peptides of Gnai3. In most cases there were at least 2 transitional states used for a given peptide mass (table at the end of document). A total of 13 unique phosphorylation sites in the Gnai3 protein were detected by the QTRAP 5500. To explore the possibility of the presence of other phosphorylation sites in Gnai3 protein, we used another 10 μL of the same tryptic sample used in the previous MRM experiment, to run the QTRAP 5500 mass spectrometer in the precursor ion scanning mode either for an ion at m/z

79 in negative ion mode for serine and threonine phosphorylation, or an ion at m/z 216.043 for tyrosine phosphorylation in the positive ion mode. Once the precursor ions are detected, the instrument switches to positive ion trap scanning mode to isolate the parent ions and to carry out MSMS analysis on these ions. The collected MSMS spectra were analyzed using the ProteinPilot search engine to identify the matching protein sequence from a database.

Statistical analysis

Each experiment presented in the figures is representative of at least three independent repeats (with at least two technical repeats for each condition within each repeat). Statistical significance between the differences of means was calculated using multiple comparisons in one-way nonparametric ANOVA. All statistics and graphical data presented were prepared using GraphPad Prism v.7. Histograms of MD simulation data were generated in R v.3.4.4. All error bars are standard deviation.

Acknowledgements

We thank Bridgett Simmons (AB SCIEX, CANADA) for technical assistance with mass spectrometry experiments. This work was supported by NIH R01 grants CA100768, CA160911 and DK099226, as well as by an NIH predoctoral fellowship (F31 CA206426) and T32 training grants T32CA067754 and T32DK007202.

Chapter 3 in part is material being prepared to be submitted for publication in: **Kalogriopoulos NA**, Lopez-Sanchez I, Lin C, Aznar N, Murray F, Garcia-Marcos M, Kufareva I, Ghassemian M, and Ghosh P. “Receptor tyrosine kinases activate Gi proteins by phosphorylating within the interdomain cleft of Gαi.” The dissertation author was the primary author.

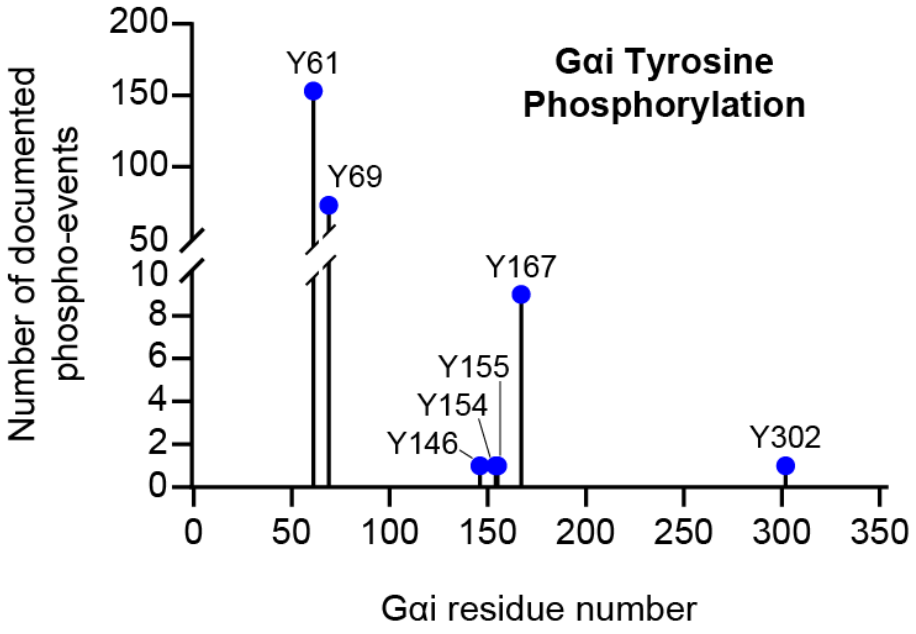

Figure 3.1: Tyrosine phosphorylation of Gαi. a, Lollipop diagram displaying all documented tyrosine phosphorylation events on Gαi1, Gαi2, and Gαi3. Data were collected from cBioPortal.

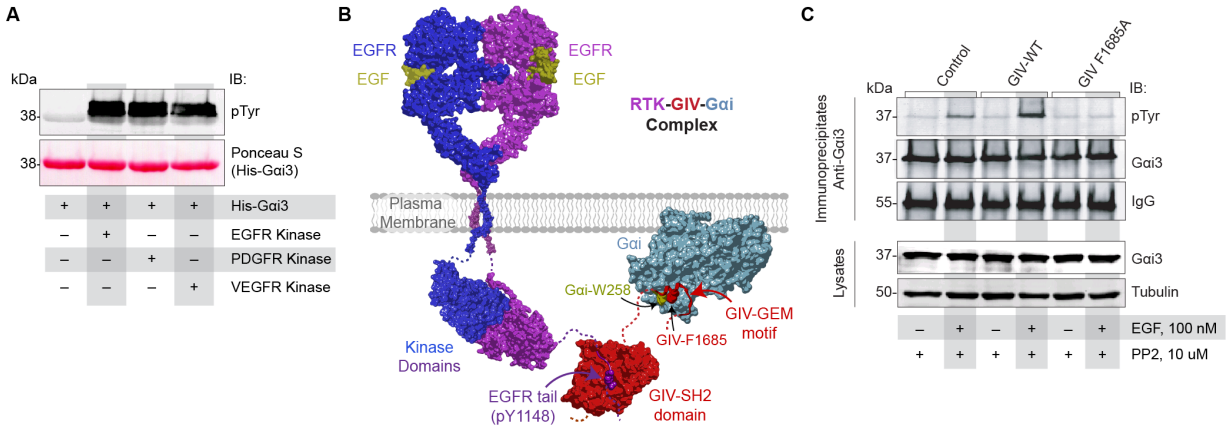

Figure 3.2: RTKs phosphorylate Gαi in a GIV-dependent manner. a, In vitro kinase assay of multiple RTKs with His-Gαi3. b, Schematic showing the RTK-GIV-Gαi ternary complex. Key residues in the GIV-Gαi interaction are also highlighted. c, Immunoprecipitation of Gαi3 from EGF-stimulated HeLa control, GIV-WT or GIV-F1685A expressing cells.

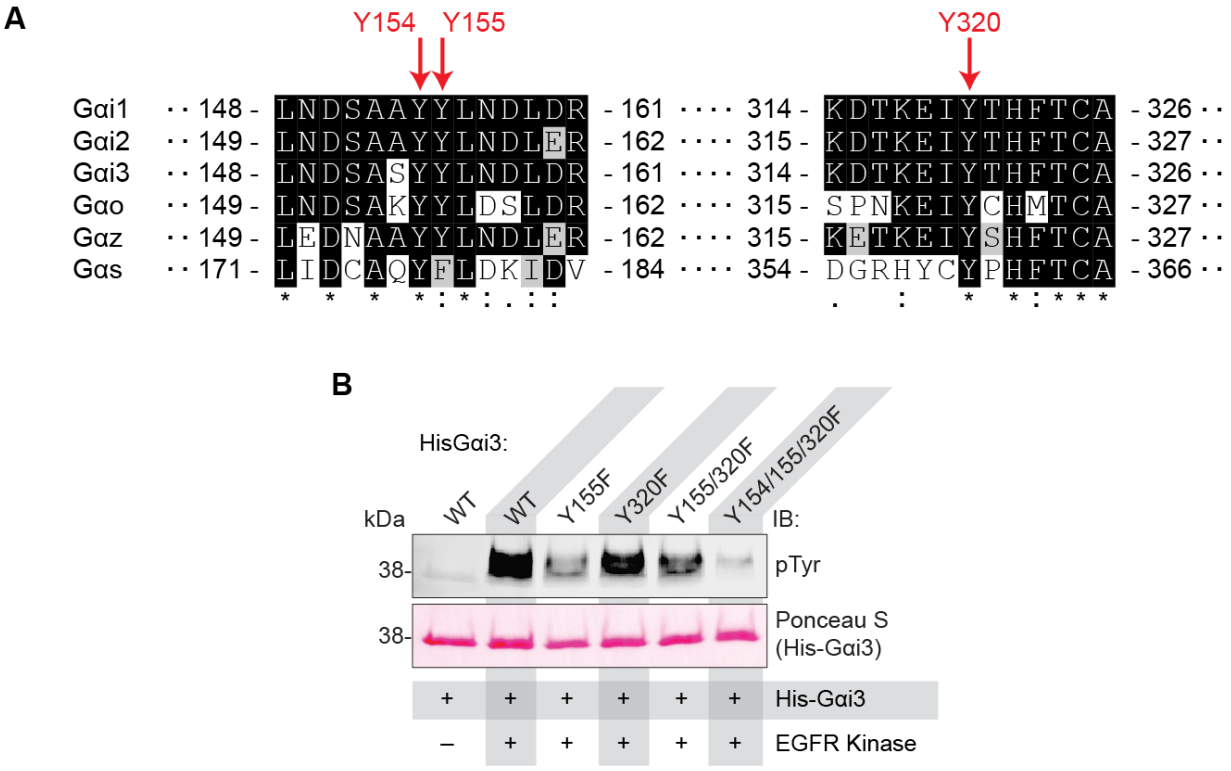

Figure 3.3: RTKs directly phosphorylate Gαi on Y154, 155, and Y320. a, Protein sequence alignment of all G proteins previously shown to bind GIV. RTK tyrosine phosphorylation sites are highlighted. b, In vitro kinase assay of EGFR with His-Gαi3-WT and various non-phosphorylatable Tyr to Phe mutants.

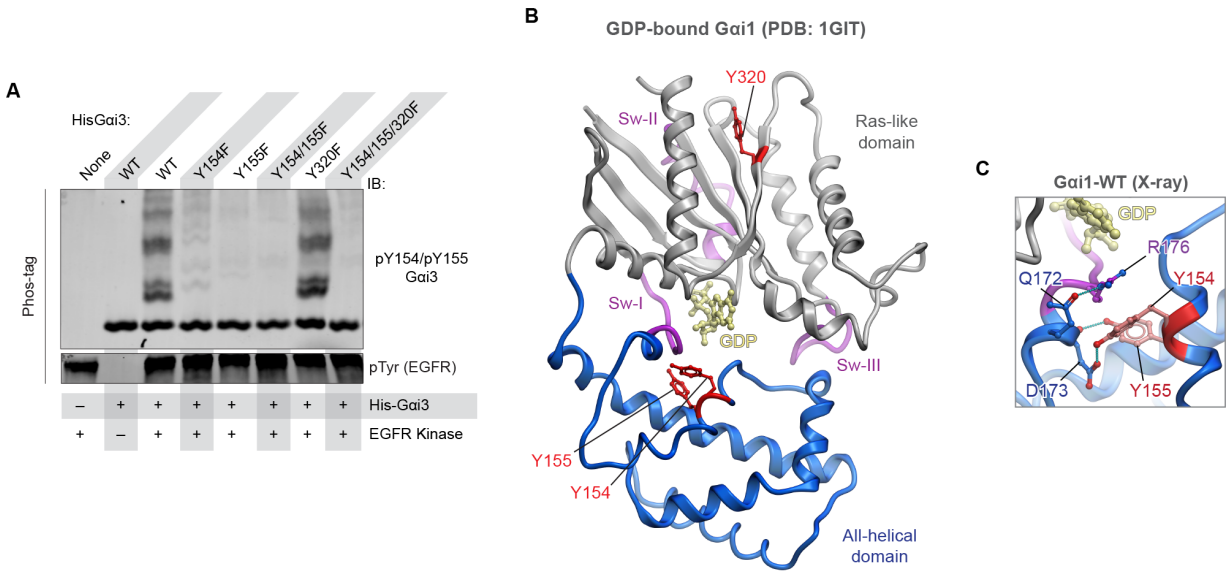

Figure 3.4: RTKs phosphorylate Gαi within the interdomain cleft. a, In vitro kinase assay of EGFR with His-Gαi3-WT and various non-phosphorylatable YF mutants run on Phos-tag gel and immunoblotted with custom pYpY-Gαi3 antibody. b, Crystal structure of Gαi1 (PDB 1GIT), highlighting key structural regions and the RTK tyrosine phosphorylation sites. c, Structure of Gαi1 highlighting the hydrogen bonding between Y154/Y155 and neighboring residues (PDB 1GIT).

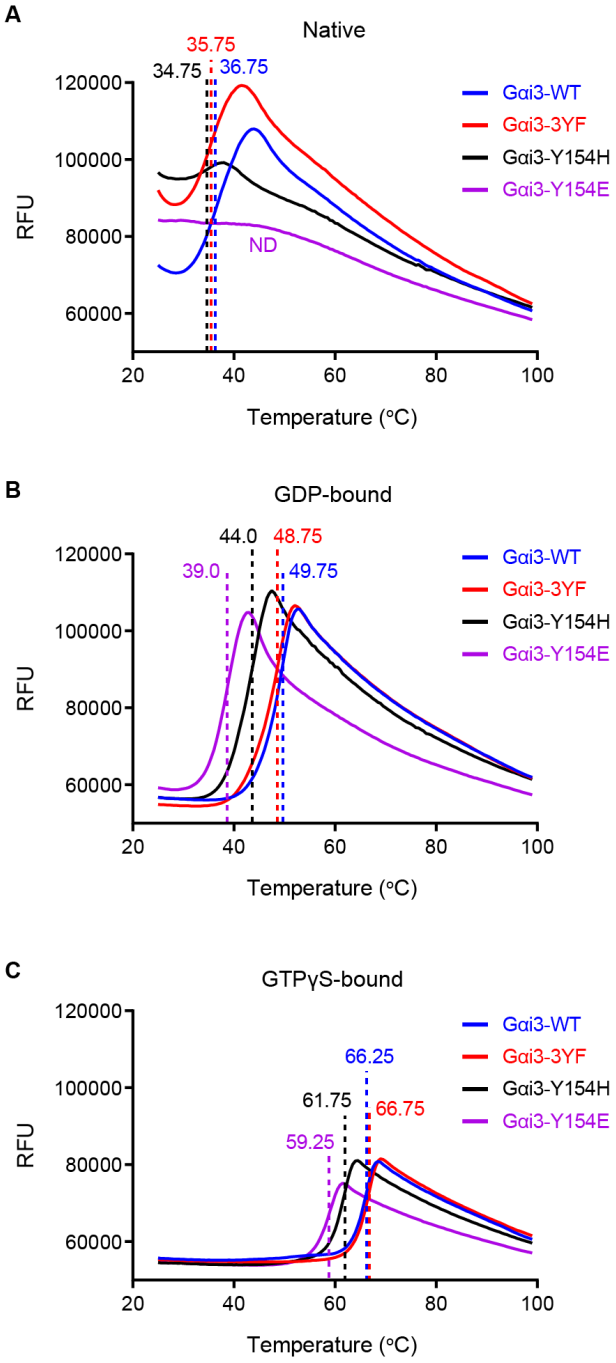

Figure 3.5: Phospho-tyrosine-mimic and cancer mutation at Y154 make Gαi less thermally stable. a-c, Thermal shift assays of WT, 3YF, Y154H, and Y154E Gαi3 proteins in the native (a), GDP-bound (b), and GTPγS-bound (c) states. Vertical dotted lines and displayed values indicate melting temperature for each condition. Not determined (ND) indicates that the Tm was not able to be determined from these experiments.

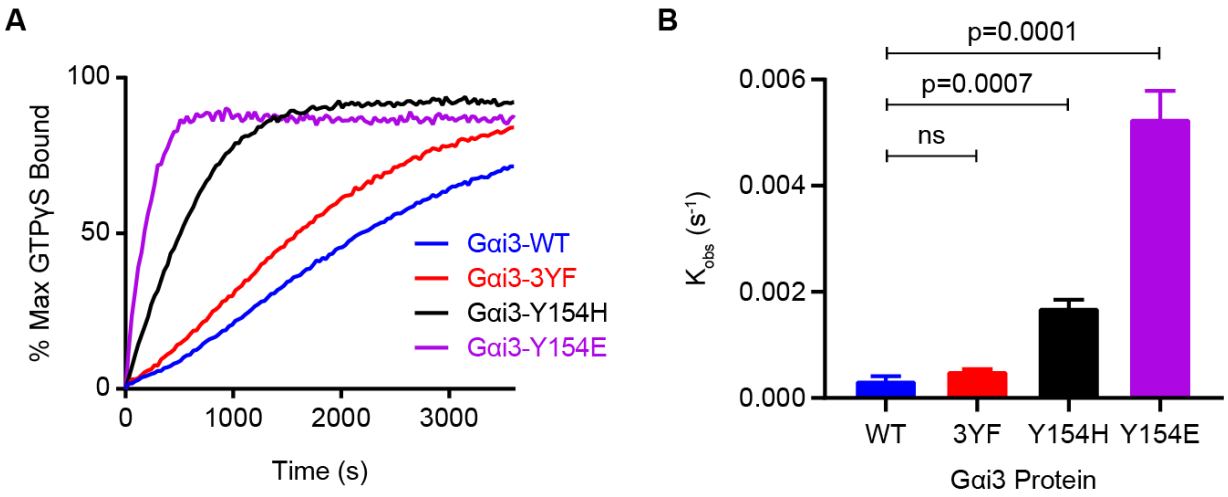

Figure 3.6: Phospho-tyrosine-mimic and cancer mutation at Y154 make Gαi hyperactive. a, Line graph showing GTPγS incorporation into WT and mutant Gαi3 proteins over time. b, Bar graph displaying observed K rates of GTPγS incorporation into WT and mutant Gαi3 proteins measured from (a).

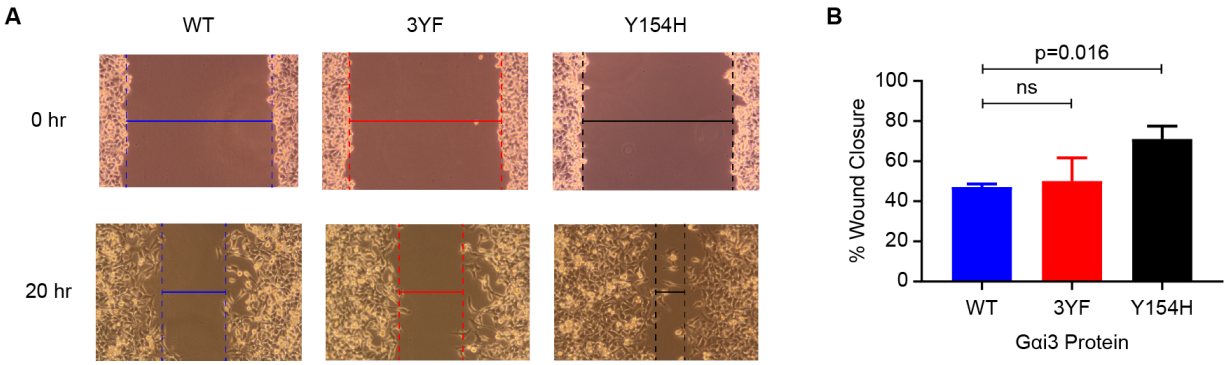

Figure 3.7: Gαi3-Y154H expressing cells display increased cell migration. a, Representative images of 2D scratch wound migration assays. Images of HeLa cells expressing WT, 3YF, or Y154H Gαi3 are shown from the 0 hr and 20 hr time points. b, Bar graph displaying the percent wound closure determined from 2D scratch wound migration assays.

Chapter 4

Conclusion: From the Past 5 Years to the Not-so-distant Future and Beyond

We have come a long way from where the field was before I started my Ph.D. Throughout these past 5 years, significant structural insights into GIV-dependent G protein signaling have been gained, and a new mechanism of GIV-dependent RTK-G protein cross-talk has been defined (Figure 4.1). In this final chapter, I will summarize these advances and conclude with my thoughts on the broader implications of my work, what questions still remain, and where the field of GIV biology and non-canonical G protein signaling as a whole is headed next.

4.1 Advances from past work

Before I began my dissertation work, the established ability of GIV to serve as a central hub for signal integration downstream of a variety of different receptors had already implicated it in a wide range of biologic processes and diseases, from cancer cell migration/invasion and

tumor angiogenesis to liver fibrosis, memory formation, vascular repair (Dunkel et al., 2016, Ghosh, 2015, Weng et al., 2010, Dunkel et al., 2012, Ma et al., 2015a, Lopez-Sanchez et al., 2014). My work mainly focused on understanding the structural and molecular mechanisms of GIV-dependent G protein activation, especially downstream of RTKs. I will spend the next subsections summarizing these works and the scientific advances they make.

Structural studies of the GIV-Gαi interaction (Chapter 2)

Previous work by our group and others has suggested that disrupting the GIV-Gαi interaction would be a viable therapeutic option for a wide range of diseases. Experimentally validated models have revealed that GIV's binding site on Gαi does not overlap with the binding site of GPCRs; this gave birth to the notion that the GIV-Gαi interface could be selectively disrupted without affecting the Gαi-GPCR interface. Biochemistry and enzymology studies on multiple G protein mutants that disrupt the GIV-Gαi interface (Garcia-Marcos et al., 2010, Garcia-Marcos et al., 2009) also support the notion that it is possible to selectively abolish non-canonical G protein signaling via GIV without affecting canonical signaling via GPCRs. Based on the broad range of receptor-initiated signals that converge on GIV and the variety of signaling pathways within disease networks that are modulated via GIV's GEM function, it is predicted that disrupting the GIV-Gαi interface will be an effective and specific approach for modulating multi-receptor signaling via GIV. Such an approach is expected to have the tremendous advantage of allowing network-based therapy irrespective of the receptor of origin (Ghosh, 2015).

In order to even begin developing a small-molecule drug to target this interaction, there were still substantial hurdles that needed to be overcome. The major hurdle that remained was the absence of high-resolution structures. In the absence of such structural information, it is

incredibly challenging to rationally design or optimize potential small molecule drugs. Computational modeling provided some clues into the druggability of the GIV-Gαi interface (Garcia-Marcos et al., 2010, Garcia-Marcos et al., 2009), but high-resolution structures were required to continue advancing toward our goal of developing a drug. A major goal of my dissertation was to address this gap in knowledge and solve a high-resolution structure to gain atomic level insights into the GIV-Gαi interaction and structural mechanism of GIV-mediated G protein activation.

We were able to successfully co-crystallize the GEM motif of GIV with GDP-bound Gαi3 and determine the structure to a 2.0 Å resolution. Using structural, computation, biophysical, and biochemical approaches, we revealed the structural and dynamical basis for GPCR-independent Gαi activation by GEMs and identified key similarities and differences between GPCR-dependent and -independent G protein activation. Binding of GIV-GEM to Gαi stabilizes an elevated Sw-II conformation and releases conformational constraints on Sw-I and β2-β3 strands of Gαi, allowing for inward collapse of the former and higher mobility of the latter. This perturbation propagates to the hydrophobic core in the center of the GTPase domain that was previously shown to contribute to both basal and GPCR-accelerated nucleotide exchange in Gαi (Kaya et al., 2014, Kaya et al., 2016). Structures of GPCR-bound G proteins demonstrate that GPCRs perturb the hydrophobic core directly by displacing the C-terminal α5 helix of Gαi and also inserting a hydrophobic residue from the intracellular loop 2 into the core (Rasmussen et al., 2011, Koehl et al., 2018, Carpenter et al., 2016, Draper-Joyce et al., 2018). Thus, our findings suggest that despite binding at non-overlapping interfaces on Gαi, GEMs and GPCRs converge on a similar mechanism for acceleration of GDP release by either directly or allosterically perturbing the intramolecular packing in the hydrophobic core of the GTPase domain of Gαi. Atomic-level insights gained here will aid structure-based efforts to selectively target the

non-canonical G protein activation.

RTK phosphorylation of Gα subunits as a cross-talk mechanism (Chapter 3)

Although our structural studies elucidated much of the mechanism and effect of GIV-GEM binding to Gαi, in order to fully understand GIV's function downstream of RTKs, we needed to take a step back and ask what other effects or regulation might be taking place in the context of the RTK-GIV-Gαi signaling complex. Because ligand-stimulated recruitment of GIV to the RTK allows for the direct phosphorylation of GIV by the RTK (Lin et al., 2011), we asked whether recruitment of Gαi in the RTK-GIV-Gαi ternary complex may also allow for direct phosphorylation of the G protein by the RTK. Some studies had already suggested that in certain cases RTKs may directly phosphorylate G proteins (Poppleton et al., 2000, Patel, 2004, Poppleton et al., 1996), however the evidence that this occurs in cells was lacking and thus the phenomenon as a whole has remained controversial.

Prior to my arrival, the lab discovered that RTK phosphorylation of G proteins does occur in cells but is dependent on the presence of GIV and its ability to recruit G proteins to the RTKs. This of course may be dependent on the cellular context in which this RTK-G protein cross-talk is occurring. Using a combination of in vitro biochemical and cell-based assays, we found that within the RTK-GIV-Gαi ternary complex, the binding of GIV to Gαi stimulates structural changes and GDP release, facilitating the exposure of Y154 and Y155 on Gαi, and results in direct phosphorylation of these tyrosines by the RTK. Our data suggest that RTK phosphorylation of Gαi enhances G protein activation and promotes downstream signaling. These findings expand the essential role of GIV in RTK-dependent non-canonical G protein activation and downstream signaling. Furthermore, cancers may be able to take advantage of this RTK-G protein cross-talk

mechanism by mutating these key tyrosine residues to promote a pro-metastatic phenotype.

4.2 Broad impact of the work

Impact of the work on signal transduction research

As two major hubs of signal transduction inside eukaryotic cells, RTKs and GPCRs/G proteins have been the center of attention for signal transduction research for decades. Investigation into the mechanism and function of each of these hubs individually has revolutionized how we think about cell signaling and cell biology. More recently, it has been widely demonstrated that the RTK and GPCR/G protein pathways cross-talk to form an integrated signaling network. Bidirectional communication can occur by several mechanisms, including stimulation of one receptor leading to ligand production of the other or by physical interaction between RTKs and GPCRs.

Many previous studies also implicated G proteins in the cellular response to stimuli that are not traditionally thought to activate trimeric G proteins; the mechanisms of how these signals are transduced to G proteins however were unidentified. These studies need to be revisited in light of recent developments in the field of non-canonical G protein signaling. The discovery of GIV and its ability to link G proteins to a variety of cell surface receptors has broadened the already massive scope of G protein signaling. Further investigations could reveal that GIV may be the missing link between more diverse stimuli and G protein signaling in these previously unresolved studies. Moreover, other GEMs and the identification of novel GEMs will continue this theme of introducing unique mechanisms of linking G proteins to other signal transducers.

In addition, our identification of the RTK phosphorylation sites within Gαi should serve

as a cornerstone for future research in G protein phosphorylation. The RTK phosphorylated tyrosines in Gαi, Y154 and Y155, are within the inter-domain cleft of the G protein on the small αE helix and are not accessible for phosphorylation in any currently known structure of Gαi in any state (GDP-bound, GTP-bound, or nucleotide free). It is also well-established that kinases prefer linear substrates. This indicates that there are still unknown dynamic motions within the G protein activation cycle that allow for the exposure and subsequent phosphorylation of these tyrosines, and this should be an active area of research for years to come; utilization of diverse techniques that provide not only high-resolution information but also provide temporal/dynamic information will be essential. This observation should be an important reminder for structural biologists and biochemists: although high-resolution protein structures provide incredible insight, they are a static image, a snapshot of one conformation in the infinite possible protein conformations. In time, I believe there will be increasing examples of buried regions of proteins being post-translationally modified and regulating protein function.

Finally, it has been postulated that a common ancestor of the GTPase fold provided a structural framework that can be perturbed by the interruption of α5-α1 contacts. GPCRs trigger the perturbation by directly binding to α5 of their effector trimeric G protein, whereas GEFs of small GTPases typically act via binding to Sw-I and Sw-II. Our structural study not only supports the conserved nature of the ancestral α5-α1 activation mechanism, but also suggests that similarities between monomeric GTPases and trimeric G proteins extend beyond it, because just like for small GTPases, Sw-I and Sw-II in Gαi may serve as allosteric handles by which the conserved exchange mechanism is accessed by modulators. These insights should shape the way the field thinks about the key structural determinants of both trimeric and monomeric GTPases alike.

Impact of the work for therapeutics

The growing number of physiologic and pathophysiologic processes that GIV is implicated in continues to increase the potential for GIV to serve as a target for personalized medicine through pharmacogenomics in several disease states. In the context of cancer progression, for example, our group and others have reported that expression of GIV at high levels correlates with tumor aggressiveness and poor survival across a variety of solid tumors (Ghosh, 2015). A consensus has emerged that patients with GIV-positive tumors are at highest risk for cancer progression and may maximally benefit from systemic chemotherapy. Ongoing clinical trials assessing the expression of GIV in primary tumors as well as on tumor cells isolated from the peripheral circulation are likely to provide a more complete assessment of the prognostic and predictive impact of GIV as biomarker for cancer progression. Our identification of phosphorylation of Y154 and Y155 in Gαi may ultimately serve as another useful biomarker of enhanced GIV-dependent G protein activation in disease contexts, though much more investigation is needed to support this idea.

GIV's potential as a biomarker in diverse diseases is underscored by its active role in regulating the cellular processes that contribute to the development of those diseases. Proof of principle studies assessing the efficacy of disrupting the GIV-Gαi interaction in various disease contexts verified that exogenous modulation of the GIV-Gαi signaling node is possible and can be used to regulate broad signaling networks and alter disease phenotypes. The structural studies presented here lay the foundation for the development of other more clinically accessible approaches for modulating the GIV-Gαi interface for novel therapeutics in a wide range of diseases, such as the development of a small molecule inhibitor. In fact, work conducting small molecule screens for inhibitors has already begun, and I envision the insights gained from our

high-resolution co-crystal structure will prove to be invaluable for the rational optimization of lead compounds by synthetic chemists.

4.3 Future Directions

Though the field of non-canonical G protein signaling via GIV is quite young (about 10 years), we have already gained so much insight into the importance of GIV-dependent signal transduction. The insights gained just within the past half-decade has continued to shape a paradigm of GIV-dependent non-canonical G protein signaling by receptors that are typically not believed to signal via G proteins. Despite these insights, it is clear that a lot remains unknown.

Many questions remain regarding the newly defined RTK-G protein cross-talk via direct phosphorylation of the Gα subunit by the RTK. For one, does tyrosine phosphorylation of the G protein play a role in the unique temporal and spatial features of non-canonical G protein signaling? Our study supports the idea that G protein phosphorylation plays a role in prolonging the RTK-initiated G protein signal, but if and how tyrosine phosphorylation is involved has not been directly investigated. Moreover, is tyrosine phosphorylation of G proteins involved in how non-canonical G protein activation at the plasma membrane by GIV coordinately triggers the same processes on internal membranes? This also remains uninvestigated.

Although we have a better understanding of how RTKs transactivate G proteins via GIV, how other classes of receptors, such as GPCRs, β1 integrins, tolllike receptors (TLRs), and transforming growth factor (TGFβ) receptors, interact with GIV to transactivate G proteins remains unclear. Knowing how GIV engages receptors is of utmost importance because an indepth insight into these mechanisms will fundamentally revolutionize our understanding of the new rules of engagement of non-canonical G protein signaling via GIV. Because GIV's C-

terminus offers structural/conformational plasticity, which should directly impact protein-protein interactions, it is possible that such structural plasticity provides context-dependent engagement with a variety of receptors, some directly and others indirectly.

Therefore, my GIV-Gαi structure work is only the beginning of many structural studies to come. Gaining atomic level insights into how GIV couples to many diverse receptors will remain one of our major goals for years to come. Furthermore, GIV's action on Gαi is only one side of the coin; GIV's GEM motif not only allows GIV to bind and activate Gαi, but it also allows it to bind and inhibit Gαs. The mechanisms of these opposing actions on Gαi and Gαs is unknown, however it is intriguing to speculate that, since GIV-GEM binding to Sw-II of Gαi destabilizes Sw-I and the hydrophobic core of the G protein to stimulate GDP-release, GIV-GEM binding to Sw-II of Gαs may in fact stabilize Sw-I in the outward position away from the nucleotide binding pocket (this is the high GDP affinity Sw-I conformation that we identified) and stabilize the hydrophobic core to inhibit GDP release. Since the Sw-II sequences of Gαi and Gαs are nearly identical, other nearby residues will likely account for the differential effect of GIV-GEM binding; residues in the α3 helix may be responsible for this differential effect as they differ between Gαi and Gαs and also contact the GIV-GEM motif, though we have no evidence for this and it remains uninvestigated. High-resolution structural studies of the GIV-Gαs interaction will provide answers to these questions, and these studies are already underway. Lastly, with our new atomic level structural insights, we are now poised to begin drug development to try to target the GIV-Gαi interface. Small molecule drug screens will be a necessary first step and are also already underway.

Looking from a 10,000-foot view, GIV is the first and most well-studied GEM protein, however there are at least three more GEM proteins that remain significantly understudied.

Moreover, information gained from the GIV-Gαi crystal structure will likely facilitate the discovery of more novel GEM proteins. Lessons learned from studying GIV may provide clues in understanding newly identified GEMs, but each GEM will also surely come with its own rich, unique biology. Many unanswered questions remain, and it is expected that we will encounter many conceptual, technical, and logical problems along the way. Such challenges will be overcome by engagement of the broader scientific community through collaborations to systematically dissect this emerging paradigm of non-canonical G protein signaling from the atomic to full-organism level.

Acknowledgements

This research was funded by NIH (R01CA160911 and DK099226), as well as an NIH predoctoral fellowship (F31 CA206426) and T32 training grants T32CA067754 and T32DK007202.

Chapter 4 in part is a reprint of material published in: Aznar N, **Kalogriopoulos NA**, Midde K, Ghosh P. 2016. “Heterotrimeric G protein signaling via GIV/Girdin: Breaking the rules of engagement, space, and time.” *Bioessays.* 38:379-93.

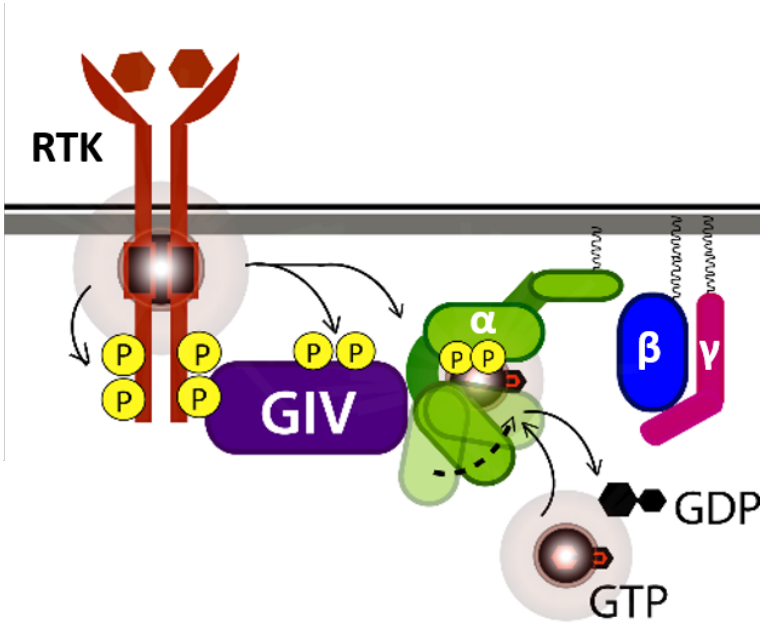

Figure 4.1: RTK-GIV-Gαi ternay complex. Schematic showing GIV-dependent formation of the RTK-GIV-Gαi complex. Direct phosphorylation of Gαi by the RTK is highlighted.

Bibliography

ABAGYAN, R. & TOTROV, M. 1994. Biased probability Monte Carlo conformational searches and electrostatic calculations for peptides and proteins. *J Mol Biol,* 235**,** 983-1002.

ADAMS, P. D., AFONINE, P. V., BUNKOCZI, G., CHEN, V. B., DAVIS, I. W., ECHOLS, N., HEADD, J. J., HUNG, L. W., KAPRAL, G. J., GROSSE-KUNSTLEVE, R. W., MCCOY, A. J., MORIARTY, N. W., OEFFNER, R., READ, R. J., RICHARDSON, D. C., RICHARDSON, J. S., TERWILLIGER, T. C. & ZWART, P. H. 2010. PHENIX: a comprehensive Python-based system for macromolecular structure solution. *Acta Crystallogr D Biol Crystallogr,* 66**,** 213-21.

ANAND, B., VERMA, S. K. & PRAKASH, B. 2006. Structural stabilization of GTP-binding domains in circularly permuted GTPases: implications for RNA binding. *Nucleic Acids Res,* 34**,** 2196-205.

ANAND, G. S., HUGHES, C. A., JONES, J. M., TAYLOR, S. S. & KOMIVES, E. A. 2002. Amide H/2H exchange reveals communication between the cAMP and catalytic subunit-binding sites in the R(I)alpha subunit of protein kinase A. *J Mol Biol,* 323**,** 377-86.

AZNAR, N., KALOGRIOPOULOS, N., MIDDE, K. K. & GHOSH, P. 2016. Heterotrimeric G protein signaling via GIV/Girdin: Breaking the rules of engagement, space, and time. *Bioessays,* 38**,** 379-93.

AZNAR, N., MIDDE, K. K., DUNKEL, Y., LOPEZ-SANCHEZ, I., PAVLOVA, Y., MARIVIN, A., BARBAZAN, J., MURRAY, F., NITSCHE, U., JANSSEN, K. P., WILLERT, K., GOEL, A., ABAL, M., GARCIA-MARCOS, M. & GHOSH, P. 2015. Daple is a novel non-receptor GEF required for trimeric G protein activation in Wnt signaling. *Elife,* 4**,** e07091.

BATTYE, T. G., KONTOGIANNIS, L., JOHNSON, O., POWELL, H. R. & LESLIE, A. G. 2011. iMOSFLM: a new graphical interface for diffraction-image processing with MOSFLM. *Acta Crystallogr D Biol Crystallogr,* 67**,** 271-81.

BEAS, A. O., TAUPIN, V., TEODOROF, C., NGUYEN, L. T., GARCIA-MARCOS, M. & FARQUHAR, M. G. 2012. Galphas promotes EEA1 endosome maturation and shuts down proliferative signaling through interaction with GIV (Girdin). *Mol Biol Cell,* 23**,** 4623-34.

BENOVIC, J. L., STRASSER, R. H., CARON, M. G. & LEFKOWITZ, R. J. 1986. Beta-adrenergic receptor kinase: identification of a novel protein kinase that phosphorylates the agonist-occupied form of the receptor. *Proc Natl Acad Sci U S A,* 83**,** 2797-801.

BHANDARI, D., LOPEZ-SANCHEZ, I., TO, A., LO, I. C., AZNAR, N., LEYME, A., GUPTA, V., NIESMAN, I., MADDOX, A. L., GARCIA-MARCOS, M., FARQUHAR, M. G. & GHOSH, P. 2015. Cyclin-dependent kinase 5 activates guanine nucleotide exchange factor GIV/Girdin to orchestrate migration-proliferation dichotomy. *Proc Natl Acad Sci U S A,* 112**,** E4874-83.

BLUME-JENSEN, P. & HUNTER, T. 2001. Oncogenic kinase signalling. *Nature,* 411**,** 355-65.

BLUMER, J. B., ONER, S. S. & LANIER, S. M. 2012. Group II activators of G-protein signalling and proteins containing a G-protein regulatory motif. *Acta Physiol (Oxf),* 204**,** 202-18.

BOCKAERT, J., CLAEYSEN, S., BECAMEL, C., PINLOCHE, S. & DUMUIS, A. 2002. G protein-coupled receptors: dominant players in cell-cell communication. *Int Rev Cytol,* 212**,** 63-132.

BOREJDO, J., RICH, R. & MIDDE, K. 2012. Mesoscopic analysis of motion and conformation of cross-bridges. *Biophys Rev,* 4**,** 299-311.

BUNEMANN, M., FRANK, M. & LOHSE, M. J. 2003. Gi protein activation in intact cells involves subunit rearrangement rather than dissociation. *Proc Natl Acad Sci U S A,* 100**,** 16077-82.

CABRERA-VERA, T. M., VANHAUWE, J., THOMAS, T. O., MEDKOVA, M., PREININGER, A., MAZZONI, M. R. & HAMM, H. E. 2003. Insights into G protein structure, function, and regulation. *Endocr Rev,* 24**,** 765-81.

CARPENTER, B., NEHME, R., WARNE, T., LESLIE, A. G. & TATE, C. G. 2016. Structure of the adenosine A(2A) receptor bound to an engineered G protein. *Nature,* 536**,** 104-7.

CHAKRAVORTY, D. & ASSMANN, S. M. 2018. G protein subunit phosphorylation as a regulatory mechanism in heterotrimeric G protein signaling in mammals, yeast, and plants. *Biochem J,* 475**,** 3331-3357.

CHE, T., MAJUMDAR, S., ZAIDI, S. A., ONDACHI, P., MCCORVY, J. D., WANG, S., MOSIER, P. D., UPRETY, R., VARDY, E., KRUMM, B. E., HAN, G. W., LEE, M. Y., PARDON, E., STEYAERT, J., HUANG, X. P., STRACHAN, R. T., TRIBO, A. R., PASTERNAK, G. W., CARROLL, F. I., STEVENS, R. C., CHEREZOV, V., KATRITCH, V., WACKER, D. & ROTH, B. L. 2018. Structure of the Nanobody-Stabilized Active State of the Kappa Opioid Receptor. *Cell,* 172**,** 55-67 e15.

CHU, J., ZHENG, H., ZHANG, Y., LOH, H. H. & LAW, P. Y. 2010. Agonist-dependent mu-opioid receptor signaling can lead to heterologous desensitization. *Cell Signal,* 22**,** 684-96.

CLAPHAM, D. E. & NEER, E. J. 1997. G protein beta gamma subunits. *Annu Rev Pharmacol Toxicol,* 37**,** 167-203.

COLEMAN, D. E., BERGHUIS, A. M., LEE, E., LINDER, M. E., GILMAN, A. G. & SPRANG, S. R. 1994. Structures of active conformations of Gi alpha 1 and the mechanism of GTP hydrolysis. *Science,* 265**,** 1405-12.

COLEMAN, D. E. & SPRANG, S. R. 1998. Crystal structures of the G protein Gi alpha 1 complexed with GDP and Mg2+: a crystallographic titration experiment. *Biochemistry,* 37**,** 14376-85.

DAUB, H., WEISS, F. U., WALLASCH, C. & ULLRICH, A. 1996. Role of transactivation of the EGF receptor in signalling by G-protein-coupled receptors. *Nature,* 379**,** 557-60.

DE ALBA, E. & TJANDRA, N. 2004. Structural studies on the Ca2+-binding domain of human nucleobindin (calnuc). *Biochemistry,* 43**,** 10039-49.

DE OPAKUA, A. I., PARAG-SHARMA, K., DIGIACOMO, V., MERINO, N., LEYME, A., MARIVIN, A., VILLATE, M., NGUYEN, L. T., DE LA CRUZ-MORCILLO, M. A., BLANCO-CANOSA, J. B., RAMACHANDRAN, S., BAILLIE, G. S., CERIONE, R. A., BLANCO, F. J. & GARCIA-MARCOS, M. 2017. Molecular mechanism of Galphai activation by non-GPCR proteins with a Galpha-Binding and Activating motif. *Nat Commun,* 8**,** 15163.

DE VRIES, L., ZHENG, B., FISCHER, T., ELENKO, E. & FARQUHAR, M. G. 2000. The regulator of G protein signaling family. *Annu Rev Pharmacol Toxicol,* 40**,** 235-71.

DEWIRE, S. M., AHN, S., LEFKOWITZ, R. J. & SHENOY, S. K. 2007. Beta-arrestins and cell signaling. *Annu Rev Physiol,* 69**,** 483-510.

DI LIBERTO, V., MUDO, G. & BELLUARDO, N. 2019. Crosstalk between receptor tyrosine kinases (RTKs) and G protein-coupled receptors (GPCR) in the brain: Focus on heteroreceptor complexes and related functional neurotrophic effects. *Neuropharmacology,* 152**,** 67-77.

DIJKMAN, P. M., CASTELL, O. K., GODDARD, A. D., MUNOZ-GARCIA, J. C., DE GRAAF, C., WALLACE, M. I. & WATTS, A. 2018. Dynamic tuneable G protein-coupled receptor monomer-dimer populations. *Nat Commun,* 9**,** 1710.

DOUGLAS, D. J., FRANK, A. J. & MAO, D. 2005. Linear ion traps in mass spectrometry. *Mass Spectrom Rev,* 24**,** 1-29.

DRAPER-JOYCE, C. J., KHOSHOUEI, M., THAL, D. M., LIANG, Y. L., NGUYEN, A. T. N., FURNESS, S. G. B., VENUGOPAL, H., BALTOS, J. A., PLITZKO, J. M., DANEV, R., BAUMEISTER, W., MAY, L. T., WOOTTEN, D., SEXTON, P. M., GLUKHOVA, A. & CHRISTOPOULOS, A. 2018. Structure of the adenosine-bound human adenosine A1 receptor-Gi complex. *Nature,* 558**,** 559-563.

DROR, R. O., GREEN, H. F., VALANT, C., BORHANI, D. W., VALCOURT, J. R., PAN, A. C., ARLOW, D. H., CANALS, M., LANE, J. R., RAHMANI, R., BAELL, J. B., SEXTON, P. M., CHRISTOPOULOS, A. & SHAW, D. E. 2013. Structural basis for modulation of a G-protein-coupled receptor by allosteric drugs. *Nature,* 503**,** 295-9.

DROR, R. O., MILDORF, T. J., HILGER, D., MANGLIK, A., BORHANI, D. W., ARLOW, D. H., PHILIPPSEN, A., VILLANUEVA, N., YANG, Z., LERCH, M. T., HUBBELL, W. L.,

KOBILKA, B. K., SUNAHARA, R. K. & SHAW, D. E. 2015. SIGNAL TRANSDUCTION. Structural basis for nucleotide exchange in heterotrimeric G proteins. *Science,* 348**,** 1361-5.

DU, Y., DUC, N. M., RASMUSSEN, S. G. F., HILGER, D., KUBIAK, X., WANG, L., BOHON, J., KIM, H. R., WEGRECKI, M., ASURU, A., JEONG, K. M., LEE, J., CHANCE, M. R., LODOWSKI, D. T., KOBILKA, B. K. & CHUNG, K. Y. 2019. Assembly of a GPCR-G Protein Complex. *Cell,* 177**,** 1232-1242 e11.

DUNKEL, Y., DIAO, K., AZNAR, N., SWANSON, L., LIU, L., ZHU, W., MI, X. Y. & GHOSH, P. 2016. Prognostic impact of total and tyrosine phosphorylated GIV/Girdin in breast cancers. *FASEB J,* 30**,** 3702-3713.

DUNKEL, Y., ONG, A., NOTANI, D., MITTAL, Y., LAM, M., MI, X. & GHOSH, P. 2012. STAT3 protein up-regulates Galpha-interacting vesicle-associated protein (GIV)/Girdin expression, and GIV enhances STAT3 activation in a positive feedback loop during wound healing and tumor invasion/metastasis. *J Biol Chem,* 287**,** 41667-83.

EMSLEY, P., LOHKAMP, B., SCOTT, W. G. & COWTAN, K. 2010. Features and development of Coot. *Acta Crystallogr D Biol Crystallogr,* 66**,** 486-501.

ERLANDSON, S. C., MCMAHON, C. & KRUSE, A. C. 2018. Structural Basis for G Protein-Coupled Receptor Signaling. *Annu Rev Biophys*.

ESTEVA, F. J. 2004. Monoclonal antibodies, small molecules, and vaccines in the treatment of breast cancer. *Oncologist,* 9 Suppl 3**,** 4-9.

EVANS, P. 2006. Scaling and assessment of data quality. *Acta Crystallogr D Biol Crystallogr,* 62**,** 72-82.

EXTON, J. H. 1996. Regulation of phosphoinositide phospholipases by hormones, neurotransmitters, and other agonists linked to G proteins. *Annu Rev Pharmacol Toxicol,* 36**,** 481-509.

FERGUSON, K. M., HIGASHIJIMA, T., SMIGEL, M. D. & GILMAN, A. G. 1986. The influence of bound GDP on the kinetics of guanine nucleotide binding to G proteins. *J Biol Chem,* 261**,** 7393-9.

FERGUSON, S. S. 2001. Evolving concepts in G protein-coupled receptor endocytosis: the role in receptor desensitization and signaling. *Pharmacol Rev,* 53**,** 1-24.

FLOCK, T., RAVARANI, C. N. J., SUN, D., VENKATAKRISHNAN, A. J., KAYIKCI, M., TATE, C. G., VEPRINTSEV, D. B. & BABU, M. M. 2015. Universal allosteric mechanism for Galpha activation by GPCRs. *Nature,* 524**,** 173-179.

FREDRIKSSON, R., LAGERSTROM, M. C., LUNDIN, L. G. & SCHIOTH, H. B. 2003. The G-protein-coupled receptors in the human genome form five main families. Phylogenetic analysis, paralogon groups, and fingerprints. *Mol Pharmacol,* 63**,** 1256-72.

GARCIA-MARCOS, M., EAR, J., FARQUHAR, M. G. & GHOSH, P. 2011a. A GDI (AGS3) and a GEF (GIV) regulate autophagy by balancing G protein activity and growth factor signals. *Mol Biol Cell,* 22**,** 673-86.

GARCIA-MARCOS, M., GHOSH, P., EAR, J. & FARQUHAR, M. G. 2010. A structural determinant that renders G alpha(i) sensitive to activation by GIV/girdin is required to promote cell migration. *J Biol Chem,* 285**,** 12765-77.

GARCIA-MARCOS, M., GHOSH, P. & FARQUHAR, M. G. 2009. GIV is a nonreceptor GEF for G alpha i with a unique motif that regulates Akt signaling. *Proc Natl Acad Sci U S A,* 106**,** 3178-83.

GARCIA-MARCOS, M., GHOSH, P. & FARQUHAR, M. G. 2015. GIV/Girdin transmits signals from multiple receptors by triggering trimeric G protein activation. *J Biol Chem,* 290**,** 6697-704.

GARCIA-MARCOS, M., KIETRSUNTHORN, P. S., PAVLOVA, Y., ADIA, M. A., GHOSH, P. & FARQUHAR, M. G. 2012. Functional characterization of the guanine nucleotide exchange factor (GEF) motif of GIV protein reveals a threshold effect in signaling. *Proc Natl Acad Sci U S A,* 109**,** 1961-6.

GARCIA-MARCOS, M., KIETRSUNTHORN, P. S., WANG, H., GHOSH, P. & FARQUHAR, M. G. 2011b. G Protein binding sites on Calnuc (nucleobindin 1) and NUCB2 (nucleobindin 2) define a new class of G(alpha)i-regulatory motifs. *J Biol Chem,* 286**,** 28138-49.

GHOSH, P. 2015. Heterotrimeric G proteins as emerging targets for network based therapy in cancer: End of a long futile campaign striking heads of a Hydra. *Aging (Albany NY),* 7**,** 469-74.

GHOSH, P., BEAS, A. O., BORNHEIMER, S. J., GARCIA-MARCOS, M., FORRY, E. P., JOHANNSON, C., EAR, J., JUNG, B. H., CABRERA, B., CARETHERS, J. M. & FARQUHAR, M. G. 2010. A G{alpha}i-GIV molecular complex binds epidermal growth factor receptor and determines whether cells migrate or proliferate. *Mol Biol Cell,* 21**,** 2338-54.

GHOSH, P., GARCIA-MARCOS, M., BORNHEIMER, S. J. & FARQUHAR, M. G. 2008. Activation of Galphai3 triggers cell migration via regulation of GIV. *J Cell Biol,* 182**,** 381-93.

GHOSH, P., GARCIA-MARCOS, M. & FARQUHAR, M. G. 2011. GIV/Girdin is a rheostat that fine-tunes growth factor signals during tumor progression. *Cell Adh Migr,* 5**,** 237-48.

GHOSH, P., RANGAMANI, P. & KUFAREVA, I. 2017. The GAPs, GEFs, GDIs and...now, GEMs: New kids on the heterotrimeric G protein signaling block. *Cell Cycle,* 16**,** 607-612.

GIBSON, S. K. & GILMAN, A. G. 2006. Gialpha and Gbeta subunits both define selectivity of G protein activation by alpha2-adrenergic receptors. *Proc Natl Acad Sci U S A,* 103**,** 212-7.

GILMAN, A. G. 1987. G proteins: transducers of receptor-generated signals. *Annu Rev Biochem,* 56**,** 615-49.

GLICK, J. L., MEIGS, T. E., MIRON, A. & CASEY, P. J. 1998. RGSZ1, a Gz-selective regulator of G protein signaling whose action is sensitive to the phosphorylation state of Gzalpha. *J Biol Chem,* 273**,** 26008-13.

GORICANEC, D., STEHLE, R., EGLOFF, P., GRIGORIU, S., PLUCKTHUN, A., WAGNER, G. & HAGN, F. 2016. Conformational dynamics of a G-protein alpha subunit is tightly regulated by nucleotide binding. *Proc Natl Acad Sci U S A,* 113**,** E3629-38.

GSCHWIND, A., FISCHER, O. M. & ULLRICH, A. 2004. The discovery of receptor tyrosine kinases: targets for cancer therapy. *Nat Rev Cancer,* 4**,** 361-70.

GU, J. L., LU, W., XIA, C., WU, X. & LIU, M. 2003. Regulation of hematopoietic-specific G-protein Galpha15 and Galpha16 by protein kinase C. *J Cell Biochem,* 88**,** 1101-11.

GUIDOLIN, D., AGNATI, L. F., MARCOLI, M., BORROTO-ESCUELA, D. O. & FUXE, K. 2015. G-protein-coupled receptor type A heteromers as an emerging therapeutic target. *Expert Opin Ther Targets,* 19**,** 265-83.

GUPTA, S. & EL-RAYES, B. F. 2008. Small molecule tyrosine kinase inhibitors in pancreatic cancer. *Biologics,* 2**,** 707-15.

GUPTA, V., BHANDARI, D., LEYME, A., AZNAR, N., MIDDE, K. K., LO, I. C., EAR, J., NIESMAN, I., LOPEZ-SANCHEZ, I., BLANCO-CANOSA, J. B., VON ZASTROW, M., GARCIA-MARCOS, M., FARQUHAR, M. G. & GHOSH, P. 2016. GIV/Girdin activates Galphai and inhibits Galphas via the same motif. *Proc Natl Acad Sci U S A,* 113**,** E5721-30.

GUREVICH, V. V. & GUREVICH, E. V. 2017. Molecular Mechanisms of GPCR Signaling: A Structural Perspective. *Int J Mol Sci,* 18.

HARTUNG, A., ORDELHEIDE, A. M., STAIGER, H., MELZER, M., HARING, H. U. & LAMMERS, R. 2013. The Akt substrate Girdin is a regulator of insulin signaling in myoblast cells. *Biochim Biophys Acta,* 1833**,** 2803-2811.

HAUSDORFF, W. P., PITCHER, J. A., LUTTRELL, D. K., LINDER, M. E., KUROSE, H., PARSONS, S. J., CARON, M. G. & LEFKOWITZ, R. J. 1992. Tyrosine phosphorylation of G protein alpha subunits by pp60c-src. *Proc Natl Acad Sci U S A,* 89**,** 5720-4.

HAUSER, A. S., CHAVALI, S., MASUHO, I., JAHN, L. J., MARTEMYANOV, K. A., GLORIAM, D. E. & BABU, M. M. 2018. Pharmacogenomics of GPCR Drug Targets. *Cell,* 172**,** 41-54 e19.

HOPKINS, A. L. & GROOM, C. R. 2002. The druggable genome. *Nat Rev Drug Discov,* 1**,** 727-30.

HUANG, W., MANGLIK, A., VENKATAKRISHNAN, A. J., LAEREMANS, T., FEINBERG, E. N., SANBORN, A. L., KATO, H. E., LIVINGSTON, K. E., THORSEN, T. S., KLING, R. C., GRANIER, S., GMEINER, P., HUSBANDS, S. M., TRAYNOR, J. R., WEIS, W. I., STEYAERT, J., DROR, R. O. & KOBILKA, B. K. 2015. Structural insights into micro-opioid receptor activation. *Nature,* 524**,** 315-21.

HUBBARD, S. R. & MILLER, W. T. 2007. Receptor tyrosine kinases: mechanisms of activation and signaling. *Curr Opin Cell Biol,* 19**,** 117-23.

HUNTER, T. 1995. Protein kinases and phosphatases: the yin and yang of protein phosphorylation and signaling. *Cell,* 80**,** 225-36.

HUNTER, T. 2015. Discovering the first tyrosine kinase. *Proc Natl Acad Sci U S A,* 112**,** 7877-82.

ICHIMIYA, H., MAEDA, K., ENOMOTO, A., WENG, L., TAKAHASHI, M. & MUROHARA, T. 2015. Girdin/GIV regulates transendothelial permeability by controlling VE-cadherin trafficking through the small GTPase, R-Ras. *Biochem Biophys Res Commun,* 461**,** 260-7.

IIRI, T., FARFEL, Z. & BOURNE, H. R. 1998. G-protein diseases furnish a model for the turn-on switch. *Nature,* 394**,** 35-8.

IMAMURA, T., VOLLENWEIDER, P., EGAWA, K., CLODI, M., ISHIBASHI, K., NAKASHIMA, N., UGI, S., ADAMS, J. W., BROWN, J. H. & OLEFSKY, J. M. 1999. G alpha-q/11 protein plays a key role in insulin-induced glucose transport in 3T3-L1 adipocytes. *Mol Cell Biol,* 19**,** 6765-74.

INSEL, P. A., TANG, C. M., HAHNTOW, I. & MICHEL, M. C. 2007. Impact of GPCRs in clinical medicine: monogenic diseases, genetic variants and drug targets. *Biochim Biophys Acta,* 1768**,** 994-1005.

JIN, J. & PAWSON, T. 2012. Modular evolution of phosphorylation-based signalling systems. *Philos Trans R Soc Lond B Biol Sci,* 367**,** 2540-55.

JOHNSTON, C. A., WILLARD, F. S., JEZYK, M. R., FREDERICKS, Z., BODOR, E. T., JONES, M. B., BLAESIUS, R., WATTS, V. J., HARDEN, T. K., SONDEK, J., RAMER, J. K. & SIDEROVSKI, D. P. 2005. Structure of Galpha(i1) bound to a GDP-selective peptide provides insight into guanine nucleotide exchange. *Structure,* 13**,** 1069-80.

KANG, Y., KUYBEDA, O., DE WAAL, P. W., MUKHERJEE, S., VAN EPS, N., DUTKA, P., ZHOU, X. E., BARTESAGHI, A., ERRAMILLI, S., MORIZUMI, T., GU, X., YIN, Y., LIU, P., JIANG, Y., MENG, X., ZHAO, G., MELCHER, K., ERNST, O. P., KOSSIAKOFF, A. A., SUBRAMANIAM, S. & XU, H. E. 2018. Cryo-EM structure of human rhodopsin bound to an inhibitory G protein. *Nature,* 558**,** 553-558.

KANT, R., ZENG, B., THOMAS, C. J., BOTHNER, B. & SPRANG, S. R. 2016. Ric-8A, a G protein chaperone with nucleotide exchange activity induces long-range secondary structure changes in Galpha. *Elife,* 5.

KAPOOR, N., MENON, S. T., CHAUHAN, R., SACHDEV, P. & SAKMAR, T. P. 2009. Structural evidence for a sequential release mechanism for activation of heterotrimeric G proteins. *J Mol Biol,* 393**,** 882-97.

KAYA, A. I., LOKITS, A. D., GILBERT, J. A., IVERSON, T. M., MEILER, J. & HAMM, H. E. 2014. A conserved phenylalanine as a relay between the alpha5 helix and the GDP binding region of heterotrimeric Gi protein alpha subunit. *J Biol Chem,* 289**,** 24475-87.

KAYA, A. I., LOKITS, A. D., GILBERT, J. A., IVERSON, T. M., MEILER, J. & HAMM, H. E. 2016. A Conserved Hydrophobic Core in Galphai1 Regulates G Protein Activation and Release from Activated Receptor. *J Biol Chem,* 291**,** 19674-86.

KELLY, E., BAILEY, C. P. & HENDERSON, G. 2008. Agonist-selective mechanisms of GPCR desensitization. *Br J Pharmacol,* 153 Suppl 1**,** S379-88.

KETTENBACH, A. N., WANG, T., FAHERTY, B. K., MADDEN, D. R., KNAPP, S., BAILEY-KELLOGG, C. & GERBER, S. A. 2012. Rapid determination of multiple linear kinase substrate motifs by mass spectrometry. *Chem Biol,* 19**,** 608-18.

KIMPLE, R. J., KIMPLE, M. E., BETTS, L., SONDEK, J. & SIDEROVSKI, D. P. 2002. Structural determinants for GoLoco-induced inhibition of nucleotide release by Galpha subunits. *Nature,* 416**,** 878-81.

KINOSHITA-KIKUTA, E., AOKI, Y., KINOSHITA, E. & KOIKE, T. 2007. Label-free kinase profiling using phosphate affinity polyacrylamide gel electrophoresis. *Mol Cell Proteomics,* 6**,** 356-66.

KINOSHITA, E., KINOSHITA-KIKUTA, E., TAKIYAMA, K. & KOIKE, T. 2006. Phosphate-binding tag, a new tool to visualize phosphorylated proteins. *Mol Cell Proteomics,* 5**,** 749-57.

KITAMURA, T., ASAI, N., ENOMOTO, A., MAEDA, K., KATO, T., ISHIDA, M., JIANG, P., WATANABE, T., USUKURA, J., KONDO, T., COSTANTINI, F., MUROHARA, T. & TAKAHASHI, M. 2008. Regulation of VEGF-mediated angiogenesis by the Akt/PKB substrate Girdin. *Nat Cell Biol,* 10**,** 329-37.

KOEHL, A., HU, H., MAEDA, S., ZHANG, Y., QU, Q., PAGGI, J. M., LATORRACA, N. R., HILGER, D., DAWSON, R., MATILE, H., SCHERTLER, G. F. X., GRANIER, S., WEIS, W. I., DROR, R. O., MANGLIK, A., SKINIOTIS, G. & KOBILKA, B. K. 2018. Structure of the micro-opioid receptor-Gi protein complex. *Nature*.

KOVALENKO, M., DENNER, K., SANDSTROM, J., PERSSON, C., GROSS, S., JANDT, E., VILELLA, R., BOHMER, F. & OSTMAN, A. 2000. Site-selective dephosphorylation of the platelet-derived growth factor beta-receptor by the receptor-like protein-tyrosine phosphatase DEP-1. *J Biol Chem,* 275**,** 16219-26.

KRUPINSKI, J., RAJARAM, R., LAKONISHOK, M., BENOVIC, J. L. & CERIONE, R. A. 1988. Insulin-dependent phosphorylation of GTP-binding proteins in phospholipid vesicles. *J Biol Chem,* 263**,** 12333-41.

KRUPNICK, J. G. & BENOVIC, J. L. 1998. The role of receptor kinases and arrestins in G protein-coupled receptor regulation. *Annu Rev Pharmacol Toxicol,* 38**,** 289-319.

KRUSE, A. C., RING, A. M., MANGLIK, A., HU, J., HU, K., EITEL, K., HUBNER, H., PARDON, E., VALANT, C., SEXTON, P. M., CHRISTOPOULOS, A., FELDER, C. C., GMEINER, P., STEYAERT, J., WEIS, W. I., GARCIA, K. C., WESS, J. & KOBILKA, B. K. 2013. Activation and allosteric modulation of a muscarinic acetylcholine receptor. *Nature,* 504**,** 101-6.

KUFAREVA, I., RUEDA, M., KATRITCH, V., STEVENS, R. C., ABAGYAN, R. & PARTICIPANTS, G. D. 2011. Status of GPCR modeling and docking as reflected by community-wide GPCR Dock 2010 assessment. *Structure,* 19**,** 1108-26.

LATORRACA, N. R., VENKATAKRISHNAN, A. J. & DROR, R. O. 2017. GPCR Dynamics: Structures in Motion. *Chem Rev,* 117**,** 139-155.

LEDDA, F. & PARATCHA, G. 2007. Negative Regulation of Receptor Tyrosine Kinase (RTK) Signaling: A Developing Field. *Biomark Insights,* 2**,** 45-58.

LEFKOWITZ, R. J. 2004. Historical review: a brief history and personal retrospective of seven-transmembrane receptors. *Trends Pharmacol Sci,* 25**,** 413-22.

LEIPE, D. D., WOLF, Y. I., KOONIN, E. V. & ARAVIND, L. 2002. Classification and evolution of P-loop GTPases and related ATPases. *J Mol Biol,* 317**,** 41-72.

LEMMON, M. A. & SCHLESSINGER, J. 2010. Cell signaling by receptor tyrosine kinases. *Cell,* 141**,** 1117-34.

LEYME, A., MARIVIN, A., PEREZ-GUTIERREZ, L., NGUYEN, L. T. & GARCIA-MARCOS, M. 2015. Integrins activate trimeric G proteins via the nonreceptor protein GIV/Girdin. *J Cell Biol,* 210**,** 1165-84.

LIANG, M. N. & GARRISON, J. C. 1991. The epidermal growth factor receptor is coupled to a pertussis toxin-sensitive guanine nucleotide regulatory protein in rat hepatocytes. *J Biol Chem,* 266**,** 13342-9.

LIN, C., EAR, J., MIDDE, K., LOPEZ-SANCHEZ, I., AZNAR, N., GARCIA-MARCOS, M., KUFAREVA, I., ABAGYAN, R. & GHOSH, P. 2014. Structural basis for activation of trimeric Gi proteins by multiple growth factor receptors via GIV/Girdin. *Mol Biol Cell,* 25**,** 3654-71.

LIN, C., EAR, J., PAVLOVA, Y., MITTAL, Y., KUFAREVA, I., GHASSEMIAN, M., ABAGYAN, R., GARCIA-MARCOS, M. & GHOSH, P. 2011. Tyrosine phosphorylation of the Galpha-interacting protein GIV promotes activation of phosphoinositide 3-kinase during cell migration. *Sci Signal,* 4**,** ra64.

LIU, W. W., MATTINGLY, R. R. & GARRISON, J. C. 1996. Transformation of Rat-1 fibroblasts with the v-src oncogene increases the tyrosine phosphorylation state and activity of the alpha subunit of Gq/G11. *Proc Natl Acad Sci U S A,* 93**,** 8258-63.

LIU, X., XU, X., HILGER, D., ASCHAUER, P., TIEMANN, J. K. S., DU, Y., LIU, H., HIRATA, K., SUN, X., GUIXA-GONZALEZ, R., MATHIESEN, J. M., HILDEBRAND, P. W. & KOBILKA, B. K. 2019. Structural Insights into the Process of GPCR-G Protein Complex Formation. *Cell,* 177**,** 1243-1251 e12.

LO, I. C., GUPTA, V., MIDDE, K. K., TAUPIN, V., LOPEZ-SANCHEZ, I., KUFAREVA, I., ABAGYAN, R., RANDAZZO, P. A., FARQUHAR, M. G. & GHOSH, P. 2015. Activation of Galphai at the Golgi by GIV/Girdin imposes finiteness in Arf1 signaling. *Dev Cell,* 33**,** 189-203.

LOHSE, M. J., NIKOLAEV, V. O., HEIN, P., HOFFMANN, C., VILARDAGA, J. P. & BUNEMANN, M. 2008. Optical techniques to analyze real-time activation and signaling of G-protein-coupled receptors. *Trends Pharmacol Sci,* 29**,** 159-65.

LOPEZ-SANCHEZ, I., DUNKEL, Y., ROH, Y. S., MITTAL, Y., DE MINICIS, S., MURANYI, A., SINGH, S., SHANMUGAM, K., AROONSAKOOL, N., MURRAY, F., HO, S. B., SEKI, E., BRENNER, D. A. & GHOSH, P. 2014. GIV/Girdin is a central hub for profibrogenic signalling networks during liver fibrosis. *Nat Commun,* 5**,** 4451.

LOPEZ-SANCHEZ, I., GARCIA-MARCOS, M., MITTAL, Y., AZNAR, N., FARQUHAR, M. G. & GHOSH, P. 2013. Protein kinase C-theta (PKCtheta) phosphorylates and inhibits the guanine exchange factor, GIV/Girdin. *Proc Natl Acad Sci U S A,* 110**,** 5510-5.

LOPEZ-SANCHEZ, I., MA, G. S., PEDRAM, S., KALOGRIOPOULOS, N. & GHOSH, P. 2015. GIV/girdin binds exocyst subunit-Exo70 and regulates exocytosis of GLUT4 storage vesicles. *Biochem Biophys Res Commun,* 468**,** 287-93.

LOWES, V. L., IP, N. Y. & WONG, Y. H. 2002. Integration of signals from receptor tyrosine kinases and g protein-coupled receptors. *Neurosignals,* 11**,** 5-19.

LUTTRELL, L. M., DAAKA, Y. & LEFKOWITZ, R. J. 1999. Regulation of tyrosine kinase cascades by G-protein-coupled receptors. *Curr Opin Cell Biol,* 11**,** 177-83.

MA, G. S., AZNAR, N., KALOGRIOPOULOS, N., MIDDE, K. K., LOPEZ-SANCHEZ, I., SATO, E., DUNKEL, Y., GALLO, R. L. & GHOSH, P. 2015a. Therapeutic effects of cell-permeant peptides that activate G proteins downstream of growth factors. *Proc Natl Acad Sci U S A,* 112**,** E2602-10.

MA, G. S., LOPEZ-SANCHEZ, I., AZNAR, N., KALOGRIOPOULOS, N., PEDRAM, S., MIDDE, K., CIARALDI, T. P., HENRY, R. R. & GHOSH, P. 2015b. Activation of G proteins by GIV-GEF is a pivot point for insulin resistance and sensitivity. *Mol Biol Cell,* 26**,** 4209-23.

MANGANELLO, J. M., HUANG, J. S., KOZASA, T., VOYNO-YASENETSKAYA, T. A. & LE BRETON, G. C. 2003. Protein kinase A-mediated phosphorylation of the Galpha13 switch I region alters the Galphabetagamma13-G protein-coupled receptor complex and inhibits Rho activation. *J Biol Chem,* 278**,** 124-30.

MARTY, C. & YE, R. D. 2010. Heterotrimeric G protein signaling outside the realm of seven transmembrane domain receptors. *Mol Pharmacol,* 78**,** 12-8.

MCCAIN, J. 2013. The MAPK (ERK) Pathway: Investigational Combinations for the Treatment Of BRAF-Mutated Metastatic Melanoma. *P T,* 38**,** 96-108.

MCCOY, A. J., GROSSE-KUNSTLEVE, R. W., ADAMS, P. D., WINN, M. D., STORONI, L. C. & READ, R. J. 2007. Phaser crystallographic software. *J Appl Crystallogr,* 40**,** 658-674.

MCINTIRE, W. E. 2009. Structural determinants involved in the formation and activation of G protein betagamma dimers. *Neurosignals,* 17**,** 82-99.

MEAGHER, K. L., REDMAN, L. T. & CARLSON, H. A. 2003. Development of polyphosphate parameters for use with the AMBER force field. *J Comput Chem,* 24**,** 1016-25.

MIDDE, K. K., AZNAR, N., LAEDERICH, M. B., MA, G. S., KUNKEL, M. T., NEWTON, A. C. & GHOSH, P. 2015. Multimodular biosensors reveal a novel platform for activation of G proteins by growth factor receptors. *Proc Natl Acad Sci U S A,* 112**,** E937-46.

MILLIGAN, G. & KOSTENIS, E. 2006. Heterotrimeric G-proteins: a short history. *Br J Pharmacol,* 147 Suppl 1**,** S46-55.

MORRIS, A. J. & MALBON, C. C. 1999. Physiological regulation of G protein-linked signaling. *Physiol Rev,* 79**,** 1373-430.

MOYERS, J. S., LINDER, M. E., SHANNON, J. D. & PARSONS, S. J. 1995. Identification of the in vitro phosphorylation sites on Gs alpha mediated by pp60c-src. *Biochem J,* 305 (Pt 2)**,** 411-7.

NAIR, B. G., PARIKH, B., MILLIGAN, G. & PATEL, T. B. 1990. Gs alpha mediates epidermal growth factor-elicited stimulation of rat cardiac adenylate cyclase. *J Biol Chem,* 265**,** 21317-22.

NATARAJAN, K. & BERK, B. C. 2006. Crosstalk coregulation mechanisms of G protein-coupled receptors and receptor tyrosine kinases. *Methods Mol Biol,* 332**,** 51-77.

NAVARRO, L., KOLLER, A., NORDFELTH, R., WOLF-WATZ, H., TAYLOR, S. & DIXON, J. E. 2007. Identification of a molecular target for the Yersinia protein kinase A. *Mol Cell,* 26**,** 465-77.

O'BRIEN, R. M., HOUSLAY, M. D., MILLIGAN, G. & SIDDLE, K. 1987. The insulin receptor tyrosyl kinase phosphorylates holomeric forms of the guanine nucleotide regulatory proteins Gi and Go. *FEBS Lett,* 212**,** 281-8.

OHTSU, H., DEMPSEY, P. J. & EGUCHI, S. 2006. ADAMs as mediators of EGF receptor transactivation by G protein-coupled receptors. *Am J Physiol Cell Physiol,* 291**,** C1-10.

OKAMOTO, T., KATADA, T., MURAYAMA, Y., UI, M., OGATA, E. & NISHIMOTO, I. 1990. A simple structure encodes G protein-activating function of the IGF-II/mannose 6-phosphate receptor. *Cell,* 62**,** 709-17.

OKAMOTO, T., MURAYAMA, Y., HAYASHI, Y., INAGAKI, M., OGATA, E. & NISHIMOTO, I. 1991. Identification of a Gs activator region of the beta 2-adrenergic receptor that is autoregulated via protein kinase A-dependent phosphorylation. *Cell,* 67**,** 723-30.

OLDHAM, W. M., VAN EPS, N., PREININGER, A. M., HUBBELL, W. L. & HAMM, H. E. 2006. Mechanism of the receptor-catalyzed activation of heterotrimeric G proteins. *Nat Struct Mol Biol,* 13**,** 772-7.

OSTMAN, A., HELLBERG, C. & BOHMER, F. D. 2006. Protein-tyrosine phosphatases and cancer. *Nat Rev Cancer,* 6**,** 307-20.

OSTROM, R. S., GREGORIAN, C., DRENAN, R. M., XIANG, Y., REGAN, J. W. & INSEL, P. A. 2001. Receptor number and caveolar co-localization determine receptor coupling efficiency to adenylyl cyclase. *J Biol Chem,* 276**,** 42063-9.

PARAG-SHARMA, K., LEYME, A., DIGIACOMO, V., MARIVIN, A., BROSELID, S. & GARCIA-MARCOS, M. 2016. Membrane Recruitment of the Non-receptor Protein GIV/Girdin (Galpha-interacting, Vesicle-associated Protein/Girdin) Is Sufficient for Activating Heterotrimeric G Protein Signaling. *J Biol Chem,* 291**,** 27098-27111.

PATEL, T. B. 2004. Single transmembrane spanning heterotrimeric g protein-coupled receptors and their signaling cascades. *Pharmacol Rev,* 56**,** 371-85.

PAWSON, T. 2004. Specificity in signal transduction: from phosphotyrosine-SH2 domain interactions to complex cellular systems. *Cell,* 116**,** 191-203.

PAWSON, T., GISH, G. D. & NASH, P. 2001. SH2 domains, interaction modules and cellular wiring. *Trends Cell Biol,* 11**,** 504-11.

PEACOCK, R. B., DAVIS, J. R., MARKWICK, P. R. L. & KOMIVES, E. A. 2018. Dynamic Consequences of Mutation of Tryptophan 215 in Thrombin. *Biochemistry,* 57**,** 2694-2703.

PERSSON, C., SAVENHED, C., BOURDEAU, A., TREMBLAY, M. L., MARKOVA, B., BOHMER, F. D., HAJ, F. G., NEEL, B. G., ELSON, A., HELDIN, C. H., RONNSTRAND, L., OSTMAN, A. & HELLBERG, C. 2004. Site-selective regulation of platelet-derived growth factor beta receptor tyrosine phosphorylation by T-cell protein tyrosine phosphatase. *Mol Cell Biol,* 24**,** 2190-201.

PIERCE, K. L., PREMONT, R. T. & LEFKOWITZ, R. J. 2002. Seven-transmembrane receptors. *Nat Rev Mol Cell Biol,* 3**,** 639-50.

PIIPER, A. & ZEUZEM, S. 2004. Receptor tyrosine kinases are signaling intermediates of G protein-coupled receptors. *Curr Pharm Des,* 10**,** 3539-45.

PITCHER, J. A., FREEDMAN, N. J. & LEFKOWITZ, R. J. 1998. G protein-coupled receptor kinases. *Annu Rev Biochem,* 67**,** 653-92.

POPPLETON, H., SUN, H., FULGHAM, D., BERTICS, P. & PATEL, T. B. 1996. Activation of Gsalpha by the epidermal growth factor receptor involves phosphorylation. *J Biol Chem,* 271**,** 6947-51.

POPPLETON, H. M., SUN, H., MULLENIX, J. B., WIEPZ, G. J., BERTICS, P. J. & PATEL, T. B. 2000. The juxtamembrane region of the epidermal growth factor receptor is required for phosphorylation of Galpha(s). *Arch Biochem Biophys,* 383**,** 309-17.

PREMONT, R. T. & GAINETDINOV, R. R. 2007. Physiological roles of G protein-coupled receptor kinases and arrestins. *Annu Rev Physiol,* 69**,** 511-34.

PRENZEL, N., ZWICK, E., DAUB, H., LESERER, M., ABRAHAM, R., WALLASCH, C. & ULLRICH, A. 1999. EGF receptor transactivation by G-protein-coupled receptors requires metalloproteinase cleavage of proHB-EGF. *Nature,* 402**,** 884-8.

QI, X., LIU, H., THOMPSON, B., MCDONALD, J., ZHANG, C. & LI, X. 2019. Cryo-EM structure of oxysterol-bound human Smoothened coupled to a heterotrimeric Gi. *Nature*.

RANA, B. K. & INSEL, P. A. 2002. G-protein-coupled receptor websites. *Trends Pharmacol Sci,* 23**,** 535-6.

RASMUSSEN, S. G., DEVREE, B. T., ZOU, Y., KRUSE, A. C., CHUNG, K. Y., KOBILKA, T. S., THIAN, F. S., CHAE, P. S., PARDON, E., CALINSKI, D., MATHIESEN, J. M., SHAH, S. T., LYONS, J. A., CAFFREY, M., GELLMAN, S. H., STEYAERT, J., SKINIOTIS, G., WEIS, W. I., SUNAHARA, R. K. & KOBILKA, B. K. 2011. Crystal structure of the beta2 adrenergic receptor-Gs protein complex. *Nature,* 477**,** 549-55.

RAW, A. S., COLEMAN, D. E., GILMAN, A. G. & SPRANG, S. R. 1997. Structural and biochemical characterization of the GTPgammaS-, GDP.Pi-, and GDP-bound forms of a GTPase-deficient Gly42 --> Val mutant of Gialpha1. *Biochemistry,* 36**,** 15660-9.

REGAD, T. 2015. Targeting RTK Signaling Pathways in Cancer. *Cancers (Basel),* 7**,** 1758-84.

REMMERS, A. E. 1998. Detection and quantitation of heterotrimeric G proteins by fluorescence resonance energy transfer. *Anal Biochem,* 257**,** 89-94.

RIBAS, C., PENELA, P., MURGA, C., SALCEDO, A., GARCIA-HOZ, C., JURADO-PUEYO, M., AYMERICH, I. & MAYOR, F., JR. 2007. The G protein-coupled receptor kinase (GRK) interactome: role of GRKs in GPCR regulation and signaling. *Biochim Biophys Acta,* 1768**,** 913-22.

ROBINSON, D. R., WU, Y. M. & LIN, S. F. 2000. The protein tyrosine kinase family of the human genome. *Oncogene,* 19**,** 5548-57.

ROE, D. R. & CHEATHAM, T. E., 3RD 2013. PTRAJ and CPPTRAJ: Software for Processing and Analysis of Molecular Dynamics Trajectory Data. *J Chem Theory Comput,* 9**,** 3084-95.

ROSS, E. M. & WILKIE, T. M. 2000. GTPase-activating proteins for heterotrimeric G proteins: regulators of G protein signaling (RGS) and RGS-like proteins. *Annu Rev Biochem,* 69**,** 795-827.

SASAKI, K., KAKUWA, T., AKIMOTO, K., KOGA, H. & OHNO, S. 2015. Regulation of epithelial cell polarity by PAR-3 depends on Girdin transcription and Girdin-Galphai3 signaling. *J Cell Sci,* 128**,** 2244-58.

SATO, M., BLUMER, J. B., SIMON, V. & LANIER, S. M. 2006. Accessory proteins for G proteins: partners in signaling. *Annu Rev Pharmacol Toxicol,* 46**,** 151-87.

SCHAFER, B., GSCHWIND, A. & ULLRICH, A. 2004. Multiple G-protein-coupled receptor signals converge on the epidermal growth factor receptor to promote migration and invasion. *Oncogene,* 23**,** 991-9.

SCHONEBERG, T., SCHULZ, A., BIEBERMANN, H., HERMSDORF, T., ROMPLER, H. & SANGKUHL, K. 2004. Mutant G-protein-coupled receptors as a cause of human diseases. *Pharmacol Ther,* 104**,** 173-206.

SHAH, B. H. & CATT, K. J. 2004. GPCR-mediated transactivation of RTKs in the CNS: mechanisms and consequences. *Trends Neurosci,* 27**,** 48-53.

SHI, J., DAMJANOSKA, K. J., SINGH, R. K., CARRASCO, G. A., GARCIA, F., GRIPPO, A. J., LANDRY, M., SULLIVAN, N. R., BATTAGLIA, G. & MUMA, N. A. 2007a. Agonist induced-phosphorylation of Galpha11 protein reduces coupling to 5-HT2A receptors. *J Pharmacol Exp Ther,* 323**,** 248-56.

SHI, J., ZEMAITAITIS, B. & MUMA, N. A. 2007b. Phosphorylation of Galpha11 protein contributes to agonist-induced desensitization of 5-HT2A receptor signaling. *Mol Pharmacol,* 71**,** 303-13.

SIDEROVSKI, D. P. & WILLARD, F. S. 2005. The GAPs, GEFs, and GDIs of heterotrimeric G-protein alpha subunits. *Int J Biol Sci,* 1**,** 51-66.

SPRANG, S. R. 2016. Invited review: Activation of G proteins by GTP and the mechanism of Galpha-catalyzed GTP hydrolysis. *Biopolymers,* 105**,** 449-62.

STADEL, J. M., NAMBI, P., SHORR, R. G., SAWYER, D. F., CARON, M. G. & LEFKOWITZ, R. J. 1983. Catecholamine-induced desensitization of turkey erythrocyte adenylate cyclase is associated with phosphorylation of the beta-adrenergic receptor. *Proc Natl Acad Sci U S A,* 80**,** 3173-7.

STOY, H. & GUREVICH, V. V. 2015. How genetic errors in GPCRs affect their function: Possible therapeutic strategies. *Genes Dis,* 2**,** 108-132.

SUN, D., FLOCK, T., DEUPI, X., MAEDA, S., MATKOVIC, M., MENDIETA, S., MAYER, D., DAWSON, R., SCHERTLER, G. F. X., MADAN BABU, M. & VEPRINTSEV, D. B. 2015. Probing Galphai1 protein activation at single-amino acid resolution. *Nat Struct Mol Biol,* 22**,** 686-694.

SUN, H., CHEN, Z., POPPLETON, H., SCHOLICH, K., MULLENIX, J., WEIPZ, G. J., FULGHAM, D. L., BERTICS, P. J. & PATEL, T. B. 1997. The juxtamembrane, cytosolic region of the epidermal growth factor receptor is involved in association with alpha-subunit of Gs. *J Biol Chem,* 272**,** 5413-20.

SUN, H., SEYER, J. M. & PATEL, T. B. 1995. A region in the cytosolic domain of the epidermal growth factor receptor antithetically regulates the stimulatory and inhibitory guanine nucleotide-binding regulatory proteins of adenylyl cyclase. *Proc Natl Acad Sci U S A,* 92**,** 2229-33.

SUN, X., SINGH, S., BLUMER, K. J. & BOWMAN, G. R. 2018. Simulation of spontaneous G protein activation reveals a new intermediate driving GDP unbinding. *Elife,* 7.

SUNAHARA, R. K., DESSAUER, C. W. & GILMAN, A. G. 1996. Complexity and diversity of mammalian adenylyl cyclases. *Annu Rev Pharmacol Toxicol,* 36**,** 461-80.

TAKEUCHI, K. & ITO, F. 2011. Receptor tyrosine kinases and targeted cancer therapeutics. *Biol Pharm Bull,* 34**,** 1774-80.

UBERSAX, J. A. & FERRELL, J. E., JR. 2007. Mechanisms of specificity in protein phosphorylation. *Nat Rev Mol Cell Biol,* 8**,** 530-41.

ULLRICH, A. & SCHLESSINGER, J. 1990. Signal transduction by receptors with tyrosine kinase activity. *Cell,* 61**,** 203-12.

UMEMORI, H., INOUE, T., KUME, S., SEKIYAMA, N., NAGAO, M., ITOH, H., NAKANISHI, S., MIKOSHIBA, K. & YAMAMOTO, T. 1997. Activation of the G protein Gq/11 through tyrosine phosphorylation of the alpha subunit. *Science,* 276**,** 1878-81.

VAN EPS, N., ALTENBACH, C., CARO, L. N., LATORRACA, N. R., HOLLINGSWORTH, S. A., DROR, R. O., ERNST, O. P. & HUBBELL, W. L. 2018. Gi- and Gs-coupled GPCRs show different modes of G-protein binding. *Proc Natl Acad Sci U S A,* 115**,** 2383-2388.

VAN EPS, N., PREININGER, A. M., ALEXANDER, N., KAYA, A. I., MEIER, S., MEILER, J., HAMM, H. E. & HUBBELL, W. L. 2011. Interaction of a G protein with an activated receptor opens the interdomain interface in the alpha subunit. *Proc Natl Acad Sci U S A,* 108**,** 9420-4.

VANHAESEBROECK, B., LEEVERS, S. J., AHMADI, K., TIMMS, J., KATSO, R., DRISCOLL, P. C., WOSCHOLSKI, R., PARKER, P. J. & WATERFIELD, M. D. 2001. Synthesis and function of 3-phosphorylated inositol lipids. *Annu Rev Biochem,* 70**,** 535-602.

VASSILATIS, D. K., HOHMANN, J. G., ZENG, H., LI, F., RANCHALIS, J. E., MORTRUD, M. T., BROWN, A., RODRIGUEZ, S. S., WELLER, J. R., WRIGHT, A. C., BERGMANN, J. E. & GAITANARIS, G. A. 2003. The G protein-coupled receptor repertoires of human and mouse. *Proc Natl Acad Sci U S A,* 100**,** 4903-8.

WALES, T. E. & ENGEN, J. R. 2006. Hydrogen exchange mass spectrometry for the analysis of protein dynamics. *Mass Spectrom Rev,* 25**,** 158-70.

WALL, M. A., COLEMAN, D. E., LEE, E., INIGUEZ-LLUHI, J. A., POSNER, B. A., GILMAN, A. G. & SPRANG, S. R. 1995. The structure of the G protein heterotrimer Gi alpha 1 beta 1 gamma 2. *Cell,* 83**,** 1047-58.

WANG, H., MISAKI, T., TAUPIN, V., EGUCHI, A., GHOSH, P. & FARQUHAR, M. G. 2015. GIV/girdin links vascular endothelial growth factor signaling to Akt survival signaling in podocytes independent of nephrin. *J Am Soc Nephrol,* 26**,** 314-27.

WANG, J., FROST, J. A., COBB, M. H. & ROSS, E. M. 1999. Reciprocal signaling between heterotrimeric G proteins and the p21-stimulated protein kinase. *J Biol Chem,* 274**,** 31641-7.

WANG, J., GARERI, C. & ROCKMAN, H. A. 2018. G-Protein-Coupled Receptors in Heart Disease. *Circ Res,* 123**,** 716-735.

WARD, C. W., LAWRENCE, M. C., STRELTSOV, V. A., ADAMS, T. E. & MCKERN, N. M. 2007. The insulin and EGF receptor structures: new insights into ligand-induced receptor activation. *Trends Biochem Sci,* 32**,** 129-37.

WENG, L., ENOMOTO, A., ISHIDA-TAKAGISHI, M., ASAI, N. & TAKAHASHI, M. 2010. Girding for migratory cues: roles of the Akt substrate Girdin in cancer progression and angiogenesis. *Cancer Sci,* 101**,** 836-42.

WETTSCHURECK, N. & OFFERMANNS, S. 2005. Mammalian G proteins and their cell type specific functions. *Physiol Rev,* 85**,** 1159-204.

WILKIE, T. M., GILBERT, D. J., OLSEN, A. S., CHEN, X. N., AMATRUDA, T. T., KORENBERG, J. R., TRASK, B. J., DE JONG, P., REED, R. R., SIMON, M. I. & ET AL. 1992. Evolution of the mammalian G protein alpha subunit multigene family. *Nat Genet,* 1**,** 85-91.

WILLETS, J. M., CHALLISS, R. A. & NAHORSKI, S. R. 2003. Non-visual GRKs: are we seeing the whole picture? *Trends Pharmacol Sci,* 24**,** 626-33.

WINN, M. D., BALLARD, C. C., COWTAN, K. D., DODSON, E. J., EMSLEY, P., EVANS, P. R., KEEGAN, R. M., KRISSINEL, E. B., LESLIE, A. G., MCCOY, A., MCNICHOLAS, S. J., MURSHUDOV, G. N., PANNU, N. S., POTTERTON, E. A., POWELL, H. R., READ, R. J., VAGIN, A. & WILSON, K. S. 2011. Overview of the CCP4 suite and current developments. *Acta Crystallogr D Biol Crystallogr,* 67**,** 235-42.

ZHANG, Y., SUN, B., FENG, D., HU, H., CHU, M., QU, Q., TARRASCH, J. T., LI, S., SUN KOBILKA, T., KOBILKA, B. K. & SKINIOTIS, G. 2017. Cryo-EM structure of the activated GLP-1 receptor in complex with a G protein. *Nature,* 546**,** 248-253.

ZHAO, J., DENG, Y., JIANG, Z. & QING, H. 2016. G Protein-Coupled Receptors (GPCRs) in Alzheimer's Disease: A Focus on BACE1 Related GPCRs. *Front Aging Neurosci,* 8**,** 58.

ZICK, Y., SAGI-EISENBERG, R., PINES, M., GIERSCHIK, P. & SPIEGEL, A. M. 1986. Multisite phosphorylation of the alpha subunit of transducin by the insulin receptor kinase and protein kinase C. *Proc Natl Acad Sci U S A,* 83**,** 9294-7.